AP1000 DESIGN CERTIFICATION REVIEW

Response to Request For Additional Information

RAI Number: 720.087

Question:

There is no reference provided in the AP1000 PRA for the assessment of ex-vessel steam explosions except to say that the results of AP600 are applicable to AP1000. The AP600 ex-vessel steam explosion analysis considers the lifting of the RPV (see Chapter 19 in NUREG-1512), and concludes that the steel containment remains intact. Please provide the justification of neglecting the potential for failure of the containment penetrations as a result of violent movement of the reactor pressure vessel subject to steam explosions-impulse loads?

Westinghouse Response:

See the response to RAI 720.075 for discussion of the applicability of the AP600 ex-vessel steam explosion assessment to AP1000. The ex-vessel steam explosion assessment for AP600 is provided in Appendix B of the AP600 PRA Report (Reference B-3 in AP1000 PRA Appendix B). The reactor pressure vessel response, including lifting and the effect on penetrations, is described in section B.3.2.2, and is appropriate for AP1000 for the reasons given in the response to RAI 720.075.

Design Control Document (DCD) Revision:

None

PRA Revision:

None

AP1000 DESIGN CERTIFICATION REVIEW

Response to Request For Additional Information

RAI Number: 720.088

Question:

In order to resolve the issue of in-vessel debris coolability due to lower head cooling for the AP1000, Westinghouse refers to a previous U. S. Department of Energy (DOE) study of the same issue for the AP600 (T. G. Theofanous, et al., "In-Vessel Coolability and Retention of a Core Melt," DOE/ID-10460, October 1996), and states that these results are directly applicable to the AP1000. The following questions are relevant to the applicability of the DOE AP600 experiments and analyses to AP1000:

A. Preliminary calculations performed for the AP1000 had shown that reactor vessel insulation based on the ULPU Configuration III gave very little margin to dryout, and, as a result, the AP1000 reactor vessel insulation was redesigned to more resemble ULPU Configuration IV (Figure 39-3 in the AP1000 PRA), for which the measured CHF was 20% to 30% higher.

(i) What are the main phenomenological reasons for the substantially higher critical heat flux that is measured for ULPU Configuration IV as compared with ULPU Configuration III?

(ii) In the DCD (e.g., Figure 5.3-7 in the AP1000 DCD), the insulation appears to resemble the Configuration III design. Please confirm the actual configuration (i.e., either Configuration III or Configuration IV) foreseen for AP1000.

(iii) Please demonstrate the influence of boiling on the structural integrity of the reactor pressure vessel insulation.

(iv) What are the experimental uncertainties associated with the measured critical heat flux for the ULPU Configuration IV design as a function of angle?

B. Debris jet impingement on the lower head was shown in the DOE AP600 study to result in an upper-bound ablation depth of about 12.5 centimeters (cm) (as compared with 15.24 cm minimum total thickness), as per calculations in which ablation depth is directly proportional to pour mass, and in which 1/3 of the AP600 total core mass was used. As this sub-issue was not specifically discussed in the AP1000 supporting documents, please provide justifications for assuming that the lower head failures due to debris impingement in the AP1000 design should be extremely unlikely even with the 26% larger total core mass in the AP1000 as compared with the AP600.

C. What is the impact of the higher fuel enrichment on the melt progression and pour rates into the lower plenum?

D. The analysis performed by Theofanous (T. G. Theofanous, et al., "In-Vessel Coolability and Retention of a Core Melt," DOE/ID-10460, October 1996) and Westinghouse, in portraying the molten pool state inside the lower head, does not consider:

(i) The potential focusing effects of a thin metal layer on top of the molten pool (with a high thermal conductivity) on the local heat flux on the vessel wall, especially considering the results of calculations for small molten steel masses documented in the study by INEEL (J. L. Rempe, et al., "Potential for AP600 In-Vessel Retention through Ex-Vessel Flooding – Technical Evaluation Report," INEEL/EXT-97-00779, Idaho National Engineering Laboratory, December 1997).

(ii) The potential influence of impurities in the debris bed that could result in stratification of the oxide pool into layers of different composition (as observed in the OECD RASPLAV and MASCA programs).

(iii) The potential influence of zirconium, steel and uranium partitioning between oxide and metallic phases, on the downward heat transfer (as observed in the OECD MASCA experiments).

Westinghouse Response:

The in-vessel melting and relocation scenario is presented in a revision to the PRA Chapter 39.

A.i Higher CHF measured in ULPU Configuration IV as compared to data obtained in ULPU Configuration III is attributed to a streamlined flow path in Configuration IV, which presents the only design difference between the two configurations.

A.ii Figure 5.3-7 in the AP1000 DCD is corrected in the revision given in the response to RAI 720.050.

Aiii Structural analysis of the vessel insulation is addressed in the response to RAI 720.050.

A.iv The ULPU concept is unique in allowing essentially full scale simulation of the reactor lower head. The elements in achieving this is a full length slice geometry and the power shaping principle. At this time we are working with Configuration V which faithfully simulates both the inlet and outlet geometries as currently conceived for AP1000. This is in addition to the streamlined geometry of Configuration IV. The Configuration IV CHF results used in the AP1000 evaluation of in-vessel retention are a conservative interpretation of the data and there is large margin, so uncertainties have been considered in a global manner.

B. An assessment of the melt impingement on the AP600 lower head is presented in Appendix H of the DOE/ID-10460. This analysis presents the relocation of 47000 kg of debris onto the lower head. The analysis neglects the effects of the water in the lower plenum.

From the AP1000 in-vessel melt and relocation assessment presented in the revision below to Chapter 39, the mass of superheat debris relocated to the lower plenum in the initial relocation is estimated to be 51200 kg. The superheat in the AP1000 debris is bounded by the superheat predicted for the AP600. Given the significant conservatism in the AP600 assessment, and that only 10% more oxide is predicted to participate in the AP1000 relocation, the conclusion of the AP600 assessment of melt impingement is considered to be applicable to the AP1000.

C. The AP1000 specific power density is used in the assessment presented in the revision below to Chapter 39.

D.i The potential for the focusing effect is considered in the assessment presented in the revision below to Chapter 39.

D.ii See the response to RAI 720.047.

D.iii The potential for the zirconium, steel and uranium partitioning between the oxide and metallic phases is addressed in the revision below to Chapter 39.

Design Control Document (DCD) Revision:

Section 19.39.5 is revised as follows

19.39.5 In-Vessel Melt Progression and Relocation

The AP1000 core and lower internals geometry has been changed from the AP600 geometry as a result of the higher power output. The core is made up of 157 fuel assemblies with a 14-foot active fuel length. To accommodate the larger reactor core, the thick stainless steel reflector has been replaced by a 7/8" thick core stainless steel shroud. The thick bottom plate of the shroud is mounted flush on the support plate. There are no former plates in the annulus between the shroud and the core barrel. The core barrel is 2" thick and hangs from the upper head flange. Cooling holes through the core shroud provide cooling flow to the shroud from the core flow.

The phenomena associated with melting the core and the relocation of the molten debris to the lower plenum play an important role in the composition and configuration of the debris pool. In turn, the characteristics of the debris pool significantly impact the heat loading to the lower head wall and the challenge to lower head integrity. Therefore, understanding the melting and relocation scenarios plays an important role in the assessment of in-vessel retention of molten core debris in the lower plenum.

The important conclusions from the analysis of the lower plenum debris pool formation are:

- **The lower plenum debris bed is cooled with water during the entire relocation process prior to contact with the support plate. Transient debris configurations are not predicted to threaten vessel integrity.**
- **The lower plenum oxide debris subsumes the lower core support plate before dry out in the lower plenum occurs. If the relocated debris is assumed to be instantaneously quenched in the lower plenum water the oxide debris contacts the lower support plate before the debris can return to a superheated condition. Therefore, the lower core support plate, core shroud and a sizeable fraction of the core barrel are subsumed in the debris bed. The focusing effect is mitigated.**
- **The lower plenum debris bed is predicted to form a metal layer over oxide pool configuration.**
- **The potential for debris interaction creating a bottom metal pool of uranium dissolved in zirconium is expected to be small.**
- **The earliest time to achieve the fully molten, circulating debris bed in the lower plenum is 2.7 hours after event initiation.**

~~The analysis of the challenge to the AP600 reactor vessel integrity due to jet impingement (Reference 19.39-1) and steam explosion (Reference 19.39-2) demonstrated very large margin to failure from these phenomena. The AP1000 reactor vessel lower head has the same geometry and thickness as the AP600. The mass and superheat characteristics of the initial debris relocation to the lower plenum are expected to be of the same order of magnitude as the AP600. The conclusions of the AP600 analyses can be extended to the AP1000. Therefore, no challenge to the lower head integrity is expected from the relocation of debris from the core region to the plenum in the AP1000.~~

~~The volume of the AP1000 lower plenum below the core support plate is slightly smaller than it was the AP600 design, because the support plate is 1 inch thicker. The volume of the oxidic core debris that can relocate to the lower plenum has increased because the AP1000 core is larger than the AP600 core. 65 to 70 percent of the molten oxidic debris are needed to relocate to the AP1000 lower plenum to contact the support plate. Therefore, the debris will melt the support plate, lower nozzles and core shroud into the lower plenum debris bed. The debris bed in the lower plenum is expected to form a molten metal layer over molten oxide pool.~~

PRA Revision:

Chapter 39 to be revised as follows:

39.5 In-Vessel Melt Progression and Relocation

In the AP600 ROAAM analysis of in-vessel retention (Reference 39-1) and in-vessel steam explosion (Reference 39-2), the melt progression and relocation to the lower plenum was analyzed. One of the conclusions from the AP600 analysis was that the reactor vessel lower internals, particularly the reflector situated inside the core barrel, significantly impacted the relocation such that:

- The debris relocation to the lower plenum occurs due to melt-through of the core barrel. The quantity of the initial mass of the molten debris that mixes with the lower plenum water is dictated by the failure size and includes only a small fraction of the debris.

- The relocation pathway to the lower plenum from the fuel region downward through the support plate is blocked by metal, which melts and re-freezes around the zirc plugs, lower fuel assembly nozzles and support plate.

- The relocation pathway to the lower plenum from the region between the reflector and the core barrel downward through the support plate is blocked by metal relocated from the failure of the core reflector.

- A fraction of the total molten UO_2 is needed to fill the lower plenum to contact the lower support plate, allowing the lower support plate and reflector to melt into the debris mass.

- The large metal mass from the melting of the reflector and support plate in the lower plenum produces a thick metal layer that mitigates any focusing effect of the metal layer and prevents a large heat flux from occurring at the top of the debris pool.

The AP1000 core and lower internals geometry has been changed from the AP600 geometry as a result of the higher power output. The core is made up of 157 fuel assemblies with a 14-foot active fuel length. To accommodate the larger reactor core, the thick stainless steel reflector has been replaced by a 7/8" thick core stainless steel shroud (Figure 39-2). The thick bottom plate of the shroud is mounted flush on the support plate. There are no former plates in the annulus between the shroud and the core barrel. The core barrel is 2" thick and hangs from the upper head flange. Cooling holes through the core shroud provide cooling flow to the shroud from the core flow.

The phenomena associated with melting the core and the relocation of the molten debris to the lower plenum play an important role in the composition and configuration of the debris pool (reference 1). In turn, the characteristics of the debris pool significantly impact the heat loading to the lower head wall and the challenge to lower head integrity (reference 2). Therefore, understanding the melting and relocation scenarios plays an important role in the assessment of in-vessel retention of molten core debris in the lower plenum. Attachment 39A provides analysis of the core melting and relocation, considering the impact of the AP1000 specific geometry, and addresses the timing and interactions of the various debris materials in the formation of a lower plenum debris bed.

The important conclusions from the Attacnment 39A analysis of the lower plenum debris pool formation are:

- **The lower plenum debris bed is cooled with water during the entire relocation process prior to contact with the support plate. Transient debris configurations are not predicted to threaten vessel integrity.**
- **The lower plenum oxide debris subsumes the lower core support plate before dry out in the lower plenum occurs. If the relocated debris is assumed to be instantaneously quenched in the lower plenum water the oxide debris contacts the lower support plate before the debris can return to a superheated condition. Therefore, the lower core support plate, core shroud and a sizeable fraction of the core barrel are subsumed in the debris bed. The focusing effect is mitigated.**
- **The lower plenum debris bed is predicted to form a metal layer over oxide pool configuration.**
- **The potential for debris interaction creating a bottom metal pool of uranium dissolved in zirconium is expected to be small.**
- **The earliest time to achieve the fully molten, circulating debris bed in the lower plenum is 2.7 hours after event initiation.**

~~The heat sink potential of the downward molten debris relocation path from the core region to the lower head is significantly greater than that of the sideward relocation pathway. Like the AP600, the downward relocation pathway through the AP1000 lower support plate to the lower plenum is expected to plug with molten metal debris frozen above the lower nozzles of the fuel assemblies. Molten oxidic debris that may melt sideward through the core shroud has no direct path from the core bypass region to the lower plenum. The cooling holes in the shroud direct the molten oxide debris back into the core region above the elevation of the downward blockage. The debris relocation to the lower head is not expected until a significant fraction of the core has melted.~~

~~Like the AP600, the initial debris relocation to the AP1000 lower plenum is expected to occur due to the melt-through of the core barrel. Only a small fraction of the debris is expected to participate in the initial relocation to the lower plenum as it pours through the failure in the core barrel. The debris relocation in the lower head is expected to be of similar mass flow rate and superheat as the AP600.~~

~~The analysis of the challenge to the AP600 reactor vessel integrity from impingement by the molten debris jet (Reference 39-1) and steam explosion (Reference 39-2) demonstrated very large margin to failure from these phenomena. The AP1000 reactor vessel lower head has the same geometry and thickness as the AP600. Given that the mass and superheat characteristics of the initial debris relocation to the lower plenum are expected to be of the same order of magnitude as the AP600, the conclusions of the AP600 analyses can be extended to the AP1000. Therefore, no challenge to the lower head integrity is expected from the relocation of debris from the core region to the plenum in the AP1000.~~

~~The volume of the AP1000 lower plenum below the core support plate is slightly smaller than it was the AP600 design, because the support plate is 1" thicker. The volume of the oxidic core debris that can relocate to the lower plenum has increased because the AP1000 core is larger than the AP600 core. Sixty-five to 70 percent of the molten oxidic debris is needed to relocate to the AP1000 lower plenum to contact the support plate. Therefore, in the case of a full core melt, the debris will melt the support plate, lower nozzles and core shroud into the lower plenum debris bed. The debris bed in the lower plenum is expected to form a molten metal layer over molten oxide pool configuration.~~

ATTACHMENT 39A

AP1000 IN-VESSEL CORE MELTING RELOCATION

39A.1 Introduction

The phenomena associated with melting the core and the relocation of the molten debris to the lower plenum play an important role in the composition and configuration of the debris pool (reference 39A-1). In turn, the characteristics of the debris pool significantly impact the heat loading to the lower head wall and the challenge to lower head integrity (reference 39A-2). Therefore, understanding the melting and relocation scenarios plays an important role in the assessment of in-vessel retention of molten core debris in the lower plenum. The purpose of this section is to investigate the core melting and relocation in detail, considering the impact of the AP1000 specific geometry, and to determine the timing and interactions of the various debris materials in the formation of a lower plenum debris bed.

39A.2 Phenomenological Issues

39A.2.1 Focusing Effect

Lower plenum debris bed configurations with a thin metallic layer on top of a molten oxide pool are postulated to produce a focusing effect in the metal layer (reference 2) that can fail the reactor vessel. A large mass of metal incorporated into the lower plenum debris bed thickens the metal layer and distributes the metal pool heat load over a larger area of the vessel wall, thus reducing the heat flux. The stainless steel of the lower support plate and core shroud, when incorporated in the debris pool before lower head debris dry out, will mitigate the focusing effect in the AP1000. This analysis will address the timing of lower plenum debris contacting the lower support plate and the potential for a large heat loading to the vessel wall from a thin metal layer.

39A.2.2 Material Interaction

References 39A-3, 4 and 5 identify potential debris interactions that could impact the formation of the lower head debris bed. This analysis considers the potential for interaction between molten zirconium and oxide debris as the core melt progresses in the AP1000 reactor vessel geometry.

39A.3 AP1000 Reactor Vessel Lower Internals Geometry

The initial lower internal geometry is presented in Figure 39A-1. The AP1000 reactor vessel has an inside diameter of 157 inches (4 m) and a hemispherical lower head (inside radius of 2 m). The vessel bottom head is 6 inches (15 cm) thick and the vessel wall is 8 inches (20 cm) thick.

The AP1000 core is comprised of 157 14-ft (4.27 m) 17x17 fuel assemblies. The bottom of the active fuel is 2 meters above the inside bottom of the reactor vessel. The flow area through the core is 3.88 m^2.

The core is surrounded by a 7/8-inch (2.2 cm) thick core shroud (Figure 39A-2). The shroud panels conform tightly to the outside perimeter of the core. The shroud supporting structure is comprised of a top plate and a bottom plate, six 12.5 in (32 cm) high ring assemblies spaced 12.5 in (32 cm) apart vertically and radial ribs that tie the panels to the rings. The core shroud sits inside the cylindrical core barrel. The core barrel has an inner diameter of 133.75 inches (3.4 m) and is 2 inches (5.1 cm) thick. The volume between the core barrel and the core shroud has a cross-sectional area of 1.5 m^2. The lower core support plate is welded to the bottom of the core barrel and the core barrel hangs from the flange of the reactor vessel.

The 15-inch (38.1 cm) thick lower core support plate supports the core and the shroud. The support plate is welded to the 2 inch (5.1 cm) thick core barrel that hangs from the flange of the reactor vessel. The bottom of the support plate is nominally 55.3 inches (1.4 meters) above the inside bottom of the vessel. Four radial keys are welded to the support plate to prevent the support plate from moving radially and give the lower support plate a total outer diameter of 148.25 in (3.77 m). An energy absorber structure is present in the lower plenum to support the lower support plate from below if it drops. The energy absorber is mounted to the bottom of the lower support plate and nominally sits 1 inch (2.54 cm) above the bottom of the lower head.

A detail of the bottom of the shroud and support plate is presented in Figure 39A-3. The bottom plate of the core shroud is 4-inch thick stainless steel that rests on the support plate. It has sixteen 0.781-inch diameter holes through the lower plate that provide cooling flow to the shroud/barrel annulus (core bypass flow). The flow is directed from the region below the core between the lower core support plate and the bottom of the active fuel. The masses of the reactor vessel lower internal components are presented in Table 39A-1.

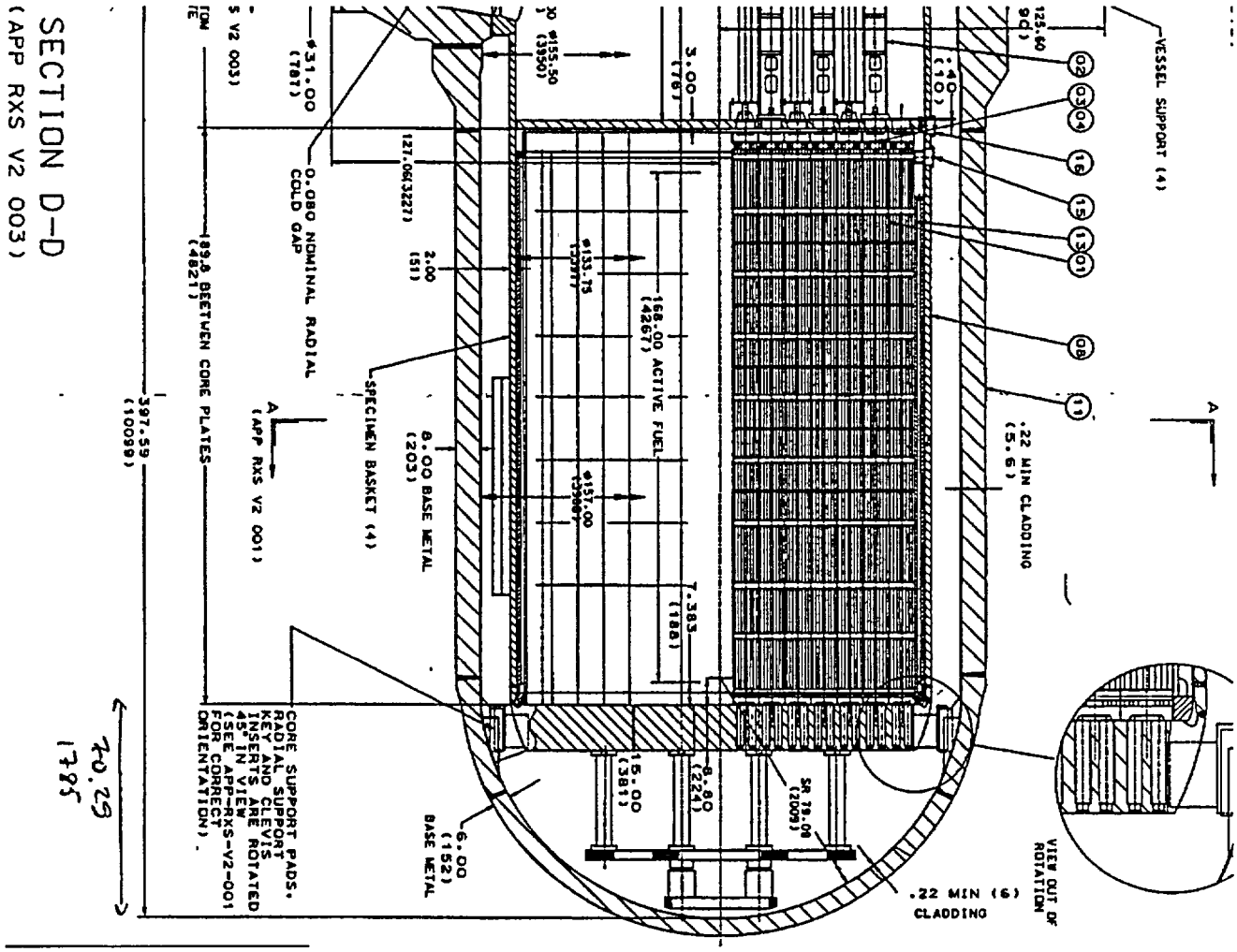

Figure 39A-1 – AP1000 RPV, Core and Lower Internals

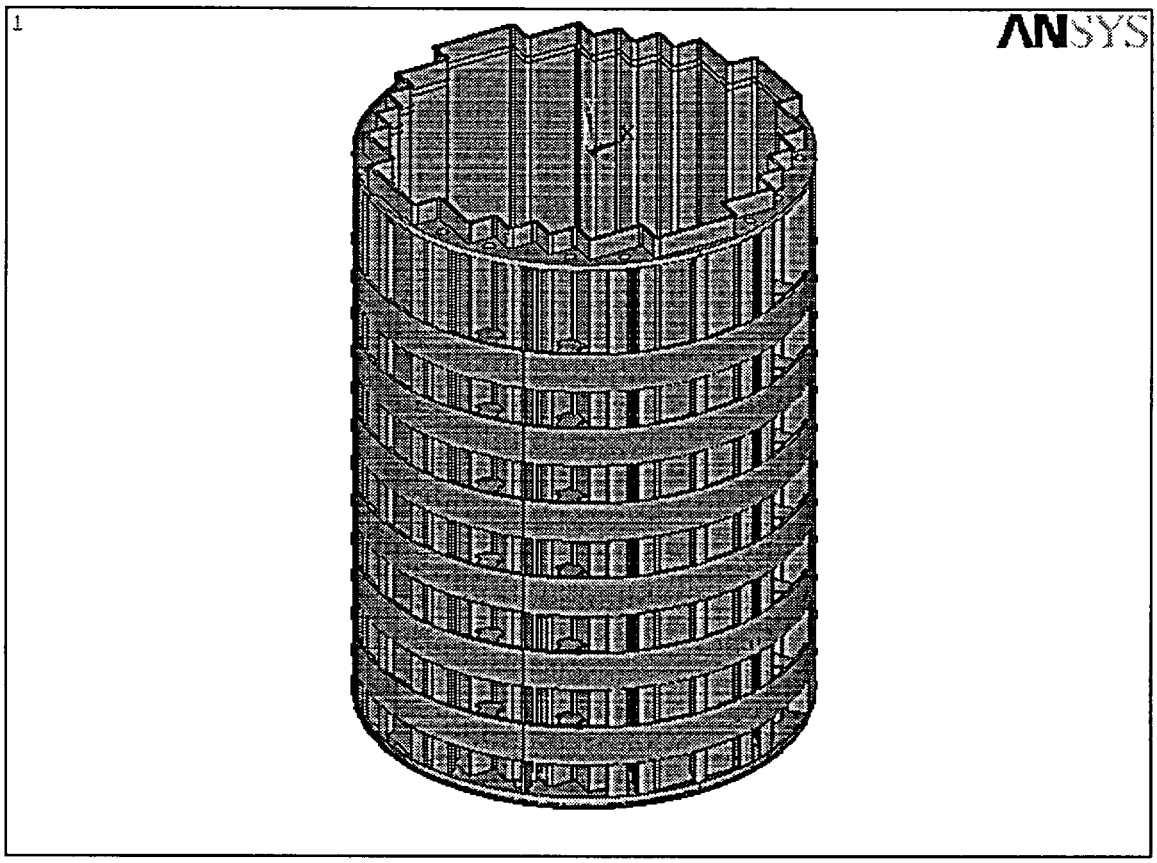

Figure 39A-2 Core Shroud

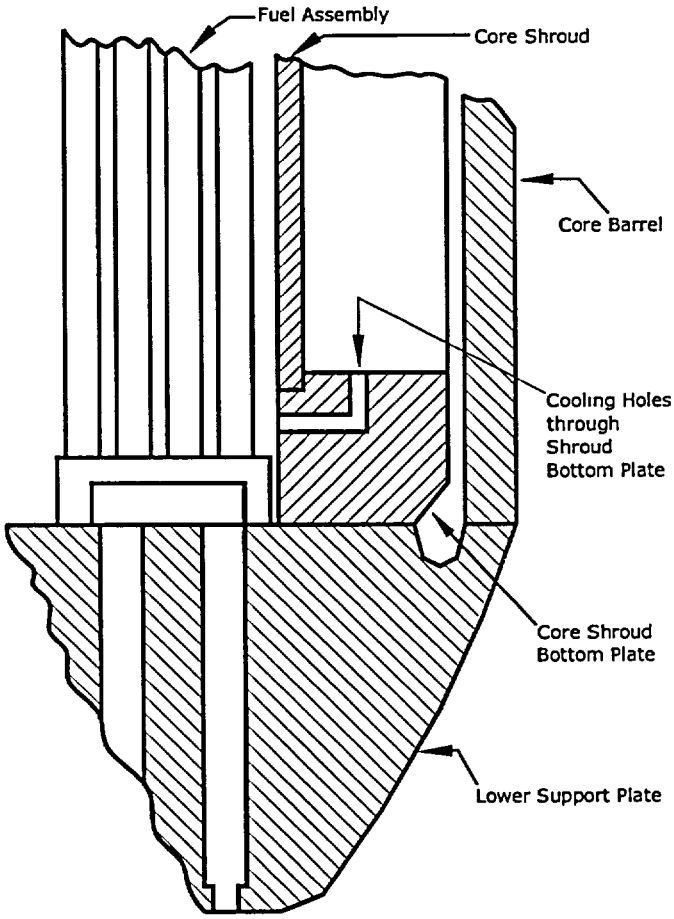

Figure 39A-3 – Bottom of Core Shroud, Core Barrel and Lower Core Support Plate (not to scale)

Table 39A-1

CORE AND LOWER INTERNALS MATERIAL INVENTORIES IN THE AP1000 REACTOR VESSEL

Component	Material	Mass (kg) x 10^{-3}	Volume (m^3)[1]
Core			
Fuel	UO_2	95.9	10.97
Active Core Cladding	Zircaloy	17.9	2.92
Additional Zirconium[2]	Zircaloy	4.8	0.78
Control Rods	Silver/Indium/Cadmium	3.9	0.58
Lower Internals (below top of active fuel)			
Core Barrel	Stainless Steel	19	2.7
Lower Support Plate[3]	Stainless Steel	25	3.4
Core Shroud	Stainless Steel	12	1.7
Shroud Support Structure	Stainless Steel	9	1.3
LP Energy Absorber	Stainless Steel	3	0.4

Notes:
1. In liquid state
2. Including zircaloy plugs at lower end of fuel rods
3. Including the lower nozzles of the fuel assemblies

39A.4 Modeling of the Core and Reactor Vessel Lower Internals Heatup

39A.4.1 MAAP4 Model

The MAAP4 code is used to investigate core uncovery and heatup in the AP1000 accident sequence. The MAAP4 code models the uncovery, melting, relocation, freezing of the fuel. It models the in-vessel debris pool formation and predicts the failure of the crust. It tracks the amount of sensible and decay heat in the debris and accounts for the release of fission products from the fuel, which decreases the decay power density in the debris.

For the MAAP4 analysis, the active core region is partitioned into 90 nodes (15 axial rows by 6 radial rings). The unfueled region below the core is modeled with 4 axial rows representing (from bottom up) the core support plate, the fuel assembly nozzles, the fuel rod zirconium plugs, and the lower plenum of the fuel rods. The unfueled region above the active core is modeled with one axial row.

Two axial power profiles are modeled: top-skewed and chopped-cosine (Figure39A-4). The radial power profile is relatively flat and is shown in (Figure39A-5).

The MAAP4 code models the core initially as a solid cylinder and the core shroud and core barrel together as one lumped stainless steel cylindrical heat sink surrounding the core. The vessel wall is a second carbon steel cylindrical heat sink surrounding the core shroud/barrel heat sink.

The MAAP4 modeling is not capable of fully modeling the complexities of the actual shroud/barrel geometry, which is not lumped, and is not a concentric cylinder around the core. The behavior of the core melting and relocation is insensitive to the heat sink modeling, but the response of the core shroud and barrel to the core melt is difficult to accurately model with the lumped cylindrical model. In the AP1000 MAAP4 model in this analysis, the core shroud/barrel heat sink was set up to conserve the total radial heat capacity and mass of the actual shroud and barrel. The mass of the core shroud panels and supporting structures in the active fuel region of the core is 17650 kg. The mass of the core barrel in the active fuel region of core is 18320 kg. Therefore, the total mass of the shroud and core barrel together provides a heat sink mass of 35970, or 2400 kg per each of the 15 axial rows of nodes in the active core model. The inside radius of the heat sink model is set to be 1.648 m (ID = 129.75 inches). The actual inside radius is 133.75 inches. The modeled radius maintains the outer radius of the core barrel (OD = 137.75 in), but makes the total thickness of the heat sink 4 inches. The increased thickness over the actual total thickness of 2.875 inches increases the thermal resistance of the heat sink model due to thermal conductivity, however it cannot completely account for the total thermal resistance due to the radiation heat transfer between the shroud panel and the core barrel.

39A.4.2 Finite Difference Modeling

To overcome the limitations of the MAAP4 code in the modeling of the core shroud and barrel, an additional analysis of the core heat up was performed using a finite difference model of the core. The finite difference model captures the geometric characteristics of the reactor vessel internals. The major limitation of the finite difference model is that the melting, relocation and freezing of the core cannot be modeled, so care must be taken to use the results conservatively. The model makes assumptions with respect to the oxidation energy input to the cladding and neglects steam cooling due to the boiling in the lower region of the core. However, all the sequences are at low pressure and the steaming rate is low during the core melting phase of the accident sequence when the core is uncovered, so the amount of steam cooling is limited.

The results of the finite difference model (see Figures 39A-6 and 39A-7), along with the MAAP4 results form the basis of the AP1000 core and lower internals heat up and melting calculation.

39A.4.3 Relocation of the In-Core Debris to the Lower Plenum

An analysis of the molten pool relocation to the lower plenum was performed using the methodology from reference 39A-1 to calculate the progressive melting of the core barrel and using initial conditions defined from the finite difference calculation.

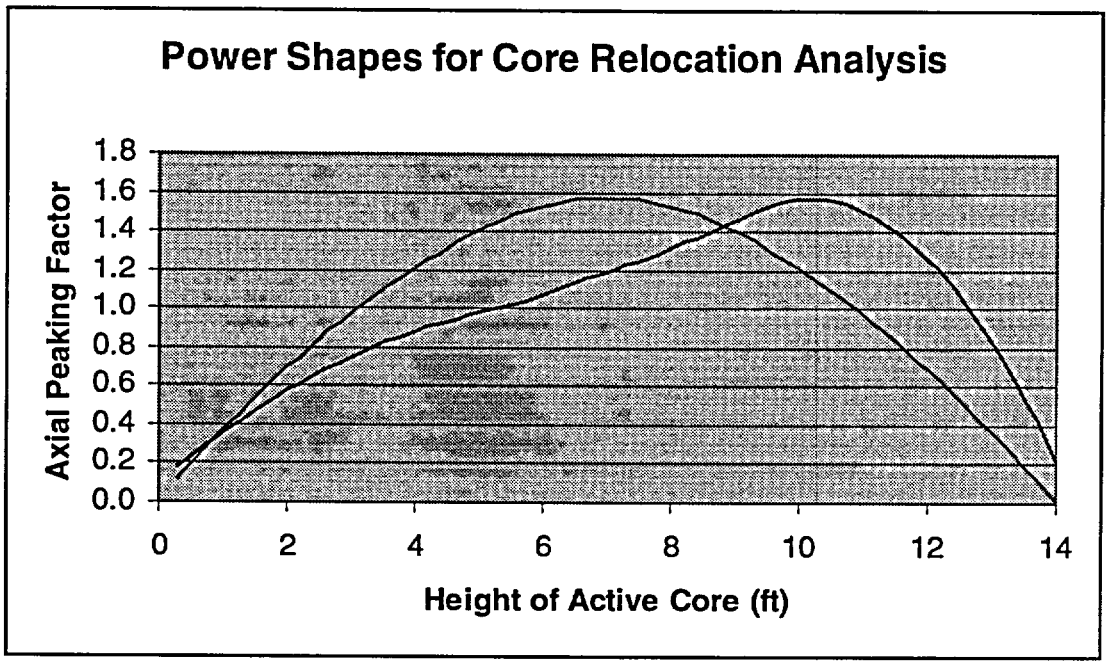

Figure 39A-4 – Axial Power Shapes Used for Core Relocation Analysis

	1	2	3	4	5	6	7	8
1	0.691	0.755	0.913	0.938	0.923	1.230	1.161	0.802
2	0.755	0.953	0.953	0.844	1.113	1.176	1.021	0.640
3	0.913	0.953	1.001	1.002	1.069	1.235	1.014	
4	0.938	0.844	1.002	0.934	1.176	1.235	0.746	
5	0.923	1.113	1.069	1.176	1.288	0.867		
6	1.230	1.176	1.235	1.235	0.867			
7	1.161	1.021	1.014	0.746				
8	0.802	0.640						

Ring	1	2	3	4	5	6
# of Asmb	1.25	8	8	11	4	7
Area Fraction	0.032	0.204	0.204	0.280	0.102	0.178
Radial Peaking Factor	0.742	0.915	1.038	1.158	1.018	0.758

Figure 39A-5 - Radial Power Shape Used for Core Relocation Analysis

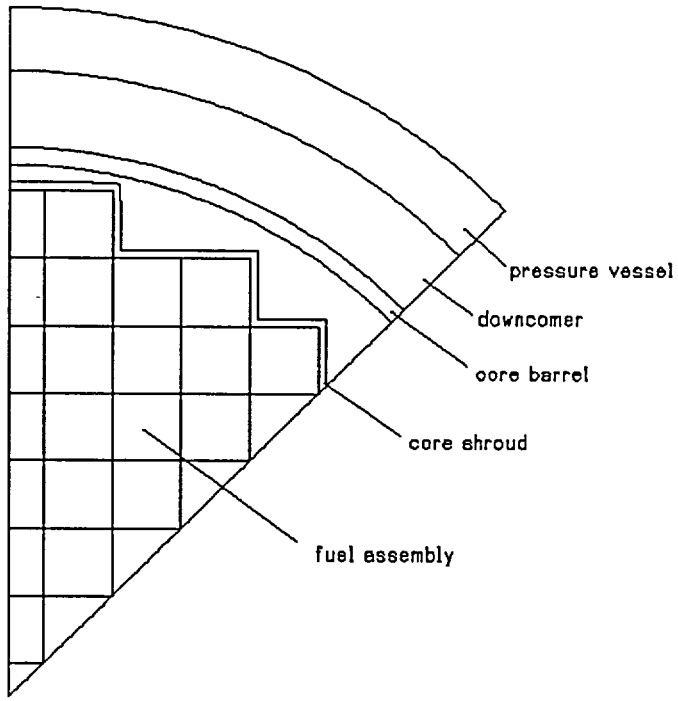

Figure 39A-6 - Cross Section Geometry of the Finite Difference Computational Model

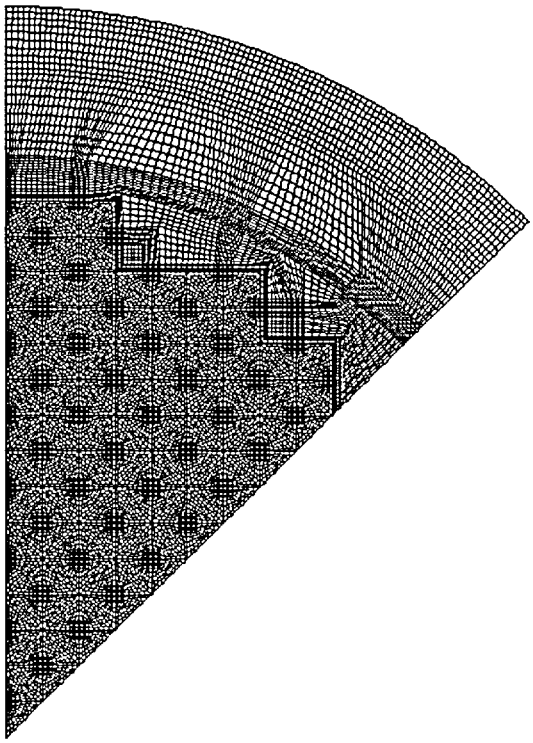

Figure 39A-7 - Computational Mesh for the Finite Difference Computational Model

39A-5 The Base Core Damage Sequence for IVR

The limiting core damage accidents for heat transfer from the core debris to the vessel wall are sequences that progress to core damage quickly and do not reflood the core debris inside the reactor vessel. Due to decay heat considerations, the accident that proceeds the most quickly to core melting and relocation is conservative. Water cooling of the core and any core debris extends the time of the core melting, potentially arrests the relocation and significantly limits the heat flux to the vessel wall from relocated debris.

IVR sequences are assumed to have successful RCS depressurization through at least two of four stage 4 ADS valves to reduce stresses on the reactor vessel wall and successful reactor cavity flooding to submerge the vessel. Therefore, the base core damage sequence is initiated by a large LOCA. The reactor coolant system is depressurized, but the failure of the gravity injection leads to core melting early in the accident sequence. In the scenario, the cavity is flooded manually by the operator after the core-exit gas temperature exceeds 1200°F, as instructed by the functional restoration guidelines. The vessel is not reflooded through the break.

This type of accident sequence is classified as accident class 3BE in the AP1000 PRA. Typically a large loss of coolant accident will reflood the core when the water level in the containment submerges the break. The largest LOCA that can reasonably be postulated with no reflooding is a spurious actuation of a stage 4 ADS valve. The ADS-4 valves have a large flow area from the reactor coolant system to the containment and open to an elevation above the maximum water level in the containment, thus preventing vessel reflooding. Therefore, the sequence timing that is considered in this analysis is based on an accident initiated by the spurious opening of a stage 4 ADS valve that proceeds to an accident class 3BE severe accident. This sequence will provide the conservatively fastest timing for establishing a lower plenum debris pool.

The MAAP4 results for the IVR base case for the top-skewed power shape case are presented in Figures 39A-8 through 16 and for the chopped cosine power shape case in Figure 39A-17 through 25.

MAAP4 AP1000 Core Melting and Relocation, Top-Skewed Power Shape
RCS Pressure

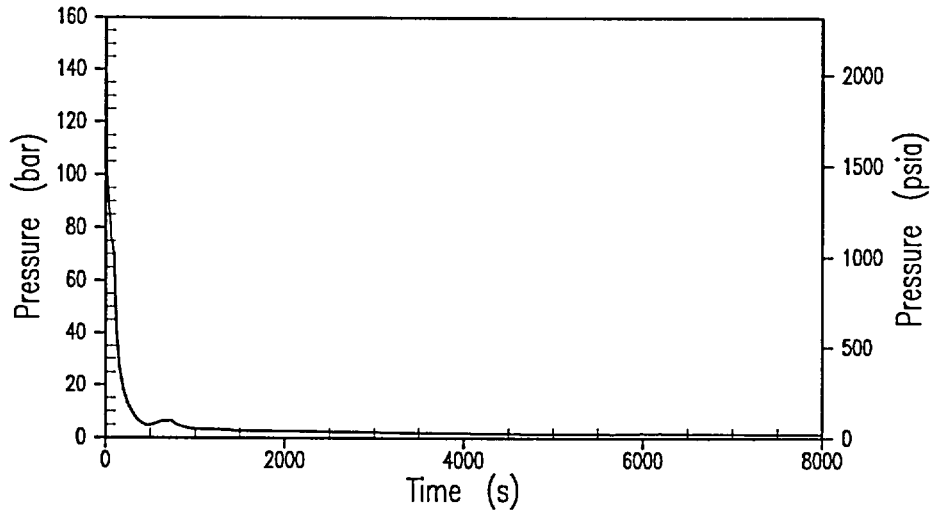

Figure 39A-8

MAAP4 AP1000 Core Melting and Relocation, Top-Skewed Power Shape
Containment and RCS Pressure

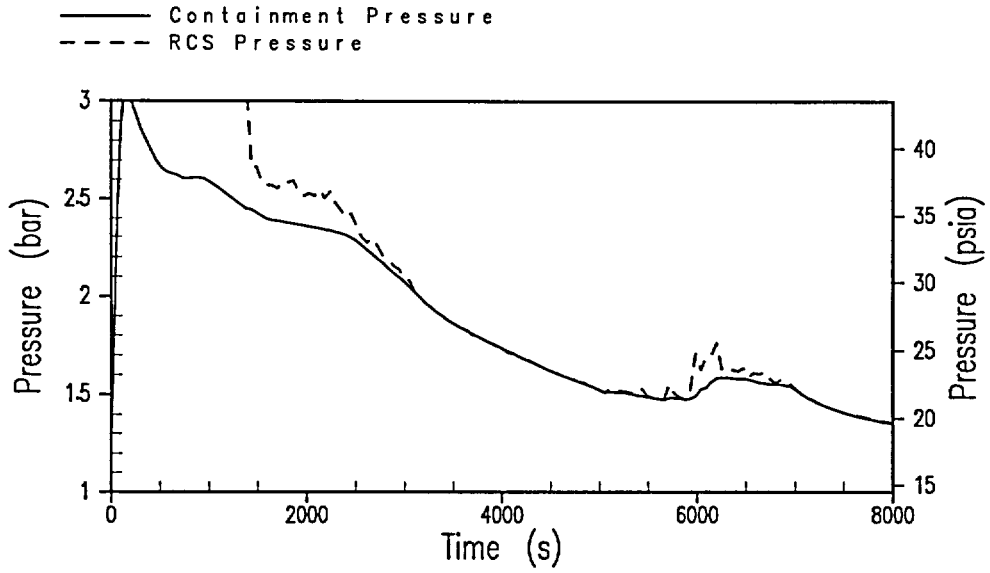

Figure 39A-9

MAAP4 AP1000 Core Melting and Relocation, Chopped Cosine Power Shape
Reactor Vessel Mixture Level

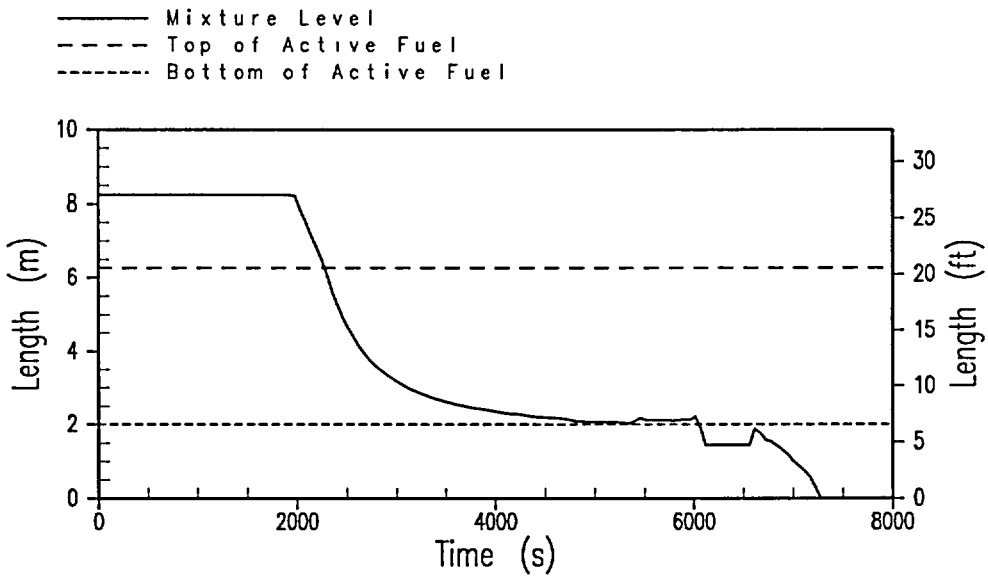

Figure 39A-10

MAAP4 AP1000 Core Melting and Relocation, Top-Skewed Power Shape
Hottest Temperature in Core

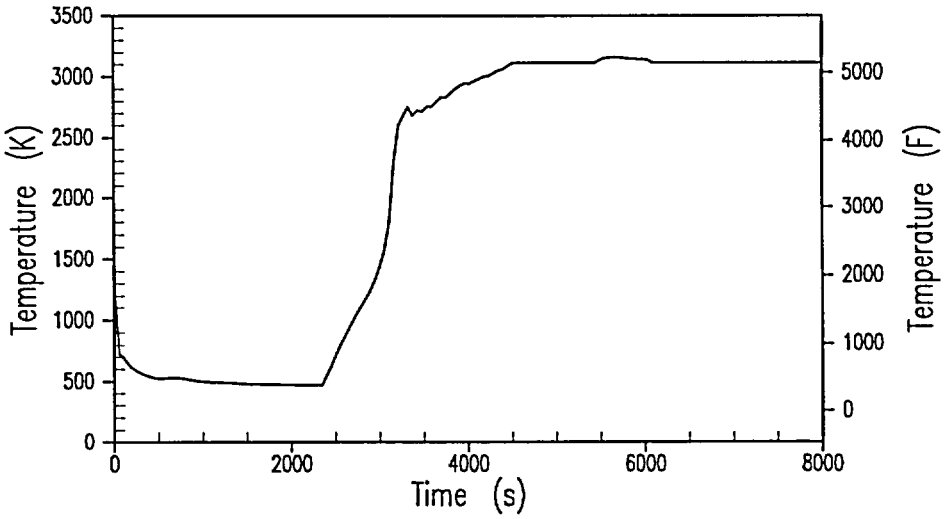

Figure 39A-11

MAAP4 AP1000 Core Melting and Relocation, Top-Skewed Power Shape
Mass of Hydrogen Generated in Core

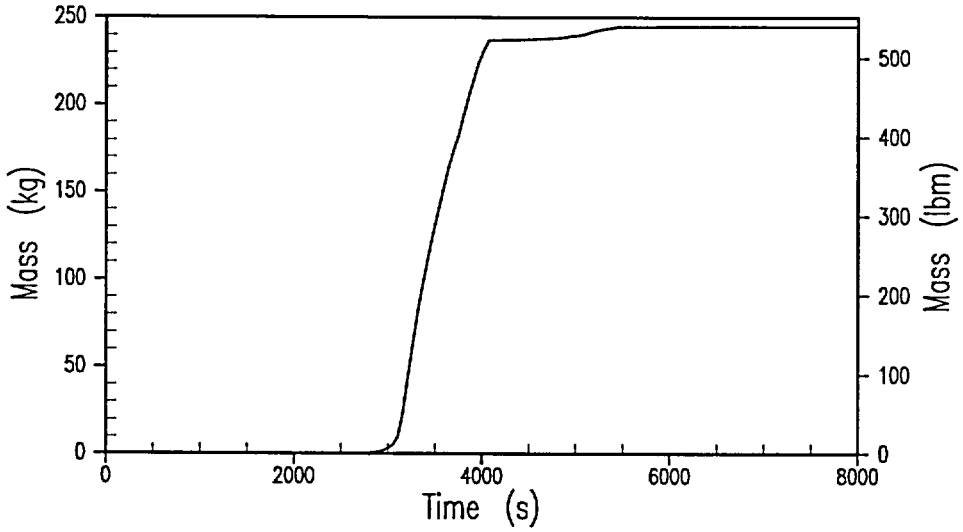

Figure 39A-12

MAAP4 AP1000 Core Melting and Relocation, Top-Skewed Power Shape
Temperature of Core Shroud/Barrel (Core Elev. 1.7 – 2.0 m)

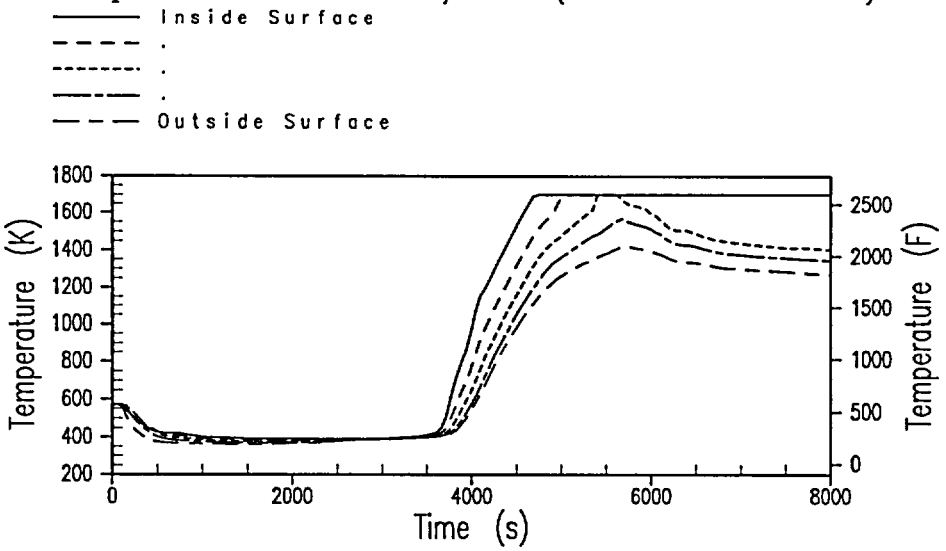

Figure 39A-13

MAAP4 AP1000 Core Melting and Relocation, Top-Skewed Power Shape
Temperature of Core Shroud/Barrel (Core Elev. 2.0 – 2.3 m)

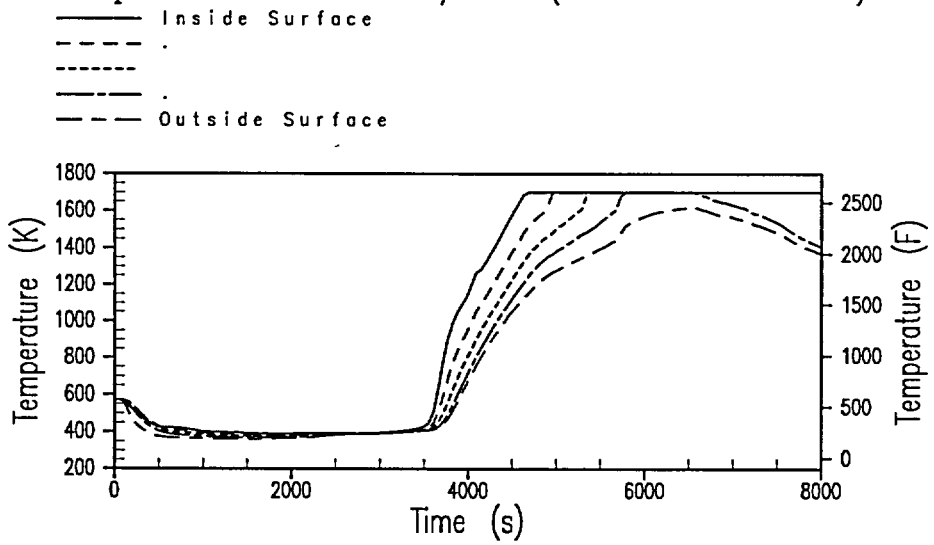

Figure 39A-14

MAAP4 AP1000 Core Melting and Relocation, Top-Skewed Power Shape
Mass of Core Shroud/Barrel

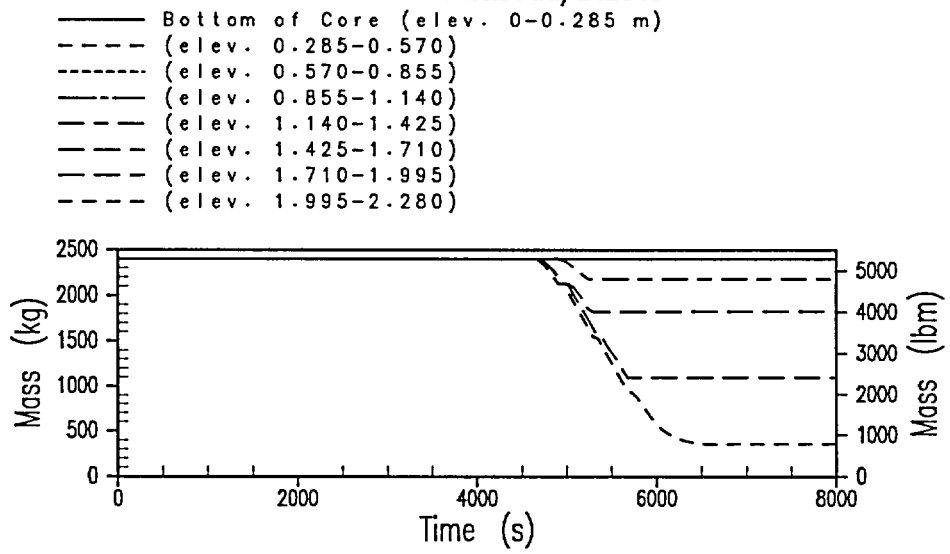

Figure 39A-15

MAAP4 AP1000 Core Melting and Relocation, Top-Skewed Power Shape
Volume of Debris in Reactor Vessel Lower Plenum

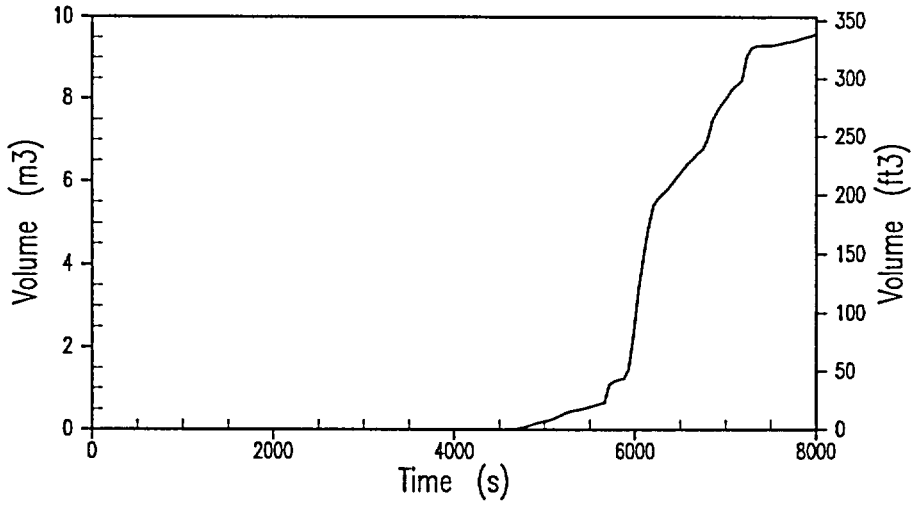

Figure 39A-16

MAAP4 AP1000 Core Melting and Relocation, Chopped Cosine Power Shape
RCS Pressure

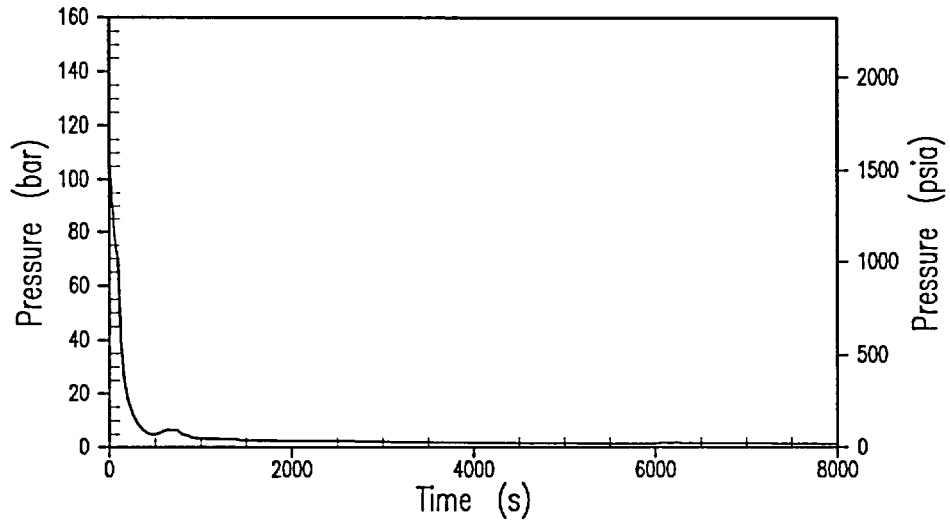

Figure 39A-17

MAAP4 AP1000 Core Melting and Relocation, Chopped Cosine Power Shape
Containment and RCS Pressure

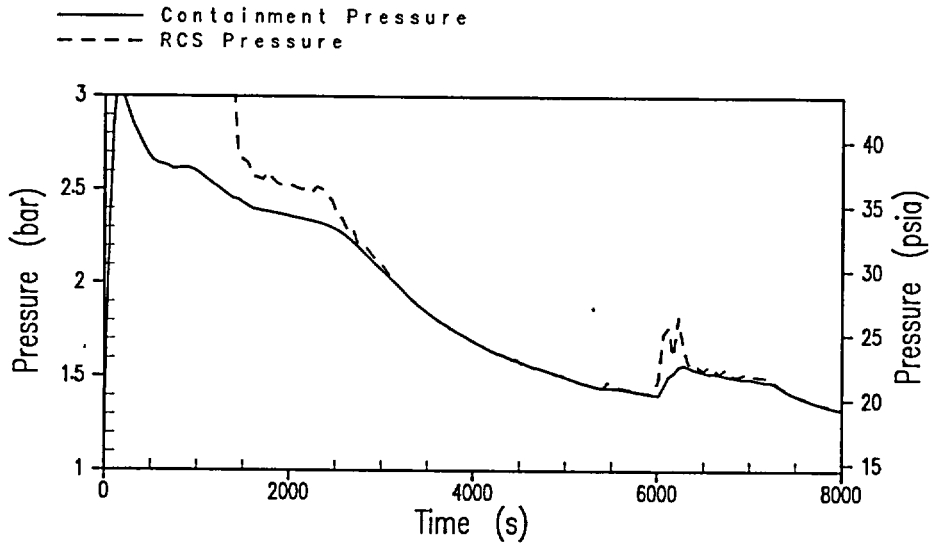

Figure 39A-18

MAAP4 AP1000 Core Melting and Relocation, Chopped Cosine Power Shape
Reactor Vessel Mixture Level

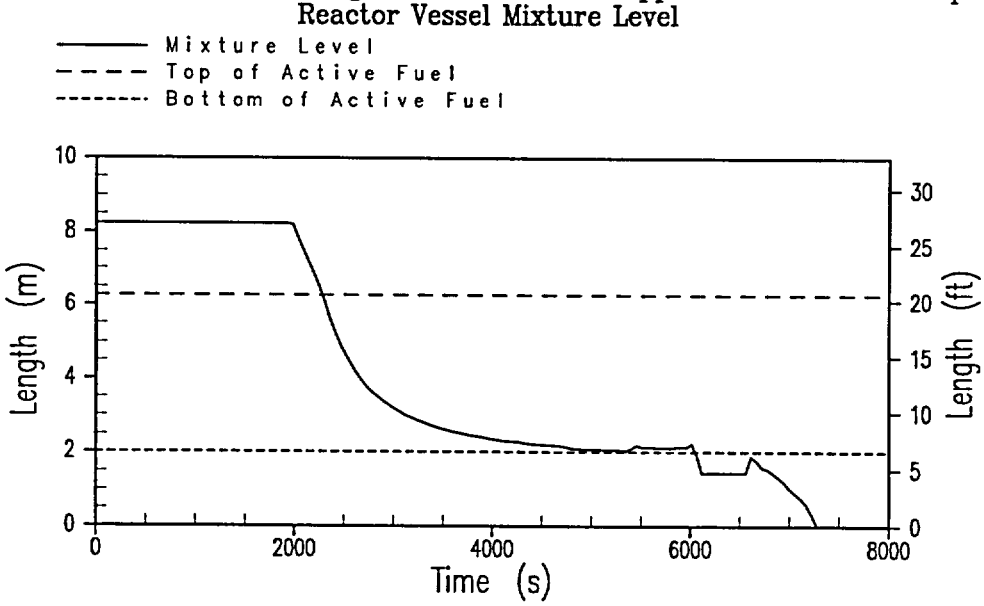

Figure 39A-19

MAAP4 AP1000 Core Melting and Relocation, Chopped Cosine Power Shape
Hottest Temperature in Core

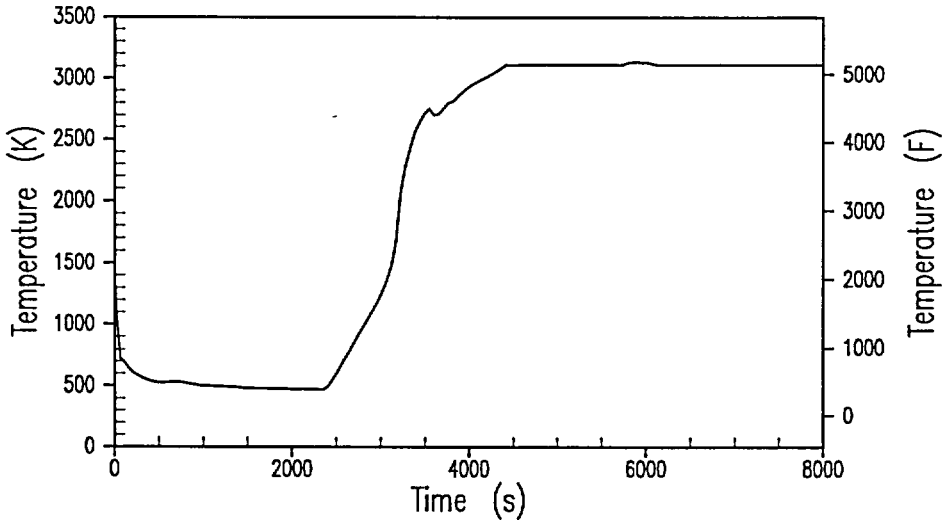

Figure 39A-20

MAAP4 AP1000 Core Melting and Relocation, Chopped Cosine Power Shape
Mass of Hydrogen Generated in Core

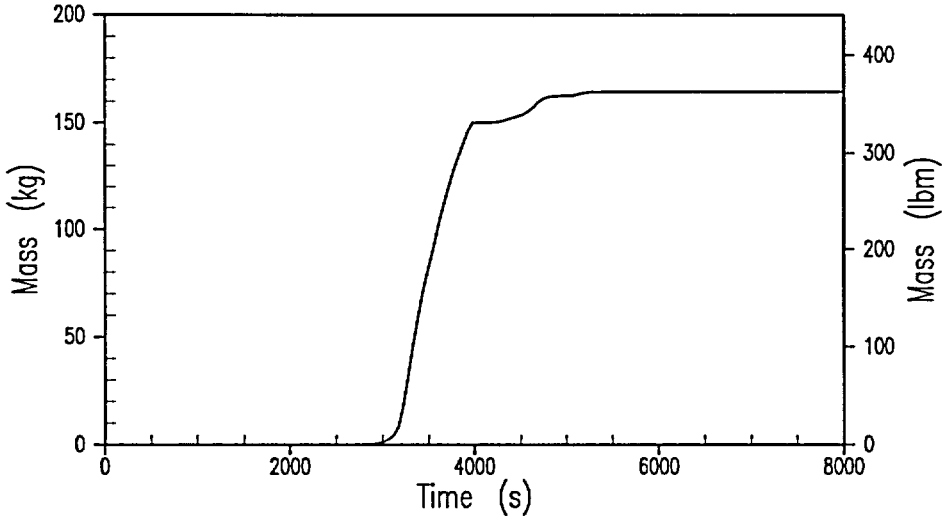

Figure 39A-21

MAAP4 AP1000 Core Melting and Relocation, Chopped Cosine Power Shape
Temperature of Core Shroud/Barrel (Core Elev. 1.1 – 1.4 m)

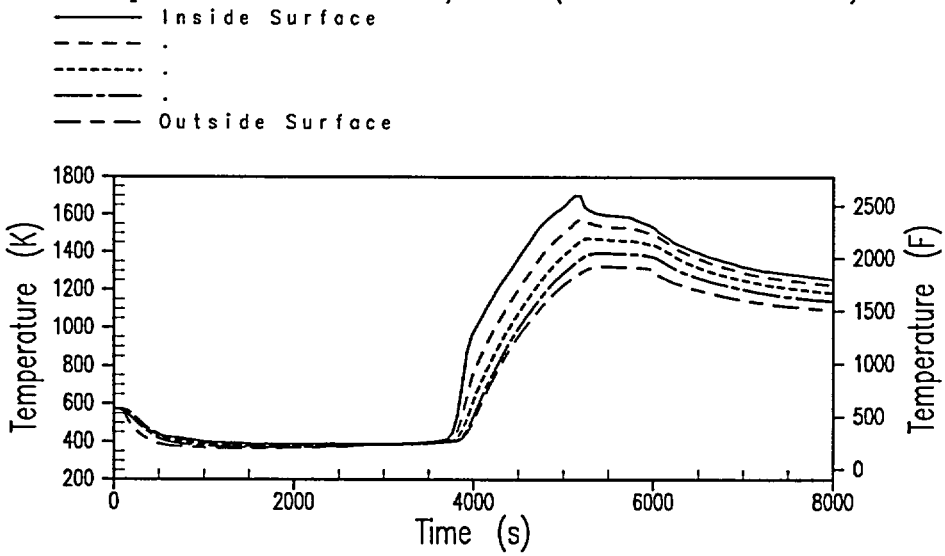

Figure 39A-22

MAAP4 AP1000 Core Melting and Relocation, Chopped Cosine Power Shape
Temperature of Core Shroud/Barrel (Core Elev. 1.4 – 1.7 m)

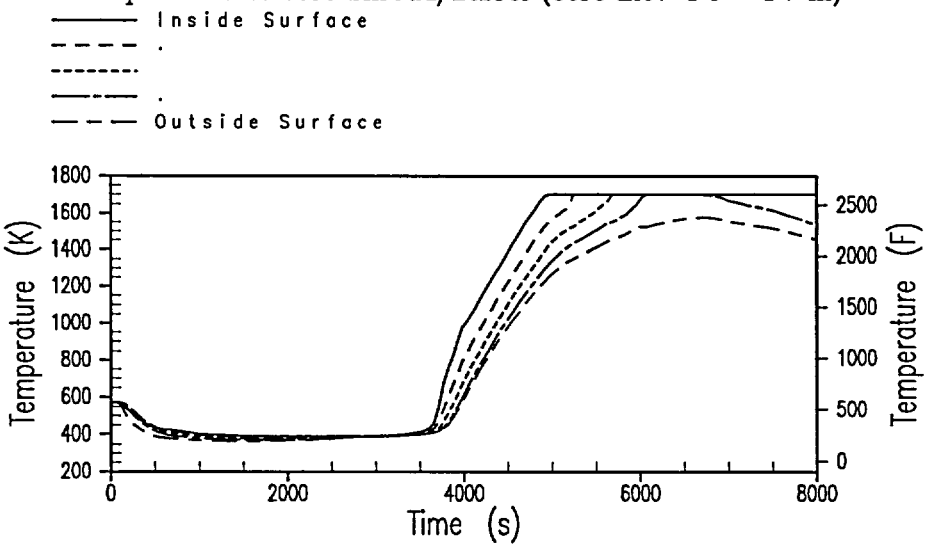

Figure 39A-23

MAAP4 AP1000 Core Melting and Relocation, Chopped Cosine Power Shape
Mass of Core Shroud/Barrel

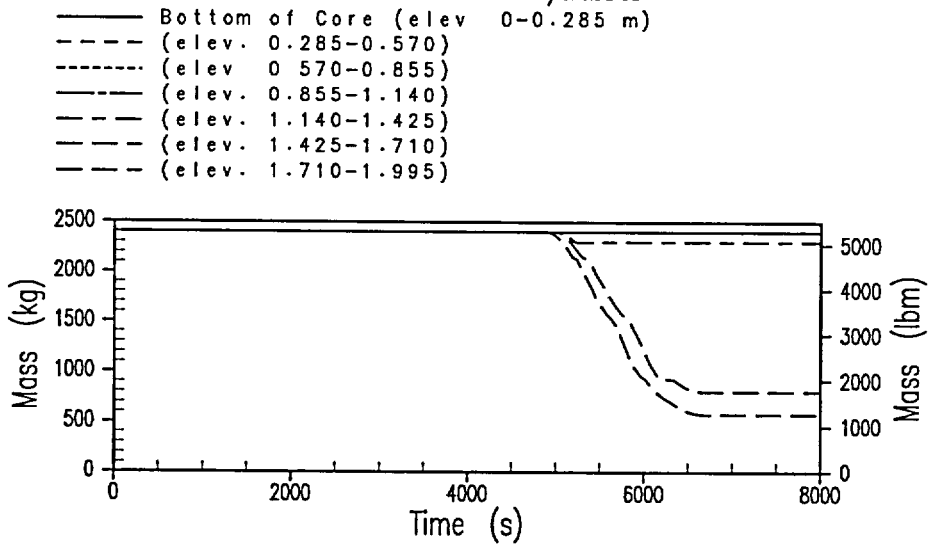

Figure 39A-24

MAAP4 AP1000 Core Melting and Relocation, Chopped Cosine Power Shape
Volume of Debris in Reactor Vessel Lower Plenum

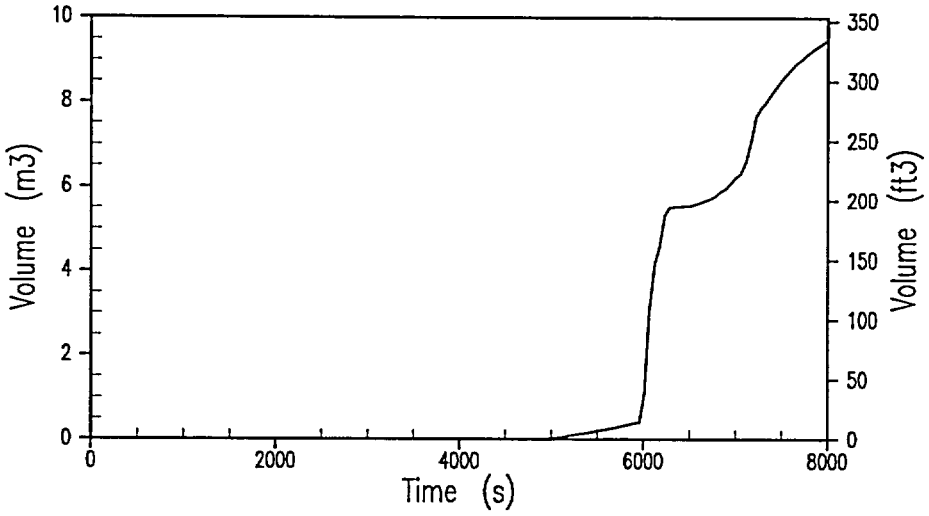

Figure 39A-25

39A.5.1 Core Heat Up and the Formation of the In-Core Molten Debris Layers

The purpose of the analysis of the in-core molten pool formation is to determine the composition, volume and power density of the debris that can relocate to the lower head and the timing of the relocation. The lower plenum debris pool needs to contact the lower support plate to melt it and thus include sufficient metal in the debris to mitigate the focusing effect. Therefore, the less initial mass that can relocate is conservative.

Based on the results of the MAAP4 code, the top of the active fuel uncovers at 2300 seconds after the initiation of the accident. The uncovered portion of the core begins to heat up from the decay heating of the fuel and the vessel mixture level continues to decrease, uncovering more of the core. Oxidation of the zircaloy cladding begins at 3000 seconds, signaling the onset of core damage and causing the core to heat up more rapidly. Unoxidized cladding and other metals in the core (such as control rod material) melt first and drain downward to the cooler regions of the core and refreeze where the temperature is less than the metal melting temperature, ~1600 to 2100°K. The melting and draining of the metal is followed by the melting of the uranium dioxide fuel and oxidized cladding, which has a much higher melting temperature, 2850 to 3100°K.

Based on the MAAP4 analyses, at the time of the onset of core damage, the water/steam mixture level in the reactor vessel is 1 m above the bottom of the active fuel (3 m above the inside bottom of the vessel). The core temperature below this elevation is initially low due to the water-cooling and the heatup rate is relatively slow because the power density of the fuel and cladding oxidation rates are lower in this region. Thus 1 m above the bottom of the active fuel is considered to be the highest elevation in the core where the bottom of the in-core molten debris pool with a refrozen oxide crust will form. The high pool assumption is conservative with respect to the mass of debris available for the initial relocation to the lower plenum.

At the time of the onset of oxidation in the core, the mass of water in the core region between the bottom of active fuel and the top of the mixture level is 1840 kg, considering an average void fraction of 0.5. If 100 percent of this water reacts with cladding, the maximum cladding oxidation is 26 percent of the cladding in the active core region, or 34% of the cladding above the initial water level.

The metal control rods and unoxidized zirconium in the core melt first, and drain downward into the cooler regions of the core below 1 meter, and continue to melt and drain as the lower regions uncover and heat up. The molten metal eventually refreezes at the top of the support plate, in the fuel assembly bottom nozzles, and bottom of the fuel rods, which are unfueled, water-cooled, and have a significant heat sink mass. Assuming maximum cladding oxidation, the total mass of unoxidized zirconium in the active core is 13265 kg, or 2.2 m^3 of zirconium. The control rod material has a

volume of 0.59 m^3. The cross-sectional flow area of the intact core is 3.88 m^2. The volume between the top of the lower support plate the bottom of the active fuel has a height of 0.2 meters and a total volume of 0.8 m^3. Therefore, the height of the metal blockage extends 54 cm above the bottom of the active core.

The fuel assemblies on the periphery of the core are cooled by radiation heat transfer to the shroud and core barrel and have a lower than average power density. The finite difference model predicts that a significant fraction of these peripheral fuel assemblies are coolable, and thus do not participate in the initial pool formation. Based on the finite difference calculation, it is assumed that half of the mass of the peripheral assemblies above the bottom of the in-core pool does not melt, and is held up from participating in the initial relocation of molten debris.

The sideward crust of the molten pool is expected to form in these outermost fuel assemblies of the core. The crust contains the debris and prevents debris relocation until the in-core debris pool develops superheat to melt the sideward crust. Given the maximum cladding oxidation, and assuming that half of the peripheral fuel assembly UO_2 or ZrO_2 melts initially, the total mass of the oxide that melts to form the molten oxide pool and crust is 72600 kg.

The height from the top of the metal blockage to the bottom of the in-core pool at 1 meter is 48 cm. The total volume fills with molten oxide, which refreezes 15700 kg of oxide material to form the bottom crust of the in-core debris pool.

When the crust fails, the molten debris drains to the volume between the core shroud and barrel (Figure 39A-26), filling the volume and draining any molten metal from the top of the in-core debris pool. The small bypass flow area through the shroud bottom plate is plugged with metal that melted from the shroud and barrel and froze in the holes. The outlets of the bypass holes are plugged with metal frozen below the active core. This "pocket" volume between the shroud and core barrel has a cross sectional area of 1.5 m^2 and will fill with debris from the molten pool. The pocket volume is initially filled with 0.35 m^3 of structure and approximately 5000 kg molten stainless steel from the melting of the shroud and core barrel during the melting (based on MAAP4 results). The volume of oxide debris that relocates into the "pocket" between the shroud and barrel is 0.7 m^3 and holds up 5730 kg of oxide.

Therefore, 51772 kg of oxide with a volume of 6.1 m^3 is molten and available to form the superheated oxide pool and participate in the initial relocation to the lower head.

The time that it takes to form the molten debris pool is estimated from the decay heat and the oxidation energy and the mass of the zirconium, UO_2 and zirconium. An adiabatic heat up calculation of the time to melt this fraction of the core is 2575 seconds. Added to the average uncovery time of 2650 seconds, the time is 5225 seconds. Based on the results of the finite difference calculation, the minimum time

that 50% of the core UO_2 is melted is 6000 seconds. The MAAP4 model predicts the relocation of approximately 6 m^3 of molten debris to the lower plenum to occur at approximately 6000 seconds. Therefore, the crust failure is predicted to occur at 6000 seconds after accident initiation or 3000 seconds after the onset of core damage.

At 6000 seconds, the power density of the oxide debris in the pool is 2.9 MW/m^3 assuming the top-skewed power shape and ANS 79 decay heat + 2 sigma uncertainty. The power density in the molten debris considers the loss of the decay heat contained in volatile fission products released from the fuel (reference 2), which is 27.5% of the total decay heat at 6000 seconds after scram. The fraction of volatile fission product that are released from the debris as taken from reference 2 is conservative with respect to the releases of barium and strontium from the debris, which can release an addition 10% of the decay heat from the oxide.

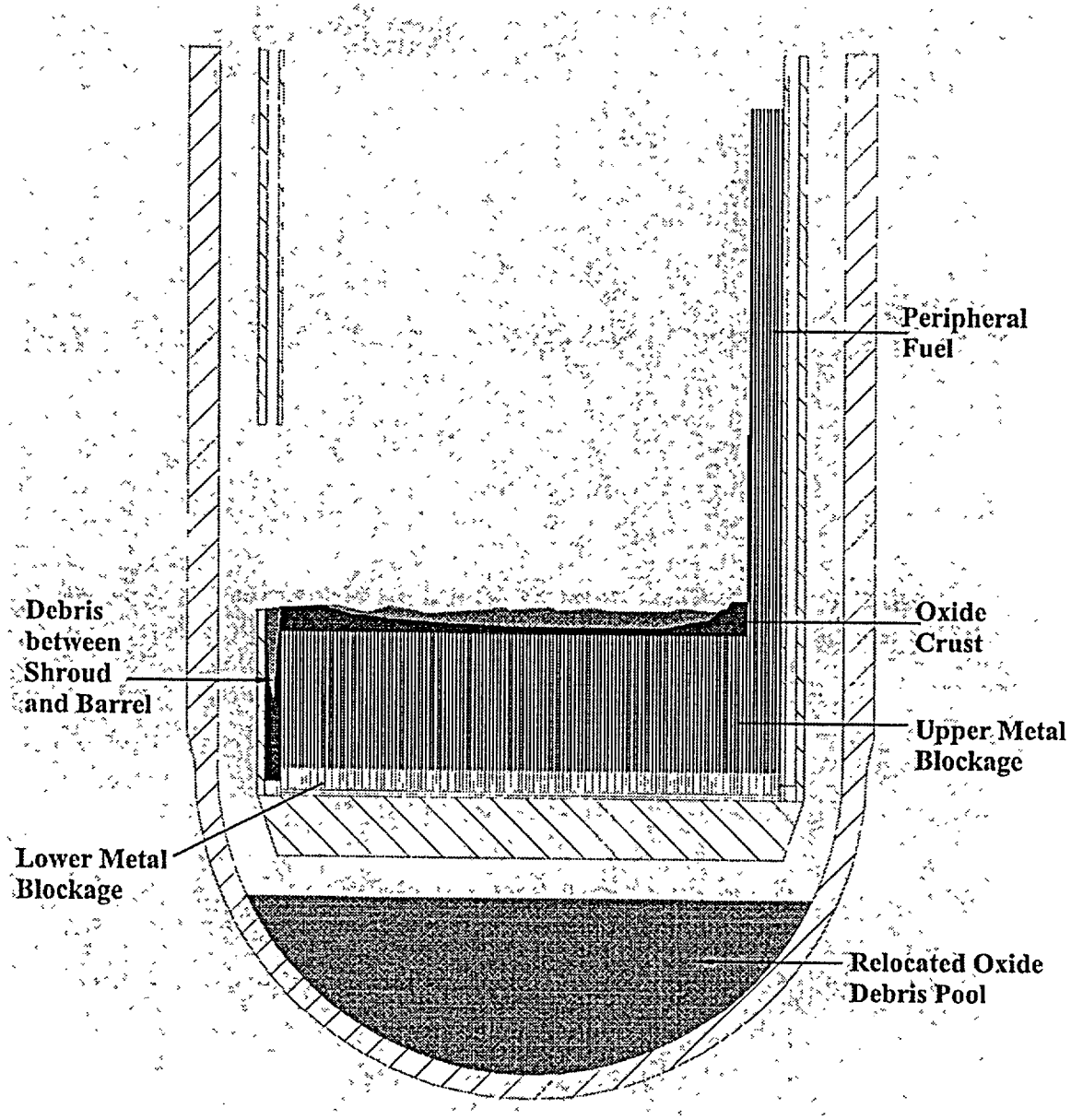

Figure 39A-26 – Initial Oxide Relocation to the Lower Plenum

39A.5.2 Melting of the Core Shroud and Core Barrel

The AP1000 core shroud and core barrel are predicted to sustain significant damage in the elevations at the top of the in-core pool after core uncovery and during the melting and relocation prior to the crust failure. The finite difference calculation in the region above where the molten debris pool is expected to form predicts that the core shroud melts before the UO_2 starts melting (Figure 39A-27 and Figure 39A-28) and that the core barrel melts significantly at the same elevation soon after the UO_2 melting begins.

The MAAP4 modeling also predicts that the core shroud melts at the 1.5 to 2 meter elevations in the core (Figure39A-28), but later in time than the finite difference model. At the time that MAAP4 predicts the debris to relocate to the lower plenum, the mass of the shroud and much of the core barrel has melted away. The remaining mass equates to a core barrel thickness of approximately 0.5 inches, with the inner surface temperature at the melting temperature of the stainless steel and the outer surface temperature at approximately 1500°K (2300°F).

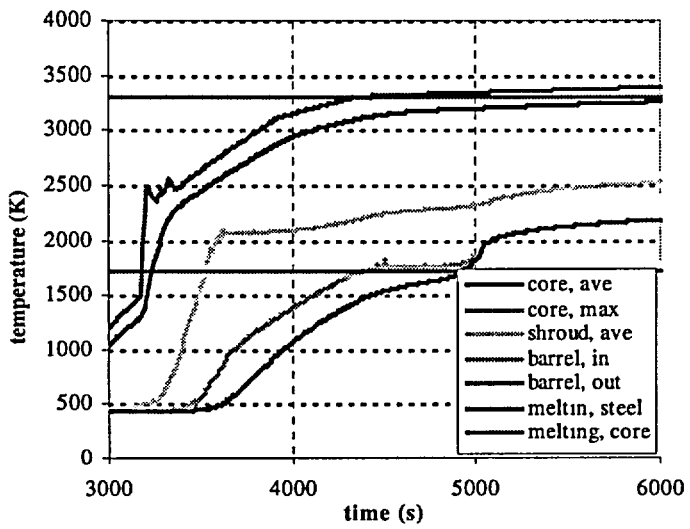

Figure 39A-27 - Finite Difference Result for Top-Skewed Power Shape at Level 5

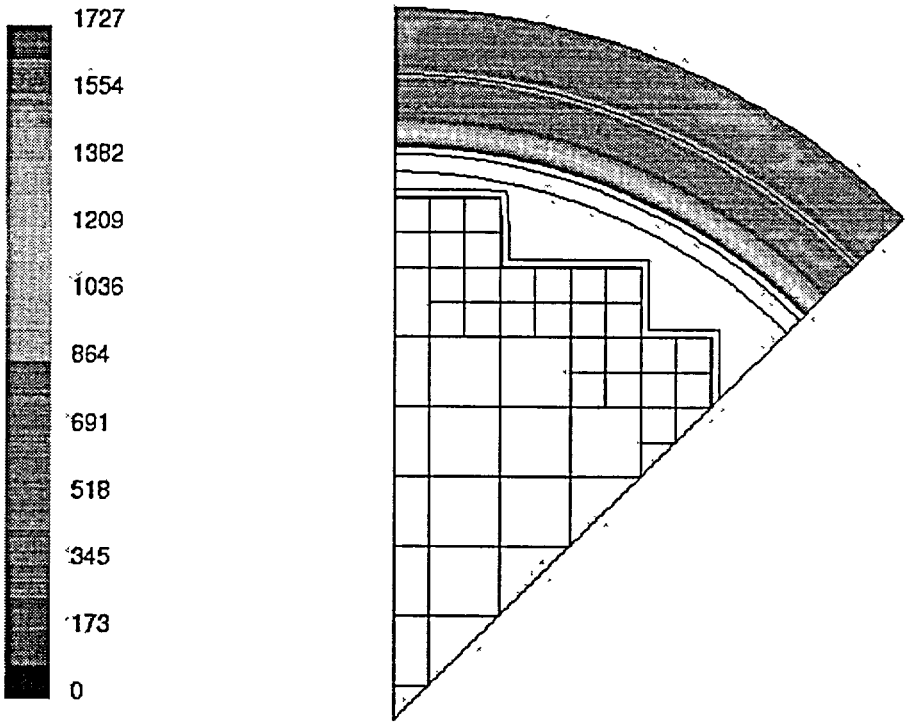

AP1000 analyses
Contours of Static Temperature (k) (Time=2.7000e+03)
Case 7, top, new alza_zo

T. Toppila, FNS
Nov 18, 2002
FLUENT 6.0 (2d, segregated, lam, unsteady)

Figure 39A-28 – Finite Difference Temperature Map Level 5 at 5380 seconds for the Top-Skewed Power Shape Case

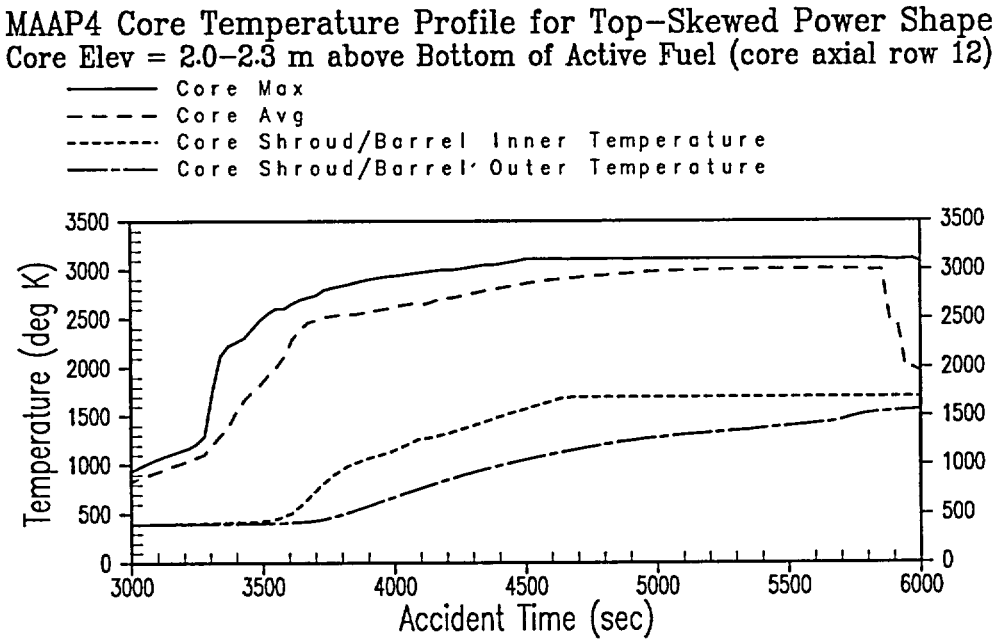

Figure 39A-29

As discussed in section 4, MAAP4 models the shroud and barrel as one lumped cylindrical heat sink, which does not model the resistance due to radiation between the components. Therefore, the whole mass heat ups more uniformly with respect to the finite difference model, delaying the time that the inner "shroud part" of the heat sink reaches the melting temperature with respect to the finite difference modeling.

Once the shroud panels melt, the radiation heat transfer from the core is directly to the core barrel, reducing the thermal resistance to the core barrel. Once melting of the inner shroud fraction of the lumped heat sink has occurred, MAAP4 models this effect and effectively models the heat sink. The mass and heat capacity of the shroud, supporting structures and the barrel are preserved in the MAAP4 model. So it is concluded that the MAAP4 results, as modeled in this analysis with the proper sideward mass and heat capacity, provide reasonable results with respect to the core barrel temperature and melting at the various elevations at and below the pool elevation.

39A.5.3 Initial Relocation of the Molten Core Debris to the Lower Plenum

The maximum heat load from the in-core debris pool to the crust occurs along the sidewall of the crust, and the heat load downward is predicted to be much less (reference 39A-1) than sideward. The crust of the in-core debris pool will fail from the side once the pool develops significant superheat. Based on the MAAP4 results, the water level in the vessel does not decrease significantly below the bottom of the active fuel until after debris relocates into the lower plenum. The bottom of the metal blockage and the lower core support plate are cooled with water prior to the initial debris relocation, and not significantly heated from above. The blockage will not fail and prevents a downward relocation of the molten pool into the lower plenum.

After the relocation of molten debris into the pocket volume between the core shroud and core barrel, the debris pool has a volume of 6.1 m^3. The total cross sectional area in the vessel between the shroud and barrel and inside the remaining peripheral fuel assemblies is 7 m^2. Therefore, the pool is anticipated to contact the core barrel up to an elevation of 1.9 m above the bottom of the active fuel.

Based on the MAAP4 results, the core shroud/barrel is thinned and weakened in the elevation 1.5 to 2.0 meters above the bottom of the active fuel (see Figures 39A-13 through 15 and 22 through 24). Below this elevation, the barrel is predicted to be overheated, yet fully intact. The heat flux from the molten pool will be highest at the top of the pool and the core barrel failure occurs azimuthally where the barrel is initially thinned near the top of the debris pool. The azimuthal length limitation is imposed by the supporting structure of the core shroud that runs vertically along the inside of the core barrel. The initial failure is postulated to occur between a vertical rib and the pinch point between the remaining peripheral assemblies and the barrel, an azimuthal distance of 1.3 m. The limiting length in the AP1000 is approximately the same as the limiting length of 1.4 m used to estimate the core barrel failure size in the

AP600 analysis (reference 1). Thus, the failure of the core barrel by the molten debris pool, and subsequent relocation to the lower head occurs essentially via the same mechanism as postulated in the AP600 (reference 39A-1).

The geometry of the core barrel (inner diameter, thickness, and material) is the same as the AP600 and the mechanism for core barrel failure is the same as the AP600. The core barrel in the AP1000 is thinned and significantly overheated, while the core barrel in the AP600 was cooler due to the presence of the reflector. Therefore, the degree of superheat in the debris needed to fail the AP1000 core barrel is bounded by the superheat in the debris that failed the AP600 core barrel (reference 39A-1). The debris pour is oxide in composition and has a superheat on the order of 150°K. The initial relocation of 52000 kg of debris into the lower plenum of the reactor vessel occurs over a duration of 500 seconds (Figure 39A-30) (reference 39A-6)

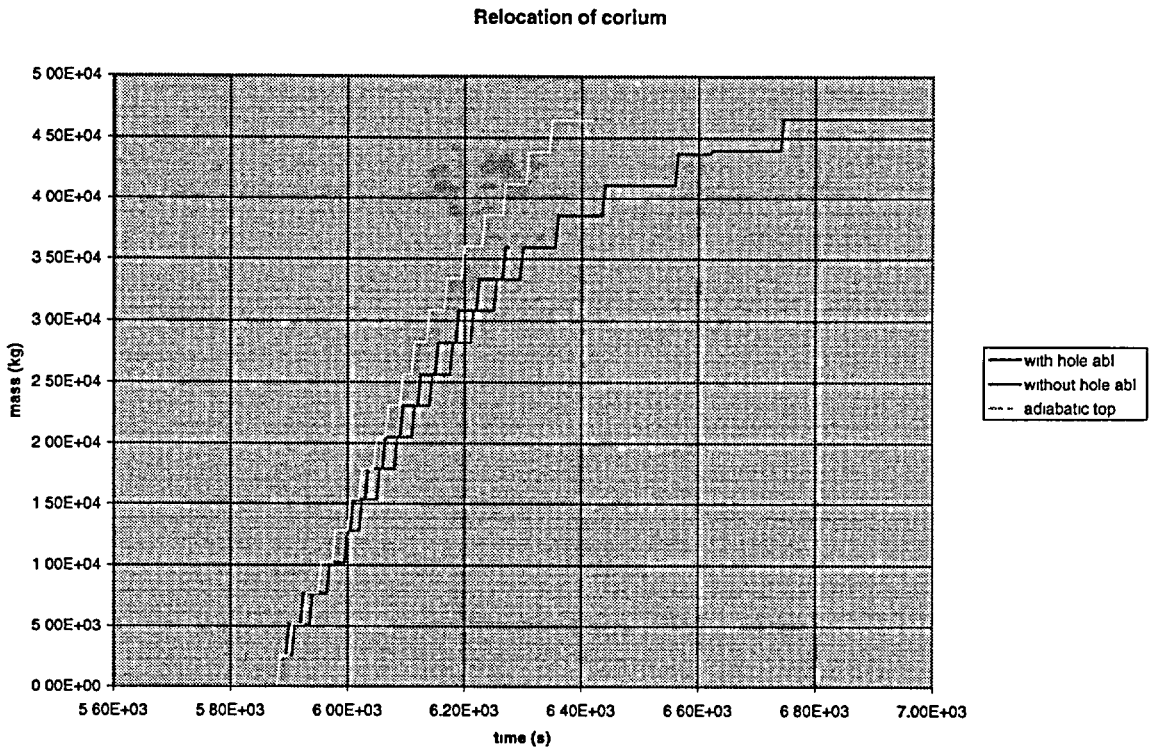

Figure 39A-30

The geometry and material composition of the reactor vessel wall and lower head of the reactor vessel are the same as the AP600. The debris composition, and mass flow rate are also the same. The superheat in the debris is bounded by the superheat predicted for the AP600. Therefore, the results and conclusions of the jet impingement analysis performed for AP600 are applicable to the AP1000, and thus the AP1000 vessel is not predicted to fail from jet impingement to the vessel wall during the relocation of molten debris to the lower plenum.

39A.5.4 Lower Plenum Debris Pool Formation

The purpose of examining the lower head debris pool formation is to determine the rate, timing and composition of material that enters the debris pool and whether oxide debris in the lower plenum subsumes the lower support plate before failing the lower head.

The lower core support plate hangs from the core barrel, which supports the weight of the core and lower internal structures. The core barrel is significantly overheated and thinned from melting prior to debris relocation and stressed by the weight it is supporting. When the debris contacts the core barrel, the core support plate will drop 1 inch until it is supported from below by the energy absorber structure in the lower plenum of the reactor vessel. When core debris begins to pour into the lower plenum, the energy absorber structure is submerged in molten oxide and melts quickly. The lower core support plate drops and rest on the radial keys (see Figure 39A-1). The keys maintain a 9 cm gap between the vessel wall and the core support plate. The volume below the collapsed lower support plate is, at most, 8.0 m^3. The volume of the molten oxide debris predicted to fill the lower plenum during the initial relocation after the crust fails is 6.1 m^3. Therefore, the initial relocation does not reach the lower core support plate.

After the initial relocation, the debris above the lower support plate will continue to melt due to the decay heating in each of the regions. There are several debris regions that are considered to be the initial condition for modeling the subsequent debris relocation that occurs after the initial debris relocation (see Figure 39A-31). The adiabatic heatup and melting timing of these regions is calculated and compared to the timing of the water depletion rate in the lower head, which is estimated conservatively.

The debris layers are lumped into four masses above the lower core support plate, which are, from top to bottom:

1. The peripheral fuel assemblies, which are assumed to collapse onto the top of the blockage after the initial relocation.

2. The oxide crust, which has frozen around unmelted UO_2 fuel.
3. The upper zirconium crust, which has frozen around unmelted UO_2 fuel.
4. The zirconium crust, below the bottom of the active fuel and the lower support plate.

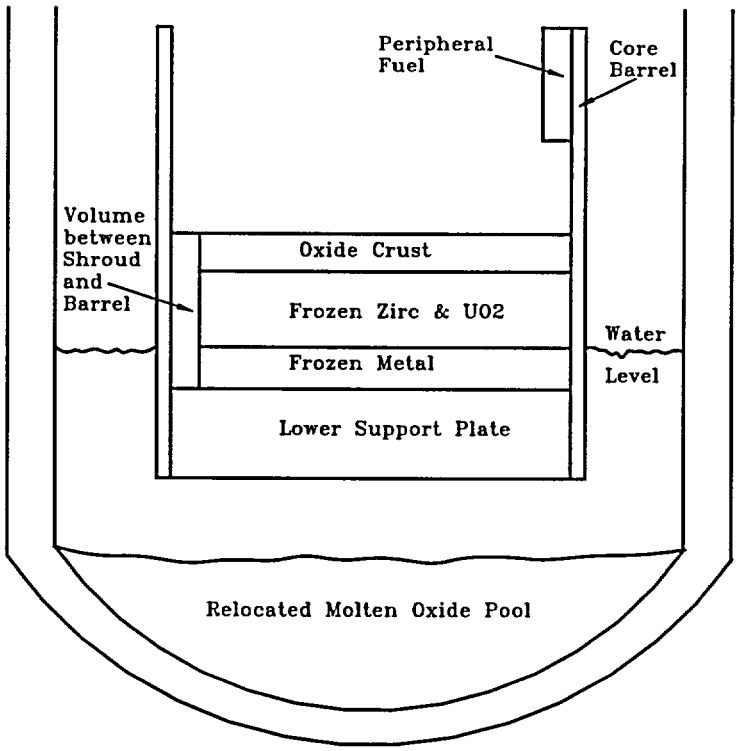

Figure 39A-31 – Model for Relocation to the Lower Plenum

39A.5.4.1 Modeling Melting and Relocation of the Layers

39A.5.4.1.1 The Peripheral Fuel Assemblies

The remaining mass of the peripheral fuel assemblies is assumed to collapse onto the top of the oxide crust upon the initial relocation of the molten pool to the lower head. This assumption is reasonable given that the oxide pool subsumes the bottom portion of the peripheral fuel assemblies during the time between crust failure and the core barrel failure. The initial temperature is estimated to be 2700°K. The temperature is based on the average temperature between the 2300°K cold edge of the temperature profile in the peripheral assemblies as calculated in the finite difference model and the 3113°K melting temperature of UO_2, which defines the hot edge of the assemblies.

The time for the peripheral assemblies to heat up to the melting temperature is found from the equation:

$$t_{mp} = \frac{m_p Cp(T_{mp} - T_i)}{Q_p V_p} + t_0 \qquad \text{(equation 1)}$$

where: t_{mp} = time to the melting point (secs)
m_p = mass of the oxide in the peripheral assemblies (kg)
Cp = heat capacity of the oxide in the peripheral assemblies (kJ/kg-°K)
T_{mp} = melting temperature of the UO_2 (°K)
T_I = initial temperature of the peripheral assemblies (°K)
Q_p = power density in peripheral assemblies (kW/m^3)
V_p = volume of the oxide debris (m^3)
t_0 = time of the initial relocation (sec)

The melting rate of the peripheral assemblies is:

$$\dot{V}_p = \frac{Q_p * V_p}{h_{LH-P} * \rho_{ox}}$$

(equation 2)

where: $\dot{V}_p$ = melting rate (m^3/sec)
h_{LH-p} = latent heat of melting (kJ/kg)
ρ_{ox} = the volume averaged density of the UO_2 and ZrO_2 eutectic

The oxide latent heat of melting is found from the latent heats of UO_2 and ZrO_2 employing the following equation:

$$h_{LH-p} = \frac{f_{UO2} MW_{UO2} h_{LH-UO2} + f_{ZrO2} MW_{ZrO2} h_{LH-ZrO2}}{f_{UO2} MW_{UO2} + f_{ZrO2} MW_{ZrO2}}$$

(equation 3)

where: MW_{UO2} = the molecular weight of UO_2
MW_{ZrO2} = the molecular weight of ZrO_2
f_{UO2} = the molecular fraction of UO_2
f_{ZrO2} = the molecular fraction of ZrO_2
h_{LH-UO2} = the latent heat of melting of UO_2
$h_{LH-ZrO2}$ = the latent heat of melting of ZrO_2

39A.5.4.1.2 The Oxide Crust

The oxide crust consists of previously molten oxide material that is frozen around unmelted fuel and the mass of the debris that has accumulated in the pocket volume between the shroud and core barrel. The oxide crust and unmelted fuel is treated as a lumped mass, and the initial temperature is estimated to be 2800°K, a low bound value based on the relocated mass temperature and latent heat and the unmelted UO_2 temperature from the finite difference calculation.

The melting rate of the oxide crust is found using the same method as the peripheral fuel assemblies. The total power density is found from the volume averaged power density of the previously molten fuel and the unmelted fuel.

39A.5.4.1.3 The Upper Metal Crust

The metal crust above the bottom of oxide fuel, or the upper metal crust, is comprised of a layer of zirconium frozen around unmelted fuel rods. The initial temperature of 1800°K is estimated conservatively high from temperature of the UO_2 in level 2 from the finite difference calculation.

The melting rate of the zirconium and UO_2 are calculated using the same lumped heat capacity methodology as above. Initially, the UO_2 and zirconium heat up as a lumped mass to the zirconium melting temperature. Then all the decay heat goes into melting the zirconium. After zirconium melting is completed, the UO_2 begins to heat up again from the zirconium melting temperature until it reaches the UO_2 melting temperature.

39A.5.4.1.4 The Support Plate and Metal Crust below the Bottom of Active Fuel

The metal crust below the bottom of the active fuel, or the lower metal crust, is comprised of a layer of zirconium and control rod material frozen around the bottom plenum and zirconium plugs of the fuel rods, the stainless steel fuel assembly lower nozzles and the stainless steel lower core support plate. There is no decay heat in this layer, and the initial temperature is 400°K since the layer is cooled by water.

For success, the lower plenum debris pool must contact the bottom of the support plate before the debris dries out. The support plate begins to heat up after contact and when the debris dries out. The upward heat flux from the lower plenum oxide debris bed is 1.2 MW/m^2 and the area for heat transfer is assumed to be 11.1 m^2, the upward facing area of the oxide pool at the elevation of the bottom of the support plate. The support plate and frozen metal are assumed to heat up as a lumped mass. The support plate is considered to fail when the metal is fully molten.

39A.5.4.2 Lower Head Integrity Success Criterion for the In-Vessel Melting and Relocation

The lower head integrity success criterion for the in-vessel melting and relocation is based on the following question:

Does the debris contact the lower core support plate before the water in the lower plenum boils away and the debris heats back up to a superheated condition?

The time to boil the water away is calculated conservatively by assuming that all of the decay heat and sensible heat in the debris goes into the water. The volume of debris that contributes to the boiling is conservatively assumed to be the entire volume below the lower core support plate. Note that there is a cancellation effect on the oxide latent heat of fusion in calculating the dry out time.

$$t_{dry-out} = \frac{M_w h_{fg} - Q_{latent_{ox}} - Q_{sens_{ox}} + Q_{latent_{ox}}}{QV_{LSP}} + t_0 = \frac{M_w h_{fg} - V_{LSP}\rho_{ox}C_{p-ox}\Delta T_{SH}}{QV_{LSP}} + t_0$$

(equation 4)

where: $t_{dry-out}$ = the dry out time

Mw = the initial mass of water in the lower head (kg)

h_{fg} = the heat of vaporization of water (kJ/kg)

V_{LSP} = the volume below the lower core support plate (m^3)

ρ_{ox} = the density of the oxide debris (kg/m^3)

C_{p-ox} = the heat capacity of the molten oxide (kJ/kg-K)

ΔT_{SH} = the superheat in the debris (°K)

The superheat in the debris is volume averaged between the volume of the initial relocation debris (V_i), which has a superheat of +150°K (ΔT_{SH-I}), and the volume of debris required to fill the lower plenum, which has a superheat of +0°K.

$$\Delta T_{SH} = \frac{V_i \Delta T_{SH-i}}{V_{LSP}} \qquad \text{(equation 5)}$$

39A.5.4.3 Results

The mass distributions for the top-skewed and chopped cosine power shapes are presented in Table 39A-3, and the results of the relocation analysis are presented in Table 39A-4. The material properties used in the calculations are presented in Table 39A-5.

In both cases, the debris subsumes the lower core support plate before the water boils away in the lower plenum. There is a period of time when zirconium is melting at the same time as oxide from the peripheral fuel.

39A.6 Potential for Debris Interaction

If molten metal debris is mixed with molten oxide debris, it is postulated that there is potential for the debris to interact and produce a uranium/zirconium metal layer that may sink to the bottom of the lower plenum debris bed.

The upper metal layer consists of zirconium that is frozen around unmelted UO_2 at the bottom of the core. A fraction of the zirconium is predicted to melt during the relocation of the oxide crust or peripheral assemblies. The zirconium blockage is below the oxide crust, contained in a crucible formed by the core barrel and bottom metal blockage. Its melting temperature is much lower than the melting temperature of the oxide, maintaining the crust between the layers. Even if a fraction of the zirconium were molten, there is no pathway for it to flow to the lower plenum, where it could potentially interact with the oxide. Therefore, there is no mechanism to cause significant mixing of the metal and oxide layers even if they were melted at the same time.

39A.7 Conclusions from the Analysis of the AP1000 In-Vessel Core Melting and Relocation

The important conclusions from the analysis of the lower plenum debris pool formation analysis are:

- The lower plenum debris bed is cooled with water during the entire relocation process prior to contact with the support plate. Transient debris configurations are not predicted to threaten vessel integrity.
- The lower plenum oxide debris subsumes the lower core support plate before dry out in the lower plenum occurs. If the relocated debris is assumed to be instantaneously quenched in the lower plenum water the oxide debris contacts the lower support plate before the debris can return to a superheated condition. Therefore, the lower core support plate, core shroud and a sizeable fraction of the core barrel are subsumed in the debris bed. The focusing effect is mitigated.
- The lower plenum debris bed is predicted to form a metal layer over oxide pool configuration.
- The potential for debris interaction creating a bottom metal pool of uranium dissolved in zirconium is expected to be small.
- The earliest time to achieve the fully molten, circulating debris bed in the lower plenum is 2.7 hours after shutdown. The timeline of events is presented in Table 39A-6.

Table 39A-3 Mass and Power Distributions of the Debris Layers in the Top-Skewed Power Shape Case (Sheet 1 of 2)

	Mass	Fraction	Height	Volume	Pow Den
Mass of UO2 in periph asmbs =	6548	6.8%		0.7	
Mass of ZrO2 in periph asmbs =	561		1.63	0.1	
	7108			0.8	2.2
Mass of UO2 Relocated to LP =	47687	49.7%		5.5	
Mass of ZrO2 Relocated to LP =	4085			0.7	
	51772			6.1	2.9
Mass of reloc UO2 in pockets	5281	5.5%		0.6	
Mass or reloc ZrO2 in pockets	452			0.1	
	5734			0.7	2.9
Mass of relocated UO2 in crust =	13910	14.5%		1.6	
Mass of relocated ZrO2 in crust =	1191		0.46	0.2	
	15102			1.8	2.9
Mass unmelted UO2 in crust	10383	10.8%		1.2	
Mass of unmelted ZrO2 in crust	0		0.46	0.0	
	10383			1.2	2.7
Mass of UO2 in metal blockage	12090	12.6%		1.4	1.2
Mass of Zr in metal blockage	12488		0.54	2.1	
				3.5	
		100.0%			
Mass of zirc relocated	786			0.1	
Mass of control rod material	3900			0.6	
Mass of zirc below core	4800			0.8	0.0
Mass of FA lower nozzles	760		0.22	0.1	
Mass of support plate	25000			1.6	

Table 39A-3 Mass and Power Distributions of the Debris Layers in the Chopped Cosine Power Shape Case (sheet 2 of 2)

	Mass	Fraction	Height	Volume	Pow Den
Mass of UO2 in periph asmbs =	6548	6.8%		0.7	
Mass of ZrO2 in periph asmbs =	561		1.63	0.1	
	7108			0.8	2.1
Mass of UO2 Relocated to LP =	47687	49.7%		5.5	
Mass of ZrO2 Relocated to LP =	4085			0.7	
	51772			6.1	2.8
Mass of reloc UO2 in pockets	5281	5.5%		0.6	
Mass or reloc ZrO2 in pockets	452			0.1	
	5734			0.7	2.8
Mass of relocated UO2 in crust =	13910	14.5%		1.6	
Mass of relocated ZrO2 in crust =	1191		0.46	0.2	
	15102			1.8	2.8
Mass unmelted UO2 in crust	10383	10.8%		1.2	
Mass of unmelted ZrO2 in crust	0		0.46	0.0	
	10383			1.2	3.3
Mass of UO2 in metal blockage	12090	12.6%		1.4	1.2
Mass of Zr in metal blockage	12488		0.54	2.1	
				3.5	
		100.0%			
Mass of zirc relocated	786			0.1	
Mass of control rod material	3900			0.6	
Mass of zirc below core	4800			0.8	0.0
Mass of FA lower nozzles	760		0.22	0.1	
Mass of support plate	25000			1.6	

Table 39A-4 Results of the Top-Skewed Power Shape Case (Sheet 1 of 2)

	Material	Mass (kg)	Mole Fraction	Molten Vol (m3)	Qdk (kW/m3)	Init Temp (K)	Start Time Heatup (s)	Time to MP (s)	Time fully melted (s)
peripheral fuel rods	UO2	6548	0.84	0.7	2189.2	2700	6000	6572	7804
	ZrO2	561	0.16	0.1					
oxide crust and pockets	UO2	19192	0.89	2.2	2908.7	2800	6000	6274	7194
	ZrO2	1644	0.11	0.3					
unmelted UO2 in UO2 crust	UO2	10383		1.2	2656.6				
unmelted UO2 in zirc crust	UO2	12090		1.4	1160.9	2125	8599	12579	
zirc in the active fuel region	Zr	12488		2.0		2000	6000	6850	8599
zirc below active fuel region	Zr	5586	0.10	0.9					
support plate and nozzles	SS	29660	0.90	4.2		400	6888	8942	9662

						qup (kW/m2)	vol under LSP (m3)	Contact time LSP (s)
initial relocation molten debris in lower plenum	UO2	47687	0.84	5.5	2908.7	1200	8.0	6718
	ZrO2	4085	0.16	0.7				

		Mass (kg)	Vol (m3)	Debris Superheat (K)	Dry Out Time (sec)
Water in RPV boils away	H2O	11038	11.6	115	6888

Contact LSP (s)	Dry Out Time (sec)
6718	6888

Table 39A-4 Relocation Results of the Chopped Cosine Power Shape Case (Sheet 2 of 2)

	Material	Mass (kg)	Mole Fraction	Molten Vol (m3)	Qdk (kW/m3)	Init Temp (K)	Start Time Heatup (s)	Time to MP (s)	Time fully melted (s)
peripheral fuel rods	UO2	6548	0.84	0.7	2124.8	2700	6000	6589	7859
	ZrO2	561	0.16	0.1					
oxide crust and pockets	UO2	19192	0.89	2.2	2823.1	2800	6000	6283	7154
	ZrO2	1644	0.11	0.3					
unmelted UO2 in UO2 crust	UO2	10383		1.2	3321.7				
unmelted UO2 in zirc crust	UO2	12090		1.4	1169.3	2125	8581	12531	
zirc in the active fuel region	Zr	12488		2.0		2000	6000	6843	8581
zirc below active fuel region	Zr	5586	0.10	0.9					
support plate and nozzles	SS	29660	0.90	4.2		400	6915	8969	9689

						qup (kW/m2)		vol under LSP (m3)	Contact time LSP (s)
initial relocation molten debris in lower plenum	UO2	47687	0.84	5.5	2823.1	1200		8.0	6707
	ZrO2	4085	0.16	0.7					

		Mass (kg)	Vol (m3)	Debris Superheat (K)	Dry Out Time (sec)
Water in RPV boils away	H2O	11038	11.6	115	6915

Contact LSP (s)	Dry Out Time (sec)
6707	6915

Table 39A-5 – Material Properties Used in In-Vessel Melting and Relocation Calculation

	Material Properties Used In Calculation							
	ZrO2	UO2	Oxide	SS	Zr	Metal	Water	
Melt Temp	2911	3113	2973	1700	2125	1600		K
Density	5990	8740	8434	7020	6130		950	kg/m3
Solid Cp	0.645	0.535		0.64	0.356			kJ/kgK
Liquid Cp	0.815	0.485	0.502	0.835	0.458			kJ/kgK
Latent Heat	856.2	274	320	280	225		2226	kJ/kg
Mole Weight	123	267		56	91		18	kg/kg-mole

Table 39A-6 – Debris Relocation Time Line

		From the Onset Melt (sec)	(hr)
Time of Core Uncovery	2300		
Onset of Melting	3000	0	0.0
In-Pool Crust Failure	6000	3000	0.8
Initial Relocation to LP starts	6000	3000	0.8
Sec. Oxide Relocation starts	6283	3283	0.9
Initial Relocation to LP ends	6500	3500	1.0
LP debris contacts LSP	6707	3707	1.0
zirc blockage melting begins	6843	3843	1.1
LP dry out	6915	3915	1.1
Sec. Oxide Relocation ends	7859	4859	1.3
zirc blockage melting ends	8581	5581	1.6
LSP melting begins	8969	5969	1.7
LSP Melting ends	9689	6689	1.9
Unmelted oxide falls into pool	9689	6689	1.9

39A.8 References

39A-1 Theofanous, T.G., et. al, Lower Head Integrity Under In-Vessel Steam Explosion Loads, DOE/ID-10541, June 1996.

39A-2 Theofanous, T.G., et. al., In-Vessel Coolability and Retention of a Core Melt, DOE/ID-10460, July 1995.

39A-3 RASPLAV

39A-4 MASCA

39A-5 Rempe, J.L., et. al., Potential for AP600 In-Vessel Retention through Ex-Vessel Flooding, INEEL/EXT-97-00779, December 1997.

AP1000 DESIGN CERTIFICATION REVIEW

Response to Request For Additional Information

RAI Number: 720.094

Question:

What effect does the AP1000 hydrogen generation rate have on the mixture classes used in the Sherman-Berman methodology and how does this affect the probability of containment failure at node DTE in the containment event tree?

Westinghouse Response:

The probability of early time frame DDT was assessed for each of the AP1000 specific MAAP4 analyses presented in Attachment A to Chapter 41 (see response to RAI 720.042) in the revision to the PRA report. The analyses assigned a +/-2% to the hydrogen concentration at the time when the concentration was the highest or when the detonation cell width was the smallest. The probability of DDT was calculated for each compartment in the containment using the Sherman-Berman methodology. The overall detonation probability was calculated, and the most conservative result was reported.

The results of this assessment are presented in Table 720.094-1, and the corresponding probability of early DDT as used in the AP1000 PRA decomposition event tree quantification is presented for comparison. Table 720.094-2 presents the containment event tree node DTE failure probabilities quantified employing the decomposition event trees for early detonation (see Figures 720.094-1 through 720.094-6) using the new sequence probabilities conservatively. The new values are compared to the values that were used in the AP1000 PRA.

The probabilities used in the AP1000 PRA containment event tree quantification are generally conservative with respect to the new values, with exceptions in accident class 3BL, recovered accident class 1A, and recovered accident class 6 sequences. However, the early DDT failure probability for these accident classes was very small and remains small in the new analysis.

Therefore, the overall probability of early containment failure is conservative with respect to the new values quantified specifically from the AP1000 MAAP4 hydrogen analyses.

Design Control Document (DCD) Revision:

None

PRA Revision:

None

Table 720.094-1

Probability of DDT Using Sherman-Berman Methodology
for AP1000 Hydrogen Sequences Presented in Chapter 41 Attachment A

Sequence	Break Compt	Reflood	AP1000 Estimate	Corresponding Value from DET
1A-3	Loop Compt	Y	0.0E-0	0.0E-0
1A-4	Loop Compt	Y	1.0E-1	0.0E-0
1AP-3	Loop Compt	Y	1.3E-2	7.8E-2
1AP-4	Loop Compt	Y	1.2E-2	7.8E-2
1AP	CVS Compt	Y	-	1.0E0
3BE-1	PXS Compt	Y	1.7E-2	5.2E-1
3BE-2	PXS Compt	N	4.0E-3	3.5E-2
3BE-4	Loop Compt	N	0.0E-0	2.0E-3
3BE-5	Loop Compt	Y	0.0E-0	3.1E-1
3BE-6	Loop Compt	Y	1.2E-2	3.1E-1
3BL-1	Loop Compt	N	9.3E-2	2.0E-3
3BL-2	PXS Compt	N	4.3E-2	3.4E-1
3BR-1	Loop Compt	Y	0.0E-0	3.8E-1
3C-1	Loop Compt	Y	6.0E-3	3.8E-1
3D-1	Loop Compt	Slow	0.0E-0	2.5E-1
3D-2	Loop Compt	Slow	0.0E-0	2.5E-1
3D-3	PXS Compt	Slow	6.0E-1	1.9E-1
3D-5	Loop Compt	Slow	0.0E-0	2.5E-1

Table 720.094-2

CONTAINMENT EVENT TREE NODAL FAILURE PROBABILITIES

Accident Class	New	Old	Comparison (new/old)
3BE RFL Success	.008	.254	.03
3BE RFL Failure	.001	.117	.009
3BL	.042	.005	8.4
3BR	.003	.19	.02
3C	.003	.19	.02
3D/1D	.117	.115	1.0
1AP	.022	.054	0.4
1A	.100	0.0	inf.
3A	0.0	0.0	1
6	.042	.005	8.4

Figure 720.094-1

Accident Class 1AP Early Detonation Decomposition Event Tree

Node N1 Ignition Source	Node N2 Break Compartment	Node N3 DDT

0.500	No Ignition					1	No ign	0.500
0.500	Ignition	0.968	Loop Compt	0.987	No DDT	2	No DDT	0.478
				0.013	DDT	3	DDT	0.006
		0.000	PXS	0.000	No DDT	4	No DDT	0.000
				1.000	DDT	5	DDT	0.000
		0.032	CVS	0.000	No DDT	6	No DDT	0.000
				1.000	DDT	7	DDT	0.016
							Total	1.000

End State	Probability
No Ign	0.500
No DDT	0.478
CET Node DTE Failure Probability = DDT	0.022

Figure 720.094-2

Accident Class 3D/1D Early Detonation Decomposition Event Tree

Node N1 Ignition Source	Node N2 Break Compartment	Node N3 DDT

0.500	No Ignition					1	No ign	0.500
0.500	Ignition	0.610	Loop Compt	1.000	No DDT	2	No DDT	0.305
				0.000	DDT	3	DDT	0.000
		0.384	PXS	0.400	No DDT	4	No DDT	0.077
				0.600	DDT	5	DDT	0.115
		0.006	CVS	0.400	No DDT	6	No DDT	0.001
				0.600	DDT	7	DDT	0.002
							Total	1.000

	End State	Probability
	No Ign	0.500
	No DDT	0.383
CET Node DTE Failure Probability =	DDT	0.117

Figure 720.094-3

Accident Class 3C/3BR Early Detonation Decomposition Event Tree

Node N1 Ignition Source	Node N2 Break Compartment	Node N3 DDT

0.500	No Ignition					1	No ign	0.500
0.500	Ignition	1.000	Loop Compt	0.994	No DDT	2	No DDT	0.497
				0.006	DDT	3	DDT	0.003
		0.000	PXS	0.000	No DDT	4	No DDT	0.000
				1.000	DDT	5	DDT	0.000
		0.000	CVS	0.000	No DDT	6	No DDT	0.000
				1.000	DDT	7	DDT	0.000
							Total	1.000

	End State	Probability
	No Ign	0.500
	No DDT	0.497
CET Node DTE Failure Probability =	DDT	0.003

Figure 720.094-4

Accident Class 3BL Early Detonation Decomposition Event Tree

Node N1 Ignition Source	Node N2 Break Compartment	Node N3 DDT

0.500	No Ignition					1	No ign	0.500
0.500	Ignition	0.827	Loop Compt	0.907	No DDT	2	No DDT	0.375
				0.093	DDT	3	DDT	0.038
		0.149	PXS	0.957	No DDT	4	No DDT	0.071
				0.043	DDT	5	DDT	0.003
		0.024	CVS	0.957	No DDT	6	No DDT	0.011
				0.043	DDT	7	DDT	0.001
							Total	1.000

	End State	Probability
	No Ign	0.500
	No DDT	0.458
CET Node DTE Failure Probability =	DDT	0.042

Figure 720.094-5

Accident Class 3BE Early Detonation Decomposition Event Tree - Given RFL Failure

Node N1 Ignition Source		Node N2 Break Compartment		Node N3 DDT				
0.500	No Ignition					1	No ign	0.500
0.500	Ignition	0.342	Loop Compt	1.000	No DDT	2	No DDT	0.171
				0.000	DDT	3	DDT	0.000
		0.649	PXS	0.996	No DDT	4	No DDT	0.323
				0.004	DDT	5	DDT	0.001
		0.009	CVS	0.996	No DDT	6	No DDT	0.004
				0.004	DDT	7	DDT	0.000
							Total	1.000

End State	Probability
No Ign	0.500
No DDT	0.499
CET Node DTE Failure Probability = DDT	0.001

Figure 720.094-6

Accident Class 3BE Early Detonation Decomposition Event Tree - Given RFL Success

Node N1 Ignition Source	Node N2 Break Compartment	Node N3 DDT

0.500	No Ignition					1	No ign	0.500
0.500	Ignition	0.047	Loop Compt	0.692	No DDT	2	No DDT	0.016
				0.012	DDT	3	DDT	0.000
		0.953	PXS	0.482	No DDT	4	No DDT	0.230
				0.017	DDT	5	DDT	0.008
		0.000	CVS	0.457	No DDT	6	No DDT	0.000
				0.017	DDT	7	DDT	0.000
							Total	0.754

	End State	Probability
	No Ign	0.500
	No DDT	0.246
CET Node DTE Failure Probability =	DDT	0.008

AP1000 DESIGN CERTIFICATION REVIEW

Response to Request For Additional Information

RAI Number. 720.095

Question:

Why is the probability of random ignition assumed to be 1 during the intermediate time? The basis for this question is that it is not conservative to assume that ignition is guaranteed in the intermediate time when it comes to global detonations. Presumably the steam content in the uniformly mixed gases inside the containment decreases as the PCCS is allowed to cool the containment shell. In the limit (dry mixtures), the concentration of hydrogen is about 14% in the AP1000, assuming 100% active cladding reaction, or about 19% assuming 100% reaction of all core zirconium. This mixture is becoming sufficiently sensitive to undergo a transition to detonation, especially if the entire containment is viewed as one confined compartment with a lot of clutter (individual compartments below the operating deck).

Westinghouse Response:

Detonation in the intermediate time frame is considered and quantified at node DTI on the containment event tree. The intermediate time frame essentially covers the time from the end of in-vessel hydrogen generation to 24 hours after core damage. Due to the PCS heat removal, natural circulation in the containment is strong, and the containment mixes quickly. For sequences in which the igniters are not functioning, a global burn of the well-mixed gases in the containment is assumed to occur with the probability of ignition of 1.0. The global burn is evaluated for the potential for flame acceleration.

The probability of DDT in the intermediate time frame is assumed to be the same as AP600 since the containment is well mixed and the increase in zirconium mass corresponds to the increase in the containment volume. In the AP600 PRA, mixture class probability distributions are developed considering uncertainties in the degree of zirconium oxidation and steam concentration over the time frame. The gas mixture composition is considered to be the same in all compartments, except the CMT room, where it is assumed to be dry air and hydrogen. This conservatism is introduced to overcome uncertainty in steam concentration below the operating deck due to stratification caused by the condensation on the PCS shell. Additionally, the CMT room has been assigned an unfavorable geometry classification.

Therefore, the AP1000 treatment of DDT in the intermediate time frame is conservative, and the assumption of guaranteed ignition facilitates the treatment.

AP1000 DESIGN CERTIFICATION REVIEW

Response to Request For Additional Information

Design Control Document (DCD) Revision:

None

PRA Revision:

None

RAI Number: 720.098

Question:

A. Additional Design Parameter Values

Please provide values for the following AP1000 parameters needed to complete the MELCOR input deck (this list includes parameters that were not addressed in response to RAI 720.001 dated September 10, 2002).

1. The dimensions of the portion of the reactor cavity that is directly below the reactor vessel,
2. The perimeter and radial dimensions of the core shroud (preferably including a detailed radial diagram of the shroud with measurements identified),
3. If the channel head of the steam generator (SG) consists of both a cylindrical part and hemispherical part, please provide the inner diameter, height, and thickness of the cylindrical part and the inner diameter and thickness of the hemispherical part. If the channel head of the SG is a hemispherical part, only the thickness of the channel head is required,
4. The thickness of the lower and upper portions of the SG shell,
5. The thickness of the SG tube wrapper,
6. Inner and outer diameters of the guide tubes in the upper plenum region of the reactor vessel (in the region above the upper core support plate and below the upper support plate),
7. Inner and outer diameters of the instrument tubes in the upper plenum region of the reactor vessel,
8. Inner and outer diameters of the guide tubes in the dome region of the reactor vessel,
9. Inner and outer diameters of the instrument tubes in the dome region of the reactor vessel,
10. The fluid volume of a reactor coolant pump (RCP), excluding the suction and discharge piping volumes,
11. The height of the fluid volume of the RCP,
12. The wall thickness of the containment chimney,
13. The diameter of sparger tubes in the in-containment refueling water storage tank (IRWST),
14. The thickness of the containment air baffle,
15. The thickness and tube thickness of the burnable absorber rods,
16. Mass of the top and bottom Nr-Cr-Fe alloy 718 grid spacers,
17. Number and diameter (or area) of penetrations in the lower core support plate,
18. Number, material, mass, surface area, height, and elevation of steam separators in the SGs,
19. Number, material, mass, surface area, height, and elevation of dryers in the SGs,

20. The correct free-volume versus altitude table for the secondary side of the SGs (there is a discrepancy in the MAAP input in this regard - see Section B),
21. Setpoint value for "Low-2 Hot Leg Level" signal,
22. Nominal volume of water in the cask loading pit,
23. Length and inner diameter of passive residual heat removal (PRHR) inlet line, and
24. Nominal volume of condensate available for feed water systems.

B. A number of apparent inconsistencies in the AP1000 design control document (DCD) and/or MAAP input deck have been found. The most important of these with respect to the process of MELCOR modeling are documented in Table 1. Please address these discrepancies and provide the correct values for the parameters in question. Make DCD changes as necessary.

Table 1

No.	Parameter	DCD	MAAP (parameter designation in the provided input deck)
1	The height of the core from the top of the lower core support plate to the bottom of the upper core support plate	4.7843 meters (m) (See Figure 1)	4.858 m (See Figure 1)
2	Number of tubes per SG	10025 (Table 5.4-4)	1000 (NTSG)
3	Water volume in the SG inlet and outlet plena per SG	16.6503 cubic meters (m^3) Table 5.4-5	20.2 (VSGPHD) - 2.96.9 (see Figure 2) = 17.24 m^3
4	Primary water volume in the SG tubes only	42.1638 m^3 (Table 5.4-5)	61.3 (VSGPR1) - 20.2 (VSGPHD) = 41.1 m^3
5	The cross-sectional flow area for secondary side of the SG inside of the shroud (the tube bundle wrapper) (Note: This data is incorrect because AFLWSG + the cross-sectional area for the tube bundle is larger than the total area inside wrapper)	Not provided	9.54 square meters (m^2) (AFLWSG)

No.	Parameter	DCD	MAAP (parameter designation in the provided input deck)
6	The lowest elevations for various containment distributed heat sinks (Note: These elevation data in MAAP input deck are not correct because they are outside of the ranges of their respective control volumes)	Not provided	7.5784 m (ZHSRB for HS#4) 17.4284 m (ZHSRB for HS#5) 15.3084 m (ZHSRB for HS#6) 8.1584 m (ZHSRB for HS#10) 13.6484 m (ZHSRB for HS#11) 9.8584 m (ZHSRB for HS#12) 6.1684 m (ZHSRB for HS#13) 21.4284 m (ZHSRB for HS#14) 12.4584 m (ZHSRB for HS#15) 18.4184 m (ZHSRB for HS#16) 18.4184 m (ZHSRB for HS#17) 13.8384 m (ZHSRB for HS#18) 8.1784 m (ZHSRB for HS#21) 21.4284 m (ZHSRB for HS#24) 17.186 m (ZHSRB for HS#25) 8.6793 m (ZHSRB for HS#39) 8.6793 m (ZHSRB for HS#42) 8.6793 m (ZHSRB for HS#45)
7	High-3 Pressurizer Level is defined as 15.55 m from the bottom of the pressurizer (this must be incorrect because this is larger than the total height of the pressurizer).	Not provided	15.55 m (ZWPZH)

C. MAAP Results

Please provide any MAAP results for the AP1000 that are available (e.g., in the form of a list of key event timing and graphs of key variables) for dominant severe accident sequences (e.g., any of the sequences listed in Table 33-4 of the AP1000 probabilistic risk assessment).

Westinghouse Response:

A. Westinghouse letters DCP/NRC1513 dated July 24, 2002, and DCP/NRC1533 dated November 22,2002 transmitted proprietary drawings that provide most of the dimensional information requested in this RAI. The attached table A-1 provides a response to the 24 items requested, and identifies that information that can be found in these transmittal letters.

B. The discrepancies identified in this RAI are addressed in the attached tables B-1 and B-2.

C. AP1000 Level 2 MAAP analyses have been provided in the AP1000 PRA and subsequent 720 series RAI Responses.

Design Control Document (DCD) Revision:

None

PRA Revision:

None

Table A-1 AP1000 Reference Information		
No.	**Design Information**	**Reference or Value**
1.	The dimensions of the portion of the reactor cavity that is directly below the reactor vessel,	See attached sketch A-1
2.	The perimeter and radial dimensions of the core shroud (preferably including a detailed radial diagram of the shroud with measurements identified),	DCP/NRC1513 DCP/NRC1533
3.	If the channel head of the steam generator (SG) consists of both a cylindrical part and hemispherical part, please provide the inner diameter, height, and thickness of the cylindrical part and the inner diameter and thickness of the hemispherical part. If the channel head of the SG is a hemispherical part, only the thickness of the channel head is required,	DCP/NRC1513
4.	The thickness of the lower and upper portions of the SG shell,	DCP/NRC1513
5.	The thickness of the SG tube wrapper,	DCP/NRC1513
6.	Inner and outer diameters of the guide tubes in the upper plenum region of the reactor vessel (in the region above the upper core support plate and below the upper support plate),	DCP/NRC1513 DCP/NRC1533
7.	Inner and outer diameters of the instrument tubes in the upper plenum region of the reactor vessel,	DCP/NRC1513 DCP/NRC1533
8.	Inner and outer diameters of the guide tubes in the dome region of the reactor vessel,	DCP/NRC1513 DCP/NRC1533
9.	Inner and outer diameters of the instrument tubes in the dome region of the reactor vessel,	DCP/NRC1513 DCP/NRC1533
10.	The fluid volume of a reactor coolant pump (RCP), excluding the suction and discharge piping volumes,	89 ft^3 / pump
11.	The height of the fluid volume of the RCP,	Centerline of Pump Discharge Elevation = 102'-8.5" Bottom of Pump Motor Elevation = 84'-3.9"
12.	The wall thickness of the containment chimney,	Wall thickness of containment (PCS) chimney = 6 ft.
13.	The diameter of sparger tubes in the in-containment refueling water storage tank (IRWST),	DCP/NRC1513

Table A-1 AP1000 Reference Information		
No.	**Design Information**	**Reference or Value**
14.	The thickness of the containment air baffle,	Thickness of containment air baffle = 0.125 in.
15.	The thickness and tube thickness of the burnable absorber rods,	Typical discrete absorber rod: Outer Clad O.D., in = .381 (a,c)
16.	Mass of the top and bottom Nr-Cr-Fe alloy 718 grid spacers,	24 lbs / fuel assembly
17.	Number and diameter (or area) of penetrations in the lower core support plate,	DCP/NRC1513 DCP/NRC1533
18.	Number, material, mass, surface area, height, and elevation of steam separators in the SGs,	DCP/NRC1513
19.	Number, material, mass, surface area, height, and elevation of dryers in the SGs,	DCP/NRC1513
20.	The correct free-volume versus altitude table for the secondary side of the SGs (there is a discrepancy in the MAAP input in this regard - see Section B),	See Table B-2
21.	Setpoint value for "Low-2 Hot Leg Level" signal,	This analysis setpoint is a level of 0 at the bottom of the hot leg
22.	Nominal volume of water in the cask loading pit,	12,900 ft^3
23.	Length and inner diameter of passive residual heat removal (PRHR) inlet line, and	DCP/NRC1513
24.	Nominal volume of condensate available for feed water systems.	Condensate Storage Tank Nominal Capacity: 485,000 gallons

Sketch A-1

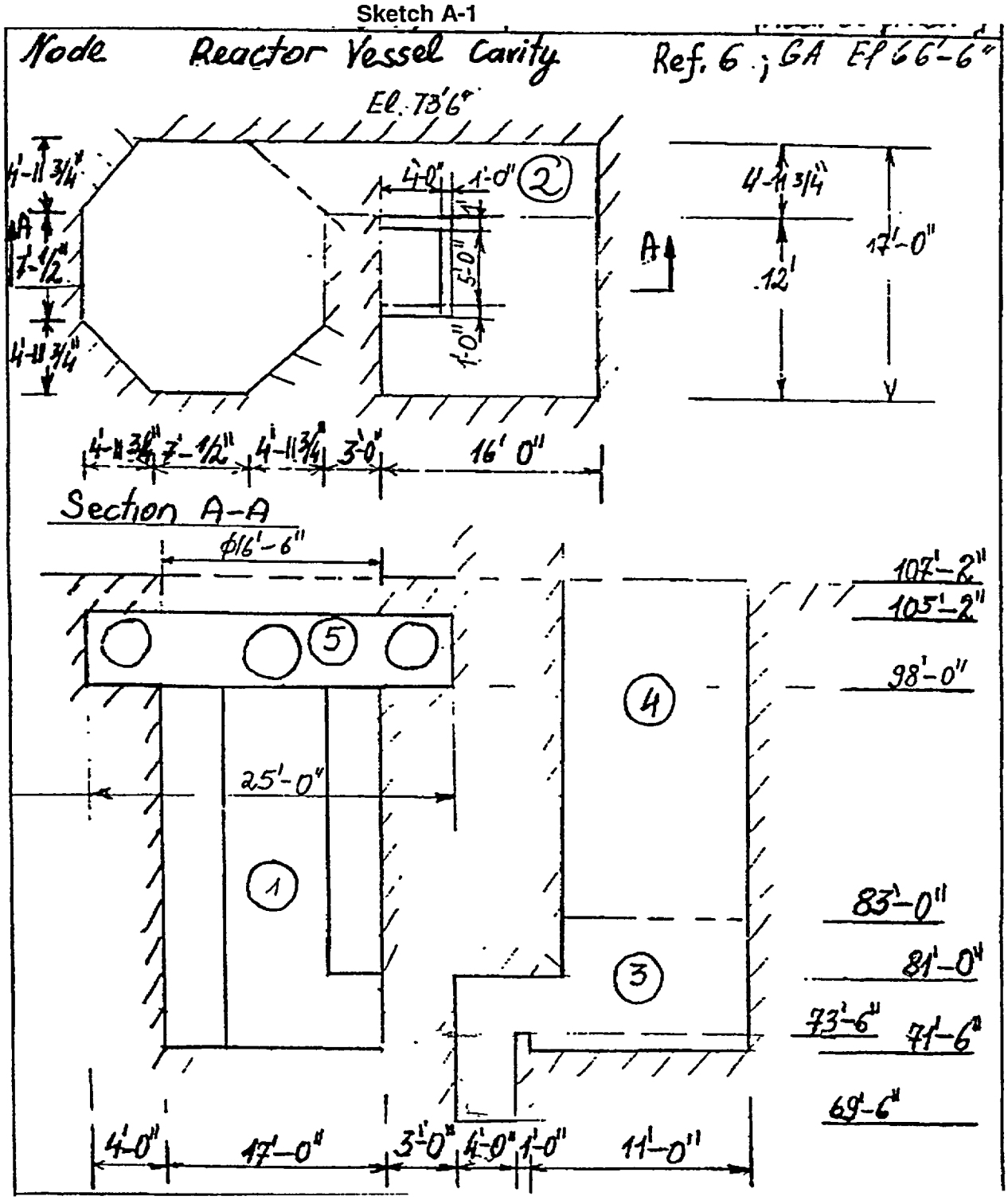
Node Reactor Vessel Cavity
Ref. 6 ; GA El 66'-6"
El. 73'6"
4'-11 3/4"
7'-1/2"
4'-11 3/4"
4'-0"
1'-0"
3'-0"
1'-0"
A
4'-11 3/4"
12'
17'-0"
4'-11 3/4"
7'-1/2"
4'-11 3/4"
3'-0"
16' 0"
Section A-A
ϕ16'-6"
107'-2"
105'-2"
98'-0"
25'-0"
83'-0"
81'-0"
73'-6"
71'-6"
69'-6"
4'-0"
17'-0"
3'-0"
4'-0"
1'-0"
11'-0"

Table B-1 AP1000 MAAP4 Discrepancies

No.	Parameter	DCD	MAAP4	Response
1	Height between core plates	4.7843 m	4.858 m	The value stated for the MAAP4 input is a composite of several input parameters. The distance between the inside surfaces of the core plates per Reactor Vessel Drawing APP-RXS-V2-002, rev 1 is 189.8 inches = 4.82 m. The difference is considered by Westinghouse to be negligible.
2	Number of steam generator tubes	10025	1000	The value in the MAAP4 parameter file is 10000, not 1000. 10000 is a number very close to 10025, and is easily within the realm of tube plugging. The difference is considered by Westinghouse to be negligible.

3	Water Volume in SG inlet and outlet plena	16.65 m^3	20.2 – 2.96
			17.24 m^3
				The volume of the steam generator tubes was calculated thusly:
				
				`** Water volume of primary head (incl. nozzles) = 661.2 ft3`
				`** number of tubes = 10000`
				`** ID of tubes = 0.607" = 0.051 ft`
				`** thickness of tubesheet = 31.13" = 2.59 ft`
				`** v = 661.2 + (10000 * pi/4 * 0.051^2 * 2.59) = 714.1 ft3`
				`**  = 20.2 m3`
				
				The calculation of the MAAP4 parameter VSGPHD only accounts for half the steam generator tube penetrations through the tubesheet. If the current value for the plenum volume and number of penetrations were properly accounted, the value for VSGPHD = 19.7 m^3. The difference is considered by Westinghouse to be negligible.

4	Primary Water Volume in SG Tubes Only	42.1638 m^3	61.3 – 20.2 = 41.1 m^3	The current value for the total primary volume of a steam generator's tubes is 1488.5 ft^3 (42.2 m^3). The difference is considered by Westinghouse to be negligible.
5	Secondary Cross Sectional Flow Area	not provided	9.54 m^2	The ID of the wrapper is 153.5 inches for a gross cross sectional area of 11.9 m^2. The OD of the tubes is 0.688 inches, so the total cross sectional area of 20000 tubes is 4.8 m^2. The net flow area through the bundle is 11.9 – 4.8 = 7.1 m^2. The calculation of the value in the MAAP4 parameter accounted for 10000 tubes in one direction. The impact of this discrepancy will be evaluated but is not anticipated to have a significant impact.
6	Heat Sink Elevations Discrepancies	not provided	See Table B-2	Corrected elevations and explanations provided in Table 1.

Table B-1 AP1000 MAAP4 Discrepancies

No.	Parameter	DCD	MAAP4	Response
7	High-3 Pressurizer Level	not provided	1.55 m	There is no hi-3 pressurizer level in the AP1000, so the value for ZWPZH in the MAAP4 parameter file is set above the elevation of the top of the pressurizer to defeat the setpoint in the code.

Table B-2 – Heat Sink Elevation Discrepancies

Heat Sink #	Node 1	Node 2	Lower Elevation (m)	Response
4	1 Loop 1	4 Cavity	30.96	Walls between the SG Compt and RPV Nozzle Gallery, which is included as part of the cavity volume. The elevation should be 98-ft = 29.87 m.
10	2 Loop 2	4 Cavity	30.96	
5	1 Loop 1	5 IRWST	44.23	Wall between SG compt and IRWST. Elev should be floor of IRWST 103'= 31.3944 m
6	1 Loop 1	6 Ucompt	38.11	Wall between SG compt and refueling canal. Elev. should be floor of refueling canal 84.5 ft = 25.76 m
11	2 Loop 2	6 Ucompt	36.45	
12	3 CMT	13 Env	32.66	Floor of CMT room. One sided heat sink (node 2 is a dummy number). Should be 107'-2" = 32.66 m.
13	3 CMT	13 Env	28.87	Walls of CMT room. Should be set to floor elev of CMT room 107'-2" = 32.66 m.
14	3 CMT	5 IRWST	44.23	Wall between CMT room and IRWST. Should be set to floor of CMT room = 107'-2" = 32.66 m.
15	3 CMT	6 Ucompt	35.26	Wall between CMT room and refueling canal. Should be set to floor of CMT room = 107'2" = 32.66 m.
16	3 CMT	6 Ucompt	41.22	Operating Deck Floor. Top Surface Elevation is 135'-3" = 41.22 m. Should be set to bottom surface elevation of 133'-3" = 40.61 m.
17	3 CMT	6 Ucompt	41.22	
18	3 CMT	11 PCS	36.64	Wall between CMT room and PCS annulus. Should be set to floor of PCS annulus = 109'-10" = 33.48 m.

21	4 Cavity	6 UCompt	30.98	Floor between refueling canal and the RPV nozzle gallery. Top surface elevation is 107'-2" = 32.66 m. Bottom surface = 105'-2" = 32.06 m.
24	5 IRWST	6 Ucompt	44.23	Wall between IRWST and Upper Compt. Should be set to the floor elev of the IRWST = 103' = 31.39 m.
25	5 IRWST	6 Ucompt	40.61	Ceiling between the IRWST and Upper Compt. Should be set to the IRWST ceiling elevation of 133.25' = 40.61 m.
39	7 PXS	3 CMT	32.1	The heat sink represents the ceiling of the PXS compartments (which is the floor of the CMT room). The elevation of the heat sink is set to the correct value of 105' 2" = 32.1 m, which is the ceiling elevation in each of the PXS compts (nodes 7 and 8) and the CVS compt (node 9).
42	8 PXS	3 CMT	32.1	
45	9 PXS	3 CMT	32.1	

AP1000 DESIGN CERTIFICATION REVIEW

Response to Request For Additional Information

RAI Number: 720.042

Question:

Westinghouse states that the overall AP1000 plant response to severe accidents as well as the mass, composition, and superheat characteristics of the initial debris relocation is very similar to the AP600, and therefore: (1) the results and insights from the AP600 hydrogen generation and mixing analyses for each accident class are applicable to the AP1000, (2) the release fractions and timing for the AP1000 release categories would be approximately the same as for the AP600, and (3) the conclusions of the AP600 analyses regarding the challenge to the lower head integrity from core debris relocation into the lower plenum and the challenge from ex-vessel steam explosions are applicable to AP1000. The premise for this conclusion is questionable given the large differences in core power and mass between the two designs, and the substantial differences in melt progression timing indicated in the results for 1A/1AP sequences in Chapter 36 of the AP1000 PRA. Also, the dominant accidents within each release category, and their relative contribution, may be different for AP1000 due to differences in the Level 1 PRA, and could lead to selection of different representative sequences for some of the release categories. Please provide AP1000-specific analyses of core melt progression and fission product releases for the dominant accident sequences within each release category, and use this information to either define AP1000-specific hydrogen releases and fission product source terms, or to substantiate the applicability of the AP600 hydrogen analyses and fission product releases to AP1000. This should include a comparison of event timing, fraction of core melted, hydrogen generation rates and quantities, mass and superheat characteristics of debris relocating into the lower plenum, and fission product release histories for representative sequences in each accident class.

Westinghouse Response:

AP1000-specific MAAP4.04 analyses for dominant accident sequences will be included in the next revision of the AP1000 PRA. The revisions to Chapter 34 and Chapter 41are attached. See the response to RAI 470.013 for the revision to Chapter 45. See the response to RAI 720.088 for the revision to Chapter 39. See the response to RAI 720.056 for the revision to Chapter 49.

Design Control Document (DCD) Revision:

DCD Section 19.34 will be revised as follows, consistent with the PRA revisions.

19.34 Severe Accident Phenomena Treatment

19.34.1 Introduction

This section describes how the AP1000 containment addresses challenges from severe accident phenomena, and how the challenges are evaluated in the probabilistic risk assessment (PRA). In the PRA, the Modular Accident Analysis Program (MAAP) version 4.04 code (Reference 19.34-8) is used to evaluate severe accident scenarios. Severe accident phenomenological uncertainties are treated with Risk-Oriented Accident Analysis Methodology (ROAMM) (Reference 19.34-2) phenomenological evaluations, with AP1000-specific decomposition event tree phenomenological evaluations or with assumptions that certain low-frequency severe accident phenomena fail the containment. The objective of these studies is to show, with a high degree of confidence, that the AP1000 containment will accommodate the effects of severe accidents in a range of scenarios for at least the first 24 hours after the onset of core damage. Such evaluations demonstrate the robustness of the containment design.

19.34.2 Treatment of Physical Processes

The following eight issues are identified in Reference 19.34-1 as being representative of the phenomenological issues pertaining to severe accident conditions:

1. Loss-of-coolant accident (LOCA)
2. Fuel-coolant interaction (steam explosion)
3. Hydrogen combustion and detonation
4. Melt attack on concrete structure or containment pressure boundary
5. High-pressure melt ejection
6. Core-concrete interaction (CCI)
7. Containment pressurization from decay heat
8. Elevated temperature (equipment survivability)

The challenge to the containment integrity from a LOCA blowdown is covered in the containment design basis and is not specifically addressed here. Treatment of physical processes affecting the remaining challenges is discussed in this chapter.

19.34.2.1 In-Vessel Retention of Molten Core Debris

In-vessel retention (IVR) of core debris by external reactor vessel cooling is a severe accident mitigation attribute of the AP1000 design; it is discussed in detail in Chapter 19.39. With the reactor vessel intact and debris retained in the lower head, phenomena such as molten core-concrete interaction and ex-vessel steam explosion, which occur as a result of core debris relocation to the reactor cavity, are prevented.

The AP1000 reactor vessel insulation and containment geometry promote in-vessel retention. Engineered design features of the AP1000 containment flood the containment reactor cavity region during accidents, and thereby, submerge the reactor vessel in water.

Chapter 39 of the AP1000 PRA presents an AP1000-specific evaluation to determine the likelihood that sufficient heat can be removed from the outside surface of the submerged reactor pressure vessel lower head to prevent reactor vessel failure and relocation of debris to containment. The methodology used to quantify the margin to vessel failure in Reference 19.34-2 for the AP600 was adapted to the AP1000. For the AP1000 the methodology assumes that:

- The RCS is depressurized.
- The reactor vessel is submerged above the 98-ft elevation in the containment.
- The reflective insulation promotes the two-phase natural circulation in the reactor vessel cooling annulus.
- The external surface treatment promotes wetability of the reactor vessel.

The containment event tree includes a node to ascertain that the reactor coolant system (RCS) is depressurized and a node to determine if adequate water is available in the cavity to achieve two-phase natural circulation. Success at both of these nodes is required to demonstrate that the conditions and assumptions of the IVR analysis are met. The AP1000 design specifies that the reactor vessel insulation is designed appropriately and that the outer surface of the reactor vessel promotes wetability.

Accounting for the uncertainties in thermal-hydraulic parameters, the heat fluxes to the vessel wall and reactor vessel internals from the debris pool are calculated. The results show large margin to failure for the reactor vessel if it is externally cooled by water.

19.34.2.2 Fuel-Coolant Interaction (Steam Explosions)

A steam explosion may occur as a result of molten metal or oxide core debris mixing with water and interacting thermally. Steam explosions are postulated to occur inside the reactor

vessel when debris relocates from the core region into the lower plenum and in the reactor cavity if the vessel fails and debris is ejected from it into water in the reactor cavity.

19.34.2.2.1 In-Vessel Fuel-Coolant Interaction

In-vessel steam explosions were studied extensively in the AP600 analyses. A ROAAM analysis of the AP600 reactor vessel lower head integrity under in-vessel steam explosion loading is presented in Reference 19.34-3. Typically, in-vessel steam explosion analyses focus on the α-mode containment failure, which is induced by the reactor vessel upper head failure. The ROAAM analysis focused on failure of the lower head since that steam explosion vessel failure mode would impair the in-vessel retention capability of the reactor vessel. The ROAAM analysis concludes that lower-head vessel failure from in-vessel steam explosion is physically unreasonable with very large margin to failure.

Based on the in-vessel core relocation scenario for the AP1000, the in-vessel steam explosion ROAAM analysis presented for the AP600 can be extended to the AP1000. The mass flow rate, superheat and composition of debris in the relocation from the upper core region to the lower head is expected to be essentially the same as the AP600. The geometry of the lower head of the AP1000 is the same as the AP600. Therefore, it is reasonable to extend the results of the AP600 in-vessel steam explosion ROAAM analysis to the AP1000.

The results of the in-vessel steam explosion ROAAM can also be extended to containment failure induced by in-vessel steam explosions (α-mode containment failure). The likelihood for vessel failure and subsequent containment failure due to in-vessel steam explosion is so small as to be negligible. This conclusion is in agreement with the conclusions of the U.S. Nuclear Regulatory Commission (NRC)-sponsored Steam Explosion Review Group (Reference 19.34-4).

19.34.2.2.2 Ex-Vessel Fuel-Coolant Interaction

The first level of defense for ex-vessel steam explosion is the in-vessel retention of the molten core debris. If molten debris does not relocate from the vessel to the containment, there are no conditions for ex-vessel steam explosion. In the event that the reactor cavity is not flooded and the vessel fails, the PRA containment event tree assumes that the containment fails in the early time frame.

An analysis of the structural response of the reactor cavity was performed for the AP600 (Reference 19.34-5, Appendix B). As in the in-vessel steam explosion analysis, the results of this AP600 ex-vessel steam explosion analysis are extended to the AP1000. The vessel failure modes for AP600 and AP1000 are the same. The initial debris mass, superheat and composition are assumed to be the same as the AP600. The reactor cavity geometry and water depth prior to vessel failure are the same as AP600. Therefore, the results of the AP600 ex-vessel steam explosion analysis are considered to be appropriate for the AP1000.

19.34.2.3 Hydrogen Combustion and Detonation

A decomposition event tree analysis discussed in Section 19.41 evaluates the potential for hydrogen combustion threatening the containment integrity during a severe accident sequence in the AP1000. The analysis examines diffusion flame burning and local detonation occurring during in-vessel hydrogen generation prior to hydrogen mixing in the containment and global deflagration and detonation, which may occur later when the hydrogen is mixed throughout the containment. Only in-vessel hydrogen generation is considered, since vessel failure and ex-vessel debris relocation is assumed to fail containment.

The AP1000 provides defense-in-depth to address hydrogen diffusion flames that may challenge containment integrity. The first level of defense is the stage four automatic depressurization system ~~lines~~ (ADS Stage 4) lines from the ~~reactor coolant system (~~RCS,~~)~~ which prevent significant hydrogen releases to the in-containment refueling water storage tank (IRWST) and PXS compartments. ADS- Stage 4 vents from the RCS hot legs to the loop compartments, which are shielded from the containment shell and have a constant source of oxygen from the natural circulation in the containment. Hydrogen can burn as a diffusion flame in the loop compartments without threatening the containment integrity. If ADS Stage 4 fails, the AP1000 has provided design considerations in ~~the in-containment refueling water storage tank~~ IRWST vents to mitigate diffusion flames near the containment walls. Vents from the passive injection system compartments and chemical volume and control system compartment are located away from the containment shell and penetrations in order to mitigate the threat from hydrogen diffusion flames.

Containment failure from a directly initiated detonation wave is not considered to be a credible event for the AP1000 containment. There are no ignition sources of sufficient energy to directly initiate a detonation in the AP1000 containment. Deflagration to detonation transition (DDT) is considered to the be the only likely mechanism to produce a detonation in the AP1000 containment.

The likelihood of DDT in the AP1000 containment is evaluated locally in confined compartments during in-vessel hydrogen generation and globally after in-vessel generation is concluded and hydrogen is mixed in the containment. For a DDT to occur, the combination of the gas mixture sensitivity to detonation and the geometric configuration potential for flame acceleration must be conducive to DDT. Since the hydrogen concentration necessary to form a detonable mixture depends on the size of the enclosure, concentration requirements for DDT in different regions of the AP1000 containment are extrapolated from the FLAME facility data (Reference 19.34-6) using scaling arguments based on the detonation cell width. The geometric requirement is evaluated considering aspects such as the degree of confinement and the extent and type of obstacles present in the postulated flame propagation path. In all cases, DDT is assumed to result in containment failure in the containment event tree analysis.

Global hydrogen deflagration and the potential for containment failure are modeled on the containment event tree. Adiabatic, isochoric, complete combustion (AICC) is assumed, and peak pressure probability distributions are developed for the accident scenarios. The probability of containment failure due to hydrogen deflagration is evaluated from the containment failure probability distribution combined with the peak pressure probability distribution.

19.34.2.4 High-Pressure Melt Ejection

The AP1000 incorporates design features that prevent high-pressure core melt. These features include the passive residual heat removal (PRHR) system and the ~~automatic depressurization system (~~ADS~~)~~. These design features provide primary system heat removal and depressurization to prevent high pressure core damage conditions. The consequences from postulated high pressure melt ejection (HPME) are mitigated by the containment layout which provides a torturous pathway to the upper compartment, and no direct pathway for the impingement of debris on the containment shell.

In high-pressure core damage sequences the potential exists for creep-rupture-induced failures of the RCS piping at the hot-leg nozzles, the surge line, the steam generator tubes and, given debris relocation to the lower plenum, in the reactor vessel lower head. Failure of the hot-leg nozzle or surge line prior to failures of other components results in the rapid depressurization of the RCS. Failure of the steam generator tubes results in a containment bypass and a large release of fission products to the environment. Failure of the lower head of the reactor vessel results in the potential for HPME.

Hot-leg nozzle failure is expected prior to steam generator tube failure, but because of large uncertainties, hot-leg nozzle creep rupture failure is not credited with preventing steam generator tube failure. In the PRA, steam generator tube failure is assumed for high-pressure sequences in the containment event tree analysis unless operator action to depressurize the RCS with the ADS is successful.

19.34.2.5 Core Debris Coolability

In accident sequences where the reactor pressure vessel failure is not prevented, core debris may be discharged into the reactor cavity. The likely vessel failure modes produce a low pressure melt ejection (LPME) to the containment. The AP1000 cavity design provides area for the core debris to spread. Condensate from the passive containment cooling system (PCS) returns to the reactor cavity, thereby providing a long-term supply of water to cool the core debris.

At vessel failure it is very likely that the cavity will be filled with water from the RCS, CMTs and accumulators to at least the 83-ft elevation. There are significant uncertainties associated

with debris spreading into a water-filled cavity. Debris-spreading is mainly a function of the highly uncertain vessel failure mode. A large-scale lower-head failure releasing debris at a high rate would enhance spreading, while a localized failure mode would release debris at a slow rate, which would most likely cause the debris to pile up under the reactor vessel and minimize spreading.

Given the uncertainties in the debris-spreading and in non-condensable gas generation and combustion, the containment event tree analysis does not credit containment integrity in the event of failure of the lower head of the vessel and relocation of the core.

A limited set of deterministic analyses of debris spreading and core-concrete interaction in the AP1000 cavity is presented in Appendix 19-B. The analyses show that basemat melt-through is not predicted to occur within 24 hours of the accident initiation. Basemat melt through is predicted to occur before pressurization of the containment by non-condensable gases challenges the containment integrity.

19.34.2.6 Containment Pressurization from Decay Heat

The AP1000 containment is cooled via the ~~Passive Containment Cooling System~~PCS (see Section 19.40). Evaporative water cooling of the containment shell provides long term containment cooling and limits the containment pressure to less than the design pressure for all severe accident events except hydrogen combustion (which is addressed separately). Containment water is provided to the top of the containment via redundant, diverse system of valves and lines, including a line that can be connected to an outside water source, such as a fire truck.

In the unlikely event that water cannot be supplied to the top of the containment shell for an extended period of time, air-only cooling by air flowing through the PCS annulus provides significant cooling to the containment. Under the right environmental conditions, the containment is expected to reach an equilibrium pressure that will not challenge containment integrity. However, under nominal to conservative environmental conditions, containment integrity by air-cooling alone cannot be assured. In this case, containment failure is predicted to occur more than 24 hours after accident initiation.

A significant amount of time is available for operator action to vent the containment under the severe accident management guidance (SAMG). Containment venting mitigates uncontrolled releases of fission products from a failed containment. The AP1000 can be vented on an ad-hoc basis under the SAMG from a number of containment penetrations. Containment venting also reduces the partial pressure of non-condensable gases in the containment, and thus creates a new containment underpressure failure mode that may occur if containment is cooled after venting.

19.34.2.7 Elevated Temperatures (Equipment Survivability)

Reference 19.34-7 states that equipment identified as being useful to mitigate the consequences of severe accidents must be designed to provide reasonable assurance that it will continue to operate in a severe accident environment for the length of time ~~duration it is~~ needed to accomplish its function. Also, 10 CFR 50.34(f) requires safety equipment to continue performing its function after being exposed to a containment environment created as a consequence of generating a quantity of hydrogen equivalent to that from 100-percent cladding oxidation. As the AP1000 design uses thermal igniters to burn hydrogen in a controlled manner, it is necessary to demonstrate that the safety equipment can continue to perform its function in the high-temperature environment created by the hydrogen burning.

The functions of the equipment in containment for which credit is taken in the AP1000 PRA were reviewed to determine if the equipment is required to operate in a severe accident environment and beyond design basis limits. The equipment and the basis for operation are the same as the AP600. Therefore, the results of the AP600 are extended to the AP1000 for equipment survivability.

19.34.2.8 Summary

The potential for and the consequences of severe accident phenomena are evaluated. The preventive and mitigative features of the AP1000 addressing the severe accident phenomena are discussed. This information is applied to the containment event trees and used in the quantification of the large release frequency.

19.34.3 Analysis Method

This section intentionally blank

19.34.4 Severe Accident Analyses

This section intentionally blank

19.34.5 Insights and Conclusions

The analyses of the severe accident phenomena for the AP1000 PRA highlight the following insights and conclusions:

- The design of the AP1000 reactor vessel, vessel insulation and reactor cavity, and the ability to flood the cavity after a severe accident reduce the potential challenges to the containment integrity by maintaining the vessel integrity.
- Should a failure of the reactor vessel occur, the design of the reactor cavity enhances the ability to cool any core debris that exits the vessel.

- Lower head vessel failure due to in-vessel steam explosions is physically unreasonable.
- The ADS and PRHR system are design features that can be used to prevent high-pressure core melt in a severe accident.
- A directly-initiated hydrogen detonation in the AP1000 containment is not a credible event.
- The equipment needed to mitigate the consequences of a severe accident is designed to provide reasonable assurance that it will continue to operate during an accident.

19.34.36 References

19.34-1 Letter from D. A. Ward, Advisory Committee on Reactor Safeguards, to K. A. Carr, Chairman, Nuclear Regulatory Commission, "Proposed Criteria to Accommodate Severe Accidents in Containment Design," dated May 17, 1991.

19.34-2 Theofanous, T. G., et al., "In-Vessel Coolability and Retention of a Core Melt," DOE/ID-10460, July 1995.

19.34-3 Theofanous, T. G., et al., "Lower Head Integrity Under In-Vessel Steam Explosion Loads," DOE/ID-10541, July 1996.

19.34-4 NUREG-1116, *A Review of the Current Understanding of the Potential for Containment Failure From In-Vessel Steam Explosions*, 1985.

19.34-5 GW-GL-021, AP600 Probabilistic Risk Assessment, August 1998.

19.34-6 Sherman, M. P., Tieszen, S. R., and Benedick, W. B., *FLAME Facility - The Effects of Obstacles and Transverse Venting on Flame Acceleration and Transition to Detonation for Hydrogen-Air Mixtures at Large Scale*, NUREG/CR-5275, April 1989.

19.34-7 Attachment to letter from D. M. Crutchfield, Office of Nuclear Reactor Regulation, to E. E. Kintner, Advanced Light Water Reactor Steering Committee, "Major Technical and Policy Issues Concerning the Evolutionary and Passive Plant Designs," dated February 27, 1992.

19.34-8 "EPRI MAAP 4.0 Users Manual"

TABLES 19.34-1 THROUGH 19.34-26 NOT INCLUDED IN THE DCD

FIGURES 19.34-1 THROUGH 19.34-391 NOT INCLUDED IN THE DCD

PRA Revision:

The following pages provide the markups of AP1000 PRA Chapters 34 and 41.

CHAPTER 34

SEVERE ACCIDENT PHENOMENA TREATMENT

34.1 Introduction

This chapter describes how the AP1000 containment addresses challenges from severe accident phenomena, and how the challenges are evaluated in the probabilistic risk assessment (PRA). In the PRA, the Modular Accident Analysis Program (MAAP) version 4.04 code (Reference 34-8) is used to evaluate severe accident scenarios. Severe accident phenomenological uncertainties are treated with Risk-Oriented Accident Analysis Methodology (ROAMM) (Reference 34-2) phenomenological evaluations, with AP1000-specific decomposition event tree phenomenological evaluations or with assumptions that certain low-frequency severe accident phenomena fail the containment. The objective of these studies is to show, with a high degree of confidence, that the AP1000 containment will accommodate the effects of severe accidents in a range of scenarios for at least the first 24 hours after the onset of core damage. Such evaluations demonstrate the robustness of the containment design.

34.2 Treatment of Physical Processes

The following eight issues are identified in Reference 34-1 as being representative of the phenomenological issues pertaining to severe accident conditions.~~:~~

1. Loss-of-coolant accident (LOCA)
2. Fuel-coolant interaction (steam explosion)
3. Hydrogen combustion and detonation
4. Melt attack on concrete structure or containment pressure boundary
5. High-pressure melt ejection
6. Core-concrete interaction (CCI)
7. Containment pressurization from decay heat
8. Elevated temperature (equipment survivability)

The challenge to the containment integrity from a LOCA blowdown is covered in the containment design basis and is not specifically addressed here. Treatment of physical processes affecting the remaining challenges is discussed in this chapter. For the AP1000 design, issues 4 and 6 above arise primarily from the same physical processes~~,~~: ex-vessel debris coolability. Therefore, they are discussed together within that subject in Section 34.2.5.

Phenomenological analyses and event trees are developed for key severe accident phenomena to provide a systematic and logical method to investigate the uncertainties in the phenomena.

34.2.1 In-Vessel Retention of Molten Core Debris

In-vessel retention (IVR) of core debris by external reactor vessel cooling is a severe accident mitigation attribute of the AP1000 design; it is discussed in detail in Chapter 39. With the reactor vessel intact and debris retained in the lower head, phenomena such as molten core-concrete interaction and ex-vessel steam explosion, which occur as a result of core debris relocation to the reactor cavity, are prevented.

The AP1000 reactor vessel insulation and containment geometry promote in-vessel retention. Engineered design features of the AP1000 containment flood the containment reactor cavity region during accidents, and thereby, submerge the reactor vessel in water. Liquid effluent released through the break during a LOCA event is directed to the reactor cavity. The AP1000 functional restoration guidelines include a provision for draining the in-containment refueling water storage tank (IRWST) water into the reactor cavity through an operator action action if automatic draining fails. Therefore, in an accident the reactor pressure vessel is most likely submerged in water.

Chapter 39 presents an AP1000-specific evaluation to determine the likelihood that sufficient heat can be removed from the outside surface of the submerged reactor pressure vessel lower head to prevent reactor vessel failure and relocation of debris to containment. The methodology used to quantify the margin to vessel failure in Reference 34-2 for the AP600 was adapted to the AP1000. For the AP1000 the methodology assumes that:

- The RCS is depressurized.
- The reactor vessel is submerged above the 98-ft elevation in the containment.
- The reflective insulation promotes the two-phase natural circulation in the reactor vessel cooling annulus.
- The external surface treatment promotes wetability of the reactor vessel.

The containment event tree includes a node to ascertain that the reactor coolant system (RCS) is depressurized and a node to determine if adequate water is available in the cavity to achieve two-phase natural circulation. Success at both of these nodes is required to demonstrate that the conditions and assumptions of the IVR analysis presented in Chapter 39 are met. The AP1000 design specifies that the reactor vessel insulation is designed appropriately and that the outer surface of the reactor vessel promotes wetability.

Accounting for the uncertainties in thermal-hydraulic parameters, the heat fluxes to the vessel wall and reactor vessel internals from the debris pool are calculated. These heat fluxes are compared to the critical heat flux limit for the downward-facing curved surface. Vessel failure is assumed if the critical heat flux is exceeded. The results show large margin to failure for the reactor vessel if it is externally cooled by water. Therefore, reactor vessel

integrity is assured at node VF in the containment event tree analysis if the reactor coolant system is depressurized and the cavity adequately flooded.

34.2.2 Fuel-Coolant Interaction (Steam Explosions)

A steam explosion may occur as a result of molten metal or oxide core debris mixing with water and interacting thermally. Steam is created at a very high rate, producing a sonic pressure front and dynamic loading on local structures. Steam explosions are postulated to occur inside the reactor vessel when debris relocates from the core region into the lower plenum and in the reactor cavity if the vessel fails and debris is ejected from it into water in the reactor cavity.

34.2.2.1 In-Vessel Fuel-Coolant Interaction

In-vessel steam explosions were studied extensively in the AP600 analyses. A ROAAM analysis of the AP600 reactor vessel lower head integrity under in-vessel steam explosion loading is presented in Reference 34-3. The analysis focused on failure of the lower head since that steam explosion vessel failure mode would impair the in-vessel retention capability of the reactor vessel. The ROAAM analysis concludes that lower-head vessel failure from in-vessel steam explosion is physically unreasonable with very large margin to failure.

Based on the in-vessel core relocation scenario for the AP1000, the in-vessel steam explosion ROAAM analysis presented for the AP600 can be extended to the AP1000. Molten debris relocation from the upper core region to the lower plenum is expected to occur as a result of a sidewall failure of the core shroud and core barrel. Downward relocation is not considered to be a reasonable relocation mode due to the large heat sink below the active fuel region formed by the fuel rod lower plenum zircaloy plugs, the bottom nozzles of the fuel assemblies and the lower core support plate. The sideward failure allows a limited mass of molten debris to initially relocate to the lower plenum. The mass flow rate, superheat and composition of debris in the relocation from the upper core region to the lower head is expected to be essentially the same as the AP600. The geometry of the lower head of the AP1000 is the same as the AP600. Therefore, it is reasonable to extend the results of the AP600 in-vessel steam explosion ROAAM analysis to the AP1000.

The results of the in-vessel steam explosion ROAAM can also be extended to containment failure induced by in-vessel steam explosions (α-mode containment failure). The sideward failure mode does not initially relocate sufficient debris to the lower head. The in-vessel fuel-coolant interaction cannot generate sufficient energy, in a short time scale, to produce a missile that could fail the AP1000 containment. The likelihood for vessel failure and subsequent containment failure due to in-vessel steam explosion is so small as to be negligible. This conclusion is in agreement with the conclusions of the U.S. Nuclear Regulatory Commission (NRC)-sponsored Steam Explosion Review Group (Reference 34-4).

34.2.2.2 Ex-Vessel Fuel-Coolant Interaction

The first level of defense for ex-vessel steam explosion is the in-vessel retention of the molten core debris. If molten debris does not relocate from the vessel to the containment, there are no conditions for ex-vessel steam explosion. In the event that the reactor cavity is not flooded and the vessel fails, the PRA containment event tree assumes that the containment fails in the early time frame.

An analysis of the structural response of the reactor cavity was performed for the AP600 (Reference 34-5, Appendix B). As in the in-vessel steam explosion analysis, the results of this AP600 ex-vessel steam explosion analysis are extended to the AP1000. The vessel failure modes for AP600 and AP1000 are the same. The initial debris mass, superheat and composition are assumed to be the same as the AP600. The mass assumption is conservative since the AP1000 vessel lower head is closer to the cavity floor resulting in less debris mass participating in the interaction. The reactor cavity geometry and water depth prior to vessel failure are the same as AP600. Therefore, the results of the AP600 ex-vessel steam explosion analysis are considered to be appropriate for the AP1000.

34.2.3 Hydrogen Combustion and Detonation

A decomposition event tree analysis discussed in Chapter 41 evaluates the potential for hydrogen combustion threatening the containment integrity during a severe accident sequence in the AP1000. The analysis examines diffusion flame burning and local detonation occurring during in-vessel hydrogen generation prior to hydrogen mixing in the containment and global deflagration and detonation, which may occur later when the hydrogen is mixed throughout the containment. Only in-vessel hydrogen generation is considered, since vessel failure and ex-vessel debris relocation is assumed to fail containment.

If the igniters are operational, the potential for diffusion-flame-induced containment failures is considered during the hydrogen generation and release from the reactor coolant system (RCS)~~RCS~~. Diffusion flames may be formed when high-concentration, nonflammable hydrogen plumes encounter oxygen and burn as a standing flame. Flames that have a large view factor or that impinge on the containment pressure boundary may fail the containment pressure boundary due to the locally high temperatures. The pathways that in-vessel hydrogen can take to containment are reviewed for potential impact on containment integrity. Locations where diffusion flames may be postulated are examined for potential failure of the containment due to creep of the containment shell at high temperature.

The AP1000 provides defense-in-depth to address hydrogen diffusion flames that may challenge containment integrity. The first level of defense is the stage four automatic depressurization system ~~lines~~ (ADS- Stage 4) lines from the ~~reactor coolant system (~~RCS,~~)~~ which prevent significant hydrogen releases to the in-containment refueling water storage tank (IRWST) and PXS compartments. The ADS- Stage 4 lines provide a path of least resistance to release hydrogen generated in-vessel to the containment. ADS- Stage 4 vents from the RCS hot legs to the loop compartments, which are shielded from the containment

shell and have a constant source of oxygen from the natural circulation in the containment. Hydrogen can burn as a diffusion flame in the loop compartments without threatening the containment integrity. If ADS- Stage 4 fails, the AP1000 has provided design considerations in the ~~in-containment refueling water storage tank~~ IRWST vents to mitigate diffusion flames near the containment walls. Vents from the passive injection system compartments and chemical volume and control system compartment are located away from the containment shell and penetrations in order to mitigate the threat from hydrogen diffusion flames.

Containment failure from a directly initiated detonation wave is not considered to be a credible event for the AP1000 containment. There are no ignition sources of sufficient energy to directly initiate a detonation in the AP1000 containment. Deflagration to detonation transition (DDT) is considered to the be the only likely mechanism to produce a detonation in the AP1000 containment.

The likelihood of DDT in the AP1000 containment is evaluated locally in confined compartments during in-vessel hydrogen generation and globally after in-vessel generation is concluded and hydrogen is mixed in the containment. For a DDT to occur, the combination of the gas mixture sensitivity to detonation and the geometric configuration potential for flame acceleration must be conducive to DDT. Since the hydrogen concentration necessary to form a detonable mixture depends on the size of the enclosure, concentration requirements for DDT in different regions of the AP1000 containment are extrapolated from the FLAME facility data (Reference 34-6) using scaling arguments based on the detonation cell width. The geometric requirement is evaluated considering aspects such as the degree of confinement and the extent and type of obstacles present in the postulated flame propagation path. In all cases, DDT is assumed to result in containment failure in the containment event tree analysis.

Global hydrogen deflagration and the potential for containment failure are modeled on the containment event tree. Adiabatic, isochoric, complete combustion (AICC) is assumed, and peak pressure probability distributions are developed for the accident scenarios. The probability of containment failure due to hydrogen deflagration is evaluated from the containment failure probability distribution combined with the peak pressure probability distribution.

34.2.4 High-Pressure Melt Ejection

The AP1000 incorporates design features that prevent high-pressure core melt. These features include the passive residual heat removal (PRHR) system and the ~~automatic depressurization system (ADS)~~. These design features provide primary system heat removal and depressurization to prevent high pressure core damage conditions. The consequences from postulated high pressure melt ejection (HPME) are mitigated by the containment layout, which provides a torturous pathway to the upper compartment~~,~~ and no direct pathway for the impingement of debris on the containment shell.

In high-pressure core damage sequences (~~that is~~i.e., non-LOCA or very small LOCA events with the ADS and ~~passive residual heat removal~~PRHR inoperable), the potential exists for creep-rupture-induced failures of the RCS piping at the hot-leg nozzles, the surge line, the steam generator tubes and, given debris relocation to the lower plenum, in the reactor vessel lower head. Failure of the hot-leg nozzle or surge line prior to failures of other components results in the rapid depressurization of the RCS. Failure of the steam generator tubes results in a containment bypass and a large release of fission products to the environment. Failure of the lower head of the reactor vessel results in the potential for HPME.

The AP1000 RCS loops have canned-motor pumps mounted to the steam generator outlet plenum. The coolant loops do not have water-trap loop seals as in conventional plant designs. A large natural-circulation flow heats the reactor coolant loop components in a relatively uniform manner. Hot-leg nozzle failure is expected prior to steam generator tube failure, but because of large uncertainties, hot-leg nozzle creep rupture failure is not credited with preventing steam generator tube failure. In the PRA, steam generator tube failure is assumed for high-pressure sequences in the containment event tree analysis unless operator action to depressurize the RCS with the ADS is successful.

34.2.5 Core Debris Coolability

In accident sequences where the reactor pressure vessel failure is not prevented, core debris may be discharged into the reactor cavity. The likely vessel failure modes produce a low pressure melt ejection (LPME) to the containment. The AP1000 cavity design provides area for the core debris to spread. Condensate from the passive containment cooling system (PCS) returns to the reactor cavity, thereby providing a long-term supply of water to cool the core debris.

To accommodate the requirements for in-vessel retention of core debris, the AP1000 provides highly reliable RCS depressurization and cavity flooding capability. At vessel failure it is very likely that the cavity will be filled with water from the RCS, CMTs and accumulators to at least the 83-ft elevation. There are significant uncertainties associated with debris spreading into a water-filled cavity. ~~Debris~~ Debris-spreading is mainly a function of the highly uncertain vessel failure mode. A large-scale lower-head failure releasing debris at a high rate would enhance spreading, while a localized failure mode would release debris at a slow rate, which would most likely cause the debris to pile up under the reactor vessel and minimize spreading.

Given the uncertainties in the ~~debris~~ debris-spreading and in non-condensable gas generation and combustion, the containment event tree analysis does not credit containment integrity in the event of failure of the lower head of the vessel and relocation of the core.

A limited set of deterministic analyses of debris spreading and core-concrete interaction in the AP1000 cavity is presented in Appendix B. The analyses show that basemat melt-through is not predicted to occur within 24 hours of the accident initiation. Basemat melt through is

predicted to occur before pressurization of the containment by non-condensable gases challenges the containment integrity.

34.2.6 Containment Pressurization from Decay Heat

The AP1000 containment is cooled via the ~~Passive Containment Cooling System~~PCS (see Chapter 40). Evaporative water cooling of the containment shell provides ~~long~~ long-term containment cooling and limits the containment pressure to less than the design pressure for all severe accident events except hydrogen combustion, ~~(~~which is addressed separately~~)~~. Containment water is provided to the top of the containment via a redundant, diverse system of valves and lines, including a line that can be connected to an outside water source~~,~~ such as a fire truck.

In the unlikely event that water cannot be supplied to the top of the containment shell for an extended period of time, air-only cooling by air flowing through the PCS annulus provides significant cooling to the containment. Under the right environmental conditions, the containment is expected to reach an equilibrium pressure that will not challenge containment integrity. However, under ~~nominal~~ nominal ~~to~~ to-conservative environmental conditions, containment integrity by air-only cooling ~~alone~~ cannot be assured. In this case, containment failure is predicted to occur more than 24 hours after accident initiation.

A significant amount of time is available for operator action to vent the containment under the severe accident management guidance (SAMG). Containment venting mitigates uncontrolled releases of fission products from a failed containment. The AP1000 can be vented on an ad-hoc basis under the SAMG from a number of containment penetrations. Once venting is concluded, the increased steam concentration in the containment improves the air-only cooling from the PCS such that no further venting is anticipated. Containment venting also reduces the partial pressure of non-condensable gases in the containment, and thus creates a new containment underpressure failure mode that may occur if containment is cooled after venting.

34.2.7 Elevated Temperatures (Equipment Survivability)

Reference 34-7 states that equipment identified as being useful to mitigate the consequences of severe accidents must be designed to provide reasonable assurance that it will continue to operate in a severe accident environment for the ~~duration it is~~ length of time needed to accomplish its function. Also, 10 CFR 50.34(f) requires safety equipment to continue performing its function after being exposed to a containment environment created as a consequence of generating a quantity of hydrogen equivalent to that from 100-percent cladding oxidation. As the AP1000 design uses thermal igniters to burn hydrogen in a controlled manner, it is necessary to demonstrate that the safety equipment can continue to perform its function in the high-temperature environment created by the hydrogen burning.

The functions of the equipment in containment for which credit is taken in the AP1000 PRA were reviewed to determine if the equipment is required to operate in a severe accident

environment and beyond design basis limits. The equipment and the basis for operation are the same as the AP600. Therefore, the results of the AP600 are extended to the AP1000 for equipment survivability. In the calculation of the large release frequency (LERF), only the containment pressure boundary is credited to perform beyond its design basis. The performance of the AP1000 containment pressure boundary beyond its design basis is evaluated in Chapter 42. Other equipment is credited in the analysis, but either the containment environmental conditions do not exceed the equipment qualification conditions at the time the function is performed, or the design basis for the equipment is a severe accident environment. The radiation environment for equipment qualification for safety-related equipment in containment is based on the severe accident source term involving significant in-vessel fuel melting described in NUREG-1465. The equipment credited in the ~~large release frequency~~LERF calculation is assumed to survive the radiation dose associated with the accidents over the time ~~it is~~ required to perform its function.

34.2.8 Summary

The potential for and the consequences of severe accident phenomena are evaluated. The preventive and mitigative features of the AP1000 addressing the severe accident phenomena are discussed. This information is applied to the containment event trees and used in the quantification of the ~~large release frequency~~LERF.

34.3 ~~References~~Analysis Method

The analyses of the fission-product source terms for the release categories discussed in Chapter 45 are completed with the MAAP4.04 computer code (Reference 34-8).

The following sections are presented for each of the accident classes for the fission-product source term MAAP4.04 analyses. First, the intact containment (IC) analyses are described, including any sensitivity analyses completed to define the most conservative system assumptions, then the relevant containment failure analyses are presented.

34.4 Severe Accident Analyses

34.4.1 Accident Class 3BE - Intact Containment

34.4.1.1 3BE-1

The sequence description and assumptions are listed below.

- DVI line break in PXS compartment (PXS is flooded through broken DVI line)
- Failure of PRHR
- 2/2 ADS stage 1 - automatic

- 2/2 ADS stage 2 - automatic
- 2/2 ADS stage 3 - automatic
- 4/4 ADS stage 4 - automatic
- 1/2 CMTs
- 1/2 accumulators
- 0/2 IRWST gravity injection lines
- 0/2 IRWST recirculation lines
- 2/2 cavity flooding lines
- Hydrogen igniters operating

No containment failure is considered, thus the release category is IC; however, normal leakage from the containment is assumed.

The main events of the case are shown in Table 34-4, while relevant plots are presented in Figures 34-1 through 34-17.

34.4.1.2 3BE-2

The sequence description and assumptions are listed below.

- DVI line break in PXS compartment (PXS is not flooded through broken DVI line)
- Failure of PRHR
- 2/2 ADS stage 1 - automatic
- 2/2 ADS stage 2 - automatic
- 2/2 ADS stage 3 - automatic
- 4/4 ADS stage 4 - automatic
- 1/2 CMTs
- 1/2 accumulators
- 0/2 IRWST gravity injection lines

- 0/2 IRWST recirculation lines
- 2/2 cavity flooding lines
- Hydrogen igniters operating

The main events of the case are shown in Table 34-5, while relevant plots are presented in Figures 34-18 through 34-34. Note that without flooding of the PXS compartment, RCS reflood does not occur.

34.4.1.3 3BE-4

The sequence description and assumptions are listed below.

- One valve of ADS Stage 4 spuriously opens
- Failure of PRHR
- 2/2 ADS stage 1 - automatic
- 2/2 ADS stage 2 - automatic
- 2/2 ADS stage 3 - automatic
- 4/4 ADS stage 4 - automatic
- 2/2 CMTs
- 2/2 accumulators
- 0/2 IRWST gravity injection lines
- 0/2 IRWST recirculation lines
- 2/2 cavity flooding lines
- Hydrogen igniters operating

The main events of the case are shown in Table 34-6, while relevant plots are presented in Figures 34-35 through 34-51.

34.4.1.4 3BE-5

The sequence description and assumptions are listed below

- 2-inch hot-leg break to steam generator compartment
- Failure of PRHR
- 2/2 ADS stage 1 - automatic
- 2/2 ADS stage 2 - automatic
- 2/2 ADS stage 3 - automatic
- 4/4 ADS stage 4 - automatic
- 2/2 CMTs
- 2/2 accumulators
- 0/2 IRWST gravity injection lines
- 0/2 IRWST recirculation lines
- 2/2 cavity flooding lines
- Hydrogen igniters operating

The main events of the case are shown in Table 34-7, while relevant plots are presented in Figures 34-52 through 34-68.

34.4.1.5 3BE-6

The sequence description and assumptions are listed below.

- 2-inch hot-leg break to steam generator compartment
- Failure of PRHR
- 2/2 ADS stage 1 - automatic
- 2/2 ADS stage 2 - automatic
- 2/2 ADS stage 3 - automatic
- 4/4 ADS stage 4 - automatic
- 2/2 CMTs

- 2/2 accumulators
- 0/2 IRWST gravity injection lines
- 0/2 IRWST recirculation lines
- 1/2 cavity flooding lines
- Hydrogen igniters operating

The main events of the case are shown in Table 34-8, while relevant plots are presented in Figures 34-69 through 34-85.

34.4.2 Accident Class 3BE - Failed Containment

34.4.2.1 3BE-7

The sequence description and assumptions are listed below.

- 2-inch hot-leg break to steam generator compartment
- Containment failure at peak of debris quench (vessel failure)
- Failure of PRHR
- 2/2 ADS stage 1 - automatic
- 2/2 ADS stage 2 - automatic
- 2/2 ADS stage 3 - automatic
- 4/4 ADS stage 4 - automatic
- 2/2 CMTs
- 2/2 accumulators
- 0/2 IRWST gravity injection lines
- 0/2 IRWST recirculation lines
- 0/2 cavity flooding lines
- Hydrogen igniters operating

The main events of the case are shown in Table 34-9, while relevant plots are presented in Figures 34-86 through 34-102.

34.4.2.2 3BE -3

The sequence description and assumptions are listed below.

- DVI line break in PXS compartment (PXS is flooded through broken DVI line)
- Hydrogen burn and containment failure after reflood
- Failure of PRHR
- 2/2 ADS stage 1 - automatic
- 2/2 ADS stage 2 - automatic
- 2/2 ADS stage 3 - automatic
- 4/4 ADS stage 4 - automatic
- 1/2 CMTs
- 1/2 accumulators
- 0/2 IRWST gravity injection lines
- 0/2 IRWST recirculation lines
- 2/2 cavity flooding lines
- No hydrogen igniters operating

The main events of the case are shown in Table 34-10, while relevant plots are presented in Figures 34-103 through 34-119.

34.4.3 Accident Class 3BL - Intact Containment

34.4.3.1 3BL-1

The sequence description and assumptions are listed below.

- 2-inch hot-leg break to steam generator compartment
- Failure of PRHR

- 2/2 ADS stage 1 - automatic
- 2/2 ADS stage 2 - automatic
- 2/2 ADS stage 3 - automatic
- 4/4 ADS stage 4 - automatic
- 2/2 CMTs
- 2/2 accumulators
- 2/2 IRWST gravity injection lines
- 0/2 IRWST recirculation lines
- Hydrogen igniters operating
- Cavity flooding unnecessary (IRWST gravity injection successful)

No containment failure is considered, thus the release category is IC; however, normal leakage from the containment is assumed. Reflooding the core via the hot leg break is not credited.

The main events of the case are shown in Table 34-11, while relevant plots are presented in Figures 34-120 through 34-136

34.4.3.2 3BL-2

This case compares the results of changes to system assumptions to the dominant sequence discussed above. The results of this comparison are used to define the system assumptions for subsequent 3BL containment failure analyses.

The sequence description and assumptions are listed below.

- DVI line break in PXS compartment (PXS is not flooded through broken DVI line)
- Failure of PRHR
- 2/2 ADS stage 1 - automatic
- 2/2 ADS stage 2 - automatic
- 2/2 ADS stage 3 - automatic
- 4/4 ADS stage 4 - automatic

- 1/2 CMTs
- 1/2 accumulators
- 1/2 IRWST gravity injection lines
- 0/2 IRWST recirculation lines
- Hydrogen igniters operating
- Cavity flooding unnecessary (IRWST gravity injection successful)

The main events of the case are shown in Table 34-12, while relevant plots are presented in Figures 34-137 through 34-153.

34.4.4 Accident Class 3BR - Intact Containment

34.4.4.1 3BR-1

The sequence description and assumptions are listed below.

- Double-ended guillotine break (DEGB) in the cold leg to the steam generator compartment
- Failure of PRHR
- 2/2 ADS stage 1 - automatic
- 2/2 ADS stage 2 - automatic
- 2/2 ADS stage 3 - automatic
- 4/4 ADS stage 4 - automatic
- 2/2 CMTs
- 0/2 accumulators
- 2/2 IRWST gravity injection lines
- 2/2 IRWST recirculation lines
- Hydrogen igniters operating
- Cavity flooding unnecessary (IRWST gravity injection successful)

No containment failure is considered, thus the release category is IC; however, normal leakage from the containment is assumed.

The main events of the case are shown in Table 34-13, while relevant plots are presented in Figures 34-154 through 34-170.

34.4.4.2 3BR-1a

The sequence description and assumptions are listed below.

- Double-ended guillotine break (DEGB) in the cold leg to the steam generator compartment
- Failure of PRHR
- 2/2 ADS stage 1 - automatic
- 2/2 ADS stage 2 - automatic
- 2/2 ADS stage 3 - automatic
- 4/4 ADS stage 4 - automatic
- 2/2 CMTs
- 0/2 accumulators
- 0/2 IRWST gravity injection lines
- 0/2 IRWST recirculation lines
- Hydrogen igniters operating
- Cavity flooding unnecessary (IRWST gravity injection successful)

No containment failure is considered, thus the release category is IC; however, normal leakage from the containment is assumed

The main events of the case are shown in Table 34-14, while relevant plots are presented in Figures 34-171 through 34-187.

34.4.6 Accident Class 3C - Intact Containment

34.4.6.1 3C-1

The sequence description and assumptions are listed below.

- Large LOCA at belt of vessel into cavity
- Failure of PRHR
- 2/2 ADS stage 1 - automatic
- 2/2 ADS stage 2 - automatic
- 2/2 ADS stage 3 - automatic
- 4/4 ADS stage 4 - automatic
- 2/2 CMTs
- 2/2 accumulators
- 2/2 IRWST gravity injection lines
- 2/2 IRWST recirculation lines
- Hydrogen igniter operating
- Cavity flooding unnecessary (IRWST gravity injection successful)

No containment failure is considered, thus the release category is IC; however, normal leakage from the containment is assumed.

The main events of the case are shown in Table 34-15, while relevant plots are presented in Figures 34-188 through 34-204.

34.4.7 **Accident Class 3C - Failed Containment**

34.4.7.1 3C-2

The sequence description and assumptions are listed below.

- Large LOCA at belt of vessel into cavity
- Containment failure at start of event
- Failure of PRHR

- 2/2 ADS stage 1 - automatic
- 2/2 ADS stage 2 - automatic
- 2/2 ADS stage 3 - automatic
- 4/4 ADS stage 4 - automatic
- 2/2 CMTs
- 2/2 accumulators
- 2/2 IRWST gravity injection lines
- 2/2 IRWST recirculation lines
- Hydrogen igniter operating
- Cavity flooding unnecessary (IRWST gravity injection successful)

The main events of the case are shown in Table 34-16, while relevant plots are presented in Figures 34-205 through 34-221.

34.4.8 Accident Class 3D - Intact Containment

34.4.8.1 3D-1

The sequence description and assumptions are listed below.

- One valve of ADS Stage 4 spuriously opens
- Failure of PRHR
- 0/2 ADS stage 1
- 0/2 ADS stage 2
- 0/2 ADS stage 3
- 0/4 ADS stage 4
- 0/2 CMTs
- 2/2 accumulators

- 0/2 IRWST gravity injection lines
- 0/2 IRWST recirculation lines
- 2/2 cavity flooding
- Hydrogen igniters operating

No containment failure is considered, thus the release category is IC; however, normal leakage from the containment is assumed.

The main events of the case are shown in Table 34-17, while relevant plots are presented in Figures 34-222 through 34-238.

34.4.8.2 3D-2

The sequence description and assumptions are listed below.

- Two valves of ADS Stage 4 spuriously open
- Failure of PRHR
- 0/2 ADS stage 1
- 0/2 ADS stage 2
- 0/2 ADS stage 3
- 0/4 ADS stage 4
- 0/2 CMTs
- 2/2 accumulators
- 0/2 IRWST gravity injection lines
- 0/2 IRWST recirculation lines
- 2/2 cavity flooding
- Hydrogen igniters operating

The main events of the case are shown in Table 34-18, while relevant plots are presented in Figures 34-239 through 34-255.

34.4.8.3 3D-3

The sequence description and assumptions are listed below.

- DVI line break in PXS compartment
- Failure of PRHR
- 0/2 ADS stage 1
- 0/2 ADS stage 2
- 0/2 ADS stage 3
- 0/4 ADS stage 4
- 1/2 CMTs (no low-2 CMT signal)
- 1/2 accumulators
- 0/2 IRWST gravity injection lines
- 0/2 IRWST recirculation lines
- 2/2 cavity flooding
- Hydrogen igniters operating

The main events of the case are shown in Table 34-19, while relevant plots are presented in Figures 34-256 through 34-272

34.4.9 Accident Class 3D - Failed Containment

34.4.9.1 3D-4

The sequence description and assumptions are listed below.

- Two valves of ADS Stage 4 spuriously open
- Failure of PRHR
- 0/2 ADS stage 1
- 0/2 ADS stage 2

- 0/2 ADS stage 3
- 0/4 ADS stage 4
- 0/2 CMTs
- 2/2 accumulators
- 0/2 IRWST gravity injection lines
- 0/2 IRWST recirculation lines
- 2/2 cavity flooding lines
- Hydrogen igniters operating
- Containment upper compartment to PCS annulus failure during hydrogen release through IRWST

The main events of the case are shown in Table 34-20, while relevant plots are presented in Figures 34-273 through 34-289.

34.4.10 Accident Class 6E - Bypass Containment

34.4.10.1 6E-1

The sequence description and assumptions are listed below.

- Coincident rupture of 5 hot side steam generator tubes
- Broken steam generator SV fails to reseat upon automatic opening
- Success of PRHR
- 0/2 ADS stage 1
- 0/2 ADS stage 2
- 0/2 ADS stage 3
- 0/4 ADS stage 4
- 2/2 CMTs
- 2/2 accumulators

- 2/2 IRWST gravity injection lines
- 2/2 IRWST recirculation lines
- 2/2 cavity flooding lines
- Hydrogen igniters operating

This is a containment bypass sequence; thus the release category is BP Note that due to the lack of ADS Stage 4, no IRWST injection flow is available to provide core cooling.

The main events of the case are shown in Table 34-21, while relevant plots are presented in Figures 34-290 through 34-306.

34.4.11 Accident Class 6L - Bypass Containment

34.4.11.1 6L-1

The sequence description and assumptions are listed below

- Coincident rupture of 5 hot side steam generator tubes
- Broken steam generator SV fails to reseat upon automatic opening
- Success of PRHR
- 2/2 ADS stage 1 - automatic
- 2/2 ADS stage 2 - automatic
- 2/2 ADS stage 3 - automatic
- 4/4 ADS stage 4 - automatic
- 2/2 CMTs
- 2/2 accumulators
- 2/2 IRWST gravity injection lines
- 0/2 IRWST recirculation lines
- Cavity flooding unnecessary (IRWST gravity injection successful)
- Hydrogen igniters operating

The main events of the case are shown in Table 34-22, while relevant plots are presented in Figures 34-307 through 34-323.

34.4.12 Accident Class 1AP

34.4.12.1 1AP-1

The sequence description and assumptions are listed below.

- 3/8-inch hot-leg break to steam generator compartment
- Creep rupture of five steam generator tubes
- Success of PRHR
- 0/2 ADS stage 1
- 0/2 ADS stage 2
- 0/2 ADS stage 3
- 0/4 ADS stage 4
- 0/2 CMTs
- 2/2 accumulators
- 0/2 IRWST gravity injection lines
- 0/2 IRWST recirculation lines
- 2/2 cavity flooding lines
- Hydrogen igniters operating

This is a containment bypass sequence; thus the release category is BP.

The main events of the case are shown in Table 34-23, while relevant plots are presented in Figures 34-324 through 34-340. The temperatures of the steam generator tubes were monitored for creep rupture potential based on the Larsen-Miller correlation (Reference 34-9).

34.4.11.2 1AP-2

The sequence description and assumptions are listed below.

- 3/8-inch hot-leg break to steam generator compartment
- Creep rupture of five steam generator tubes
- Success of PRHR
- 0/2 ADS stage 1
- 0/2 ADS stage 2
- 0/2 ADS stage 3
- 0/4 ADS stage 4
- 2/2 CMTs
- 2/2 accumulators
- 0/2 IRWST gravity injection lines
- 0/2 IRWST recirculation lines
- 0/2 cavity flooding lines
- Hydrogen igniters operating

This is a containment bypass sequence; thus the release category is BP.

The main events of the case are shown in Table 34-24, while relevant plots are presented in Figures 34-341 through 34-357. The temperatures of the hot leg and steam generator tubes were monitored for creep rupture potential based on the Larsen-Miller correlation (Reference 34-9).

34.4.12 Accident Class 1A

34.4.12.1 1A-1

The sequence description and assumptions are listed below.

- Loss of feedwater transient
- Creep rupture of five steam generator tubes
- Failure of PRHR

- 0/2 ADS stage 1
- 0/2 ADS stage 2
- 0/2 ADS stage 3
- 0/4 ADS stage 4
- 2/2 CMTs
- 2/2 accumulators
- 2/2 IRWST gravity injection lines
- 2/2 IRWST recirculation lines
- 2/2 cavity flooding lines
- Hydrogen igniters operating

This is a containment bypass sequence; thus the release category is BP.

The main events of the case are shown in Table 34-25, while relevant plots are presented in Figures 34-358 through 34-374. The temperatures of the hot leg and steam generator tubes were monitored for creep rupture potential based on the Larsen-Miller correlation (Reference 34-9).

34.4.12.2 1A-2

The sequence description and assumptions are listed below.

- Loss of feedwater transient
- Creep rupture of five steam generator tubes
- Creep rupture of hot leg
- Failure of PRHR
- 0/2 ADS stage 1
- 0/2 ADS stage 2
- 0/2 ADS stage 3

- 0/4 ADS stage 4
- 0/2 CMTs
- 2/2 accumulators
- 0/2 IRWST gravity injection lines
- 2/2 IRWST recirculation lines
- 0/2 cavity flooding lines
- Hydrogen igniters operating

This is a containment bypass sequence, thus the release category is BP

The main events of the case are shown in Table 34-26, while relevant plots are presented in Figures 34-375 through 34-391. The temperatures of the hot leg and steam generator tubes were monitored for creep rupture potential based on the Larsen-Miller correlation (Reference 34-9) The steam generator tubes failed first.

34.5 Insights and Conclusions

The analyses of the severe accident phenomena for the AP1000 PRA highlight the following insights and conclusions

- The design of the AP1000 reactor vessel, vessel insulation and reactor cavity, and the ability to flood the cavity after a severe accident reduce the potential challenges to the containment integrity by maintaining the vessel integrity.
- Should a failure of the reactor vessel occur, the design of the reactor cavity enhances the ability to cool any core debris that exits the vessel.
- Lower head vessel failure due to in-vessel steam explosions is physically unreasonable.
- The ADS and PRHR system are design features that can be used to prevent high-pressure core melt in a severe accident.
- A directly-initiated hydrogen detonation in the AP1000 containment is not a credible event.
- The equipment needed to mitigate the consequences of a severe accident is designed to provide reasonable assurance that it will continue to operate during an accident.

34.6 References

34-1 Letter from D. A. Ward, Advisory Committee on Reactor Safeguards, to K. A. Carr, Chairman, Nuclear Regulatory Commission, "Proposed Criteria to Accommodate Severe Accidents in Containment Design," dated May 17, 1991.

34-2 Theofanous, T. G., et al., "In-Vessel Coolability and Retention of a Core Melt," DOE/ID-10460, July 1995.

34-3 Theofanous, T. G., et al., "Lower Head Integrity Under In-Vessel Steam Explosion Loads," DOE/ID-10541, July 1996.

34-4 NUREG-1116, *A Review of the Current Understanding of the Potential for Containment Failure From In-Vessel Steam Explosions*, 1985.

34-5 GW-GL-021, AP600 Probabilistic Risk Assessment, August 1998.

34-6 Sherman, M. P., Tieszen, S. R., and Benedick, W. B., *FLAME Facility - The Effects of Obstacles and Transverse Venting on Flame Acceleration and Transition to Detonation for Hydrogen-Air Mixtures at Large Scale*, NUREG/CR-5275, April 1989.

34-7 Attachment to letter from D. M. Crutchfield, Office of Nuclear Reactor Regulation, to E. E. Kintner, Advanced Light Water Reactor Steering Committee, "Major Technical and Policy Issues Concerning the Evolutionary and Passive Plant Designs," dated February 27, 1992.

34-8 "EPRI MAAP 4.0 Users Manual."

34-9 Larson, F.R., Miller, J., "A Time-Temperature Relationship for Rupture and Creep Stress," Transactions of the American Society of Mechanical Engineers, pp. 765-775, July 1952.

Table 34-1

POST-ACCIDENT MONITORING EQUIPMENT

PARAMETER	PRIMARY PURPOSES	METHOD OF MEASUREMENT (OR ESTIMATE)
Steam Generator Water Level	• To determine if there is an RCS heat sink available • To determine if creep rupture of the steam generator tubes is a concern • To mitigate fission-product releases from faulty or leaking steam generator tubes	• Wide-range steam generator level • Narrow-range steam generator level
RCS Pressure	• To determine the ability to inject into the RCS • To determine if high-pressure melt ejection is a concern • To determine if there is an uncontrolled opening in the RCS	• Wide-range RCS pressure • Pressurizer pressure • Accumulator pressure • CMT flow • IRWST flow
Core Temperature (RCS Temperature or Reactor Vessel Level)	• To determine if the core is covered with water	• Core-exit thermocouples • Hot-leg/cold-leg RTDs • Subcooling margin monitor • Reactor vessel level • Source range monitor • Power range monitor

Table 34-1

POST-ACCIDENT MONITORING EQUIPMENT

PARAMETER	PRIMARY PURPOSES	METHOD OF MEASUREMENT (OR ESTIMATE)
Containment Water Level	• To determine if equipment and instruments are flooded • To determine if core cooling in the recirculation mode is possible • To determine if the outside of the reactor vessel is covered with water • To determine if the core is coolable if reactor vessel failure occurs	• Containment recirculation sump level • IRWST water level
Site Release	• To determine if release mitigation is desired	• Site-specific list
Containment Pressure	• To determine if there is a challenge to the containment due to overpressurization or due to a sub-atmospheric condition • To determine if the containment atmosphere is steam inerted	• Containment pressure • Wide-range containment pressure • Water levels that use containment as reference leg
	• To determine if there is a challenge to the containment due to hydrogen flammability	• Containment hydrogen monitor

Table 34-2

LEVEL 1 ACCIDENT CLASS

FUNCTIONAL DEFINITIONS OF LEVEL 1 ACCIDENT CLASS		
Accident Class	Subclass	Definition
1	A	Core damage with RCS at high pressure following transient or RCS leak
1	AP	Core damage with no depressurization following small LOCA and RCS leak with PRHR operating or intermediate LOCA
1	D	Core damage with partial depressurization of RCS following transient
3	A	Core damage with RCS at high pressure following ATWS or main steam line break inside containment
3	BR	Core damage following large LOCA with full RCS depressurization, but accumulator failed
3	BE	Core damage following large LOCA or other event with full depressurization
3	BL	Core damage at long term following failure of water recirculation to reactor pressure vessel (RPV) after successful gravity injection
3	C	Core damage following vessel rupture
3	D	Core damage following small, intermediate or medium LOCA with partial depressurization
6	E	Core damage following steam generator tube rupture or interfacing systems LOCA – early core damage (loss of injection)
6	L	Core damage following steam generator tube rupture – late core damage (loss of recirculation)

Table 34-3

SUMMARY OF RELEASE CATEGORIES

Release Category	Release Category Name	Release Category Description
IC	Intact Containment	Containment integrity is maintained throughout the accident, and the release of radiation to the environment is due to nominal leakage.
BP	Bypass Containment	Fission products are released directly from the RCS to the environment via the secondary system or other interfacing system bypass. Containment failure occurs prior to onset of core damage.
CI	Containment Isolation Failure	Fission products are released through a failure of the system or valves that close the penetrations between the containment and the environment. Containment failure occurs prior to onset of core damage.
CFE	Early Containment Failure	Fission products are released through a containment failure caused by dynamic severe accident phenomena occurring after the onset of core damage, but prior to core relocation. Such phenomena include hydrogen detonation, hydrogen diffusion flame, steam explosions, and vessel failure.
CFI	Intermediate Containment Failure	Fission products are released through a containment failure caused by dynamic severe accident phenomena occurring after core relocation, but before 24 hours. Such phenomena include hydrogen detonation and hydrogen deflagration.
CFL	Late Containment Failure	Fission products are released through a containment failure caused by severe accident phenomena occurring after 24 hours. Such phenomena include the failure of containment heat removal (failure of passive containment cooling).

Table 34-4

3BE-1 EVENT SUMMARY

Time (sec)	Description
0.0	DVI Line Break to PXS Compartment
20 5	Reactor Scram
25.3	Main Coolant Pump Trip
25.3	CMT Actuation
56.0	PCS Actuation
615 0	ADS Stage 1 Actuation - Automatic
735.7	ADS Stage 2 Actuation - Automatic
855.7	ADS Stage 3 Actuation - Automatic
901.0	Accumulator Water Depleted
1594.0	ADS Stage 4 Actuation - Automatic
1670 0	Cavity Water Level @ 83'
3359 3	Cavity Flooding Actuation
3405.0	Onset of Core Melting
5050.0	Cavity Water Level @ 98'
N/A	Hot Leg Submerged
N/A	PRHR Actuation
N/A	IRWST Injection Initiated
N/A	IRWST Low Level - Switchover to Recirculation
N/A	Begin Core Relocation to Lower Plenum
N/A	Lower Plenum Dryout.
N/A	Vessel Failure
N/A	Containment Failure
N/A	Creep Rupture of RCS

Table 34-5

3BE-2 EVENT SUMMARY

Time (sec)	Description
0.0	DVI Line Break to PXS Compartment
20.5	Reactor Scram
25.3	Main Coolant Pump Trip
25.3	CMT Actuation
56.0	PCS Actuation
616.0	ADS Stage 1 Actuation - Automatic
736.4	ADS Stage 2 Actuation - Automatic
856.4	ADS Stage 3 Actuation - Automatic
901.0	Accumulator Water Depleted
1500.0	Cavity Water Level @ 83'
1594.4	ADS Stage 4 Actuation - Automatic
3359.0	Cavity Flooding Actuation
3406.4	Onset of Core Melting
5100.0	Cavity Water Level @ 98'
5880.0	Begin Core Relocation to Lower Plenum
7500.0	Lower Plenum Dryout
N/A	Hot Leg Submerged
N/A	PRHR Actuation
N/A	IRWST Injection Initiated
N/A	IRWST Low Level - Switchover to Recirculation
N/A	Vessel Failure
N/A	Containment Failure
N/A	Creep Rupture of RCS

Table 34-6

3BE-4 EVENT SUMMARY

Time (sec)	Description
0.0	Spurious ADS Stage 4
5.0	Reactor Scram
5.3	Main Coolant Pump Trip
5.3	CMT Actuation
5.3	PCS Actuation
240.0	Cavity Water Level @ 83'
371.5	Accumulator Water Depleted
659.6	ADS Stage 1 Actuation - Automatic
779.6	ADS Stage 2 Actuation - Automatic
899.6	ADS Stage 3 Actuation - Automatic
1416.0	ADS Stage 4 Actuation - Automatic
3156.5	Cavity Flooding Actuation
3406.4	Onset of Core Melting
4650.0	Cavity Water Level @ 98'
5572.0	Begin Core Relocation to Lower Plenum
7400.0	Lower Plenum Dryout
N/A	Hot Leg Submerged
N/A	PRHR Actuation
N/A	IRWST Injection Initiated
N/A	IRWST Low Level - Switchover to Recirculation
N/A	Vessel Failure
N/A	Containment Failure
N/A	Creep Rupture of RCS

Table 34-7

3BE-5 EVENT SUMMARY

Time (sec)	Description
0.0	2-inch Hot Leg Break to Steam Generator Compartment
149.0	Reactor Scram
165.2	Main Coolant Pump Trip
165.2	CMT Actuation
289.3	PCS Actuation
371.5	Accumulator Water Depleted
2047.4	ADS Stage 1 Actuation - Automatic
2167.4	ADS Stage 2 Actuation - Automatic
2287.4	ADS Stage 3 Actuation - Automatic
2300.0	Cavity Water Level @ 83'
2946.0	ADS Stage 4 Actuation - Automatic
4792.3	Cavity Flooding Actuation
4847.5	Onset of Core Melting
6300.0	Cavity Water Level @ 98'
7617.0	Begin Core Relocation to Lower Plenum
N/A	Hot Leg Submerged
N/A	PRHR Actuation
N/A	IRWST Injection Initiated
N/A	IRWST Low Level - Switchover to Recirculation
N/A	Lower Plenum Dryout
N/A	Vessel Failure
N/A	Containment Failure
N/A	Creep Rupture of RCS

Table 34-8

3BE-6 EVENT SUMMARY

Time (sec)	Description
0.0	2-inch Hot Leg Break to Steam Generator Compartment
149 1	Reactor Scram
165.7	Main Coolant Pump Trip
165.7	CMT Actuation
287.8	PCS Actuation
2046.3	ADS Stage 1 Actuation - Automatic
2163.6	ADS Stage 2 Actuation - Automatic
2283 6	ADS Stage 3 Actuation - Automatic
2300.0	Cavity Water Level @ 83'
2511 5	Accumulator Water Depleted
2948.9	ADS Stage 4 Actuation - Automatic
4793 2	Cavity Flooding Actuation
4847.7	Onset of Core Melting
7525.0	Begin Core Relocation to Lower Plenum
7800.0	Cavity Water Level @ 98'
N/A	Hot Leg Submerged
N/A	PRHR Actuation
N/A	IRWST Injection Initiated
N/A	IRWST Low Level - Switchover to Recirculation
N/A	Lower Plenum Dryout
N/A	Vessel Failure
N/A	Containment Failure
N/A	Creep Rupture of RCS

Table 34-9

3BE-7 EVENT SUMMARY

Time (sec)	Description
0.0	2-inch Hot Leg Break to Steam Generator Compartment
149.0	Reactor Scram
165.2	Main Coolant Pump Trip
165.2	CMT Actuation
289.3	PCS Actuation
1949.9	ADS Stage 4 Actuation - Automatic
2044.1	ADS Stage 1 Actuation - Automatic
2164.1	ADS Stage 2 Actuation - Automatic
2284.1	ADS Stage 3 Actuation - Automatic
2400.0	Cavity Water Level @ 83'
2512.6	Accumulator Water Depleted
4782.1	Cavity Flooding Actuation
4839.0	Onset of Core Melting
7520.0	Begin Core Relocation to Lower Plenum
9000.0	Lower Plenum Dryout
11302.0	Vessel Failure
11302.0	Containment Failure
N/A	Cavity Water Level @ 98'
N/A	Hot Leg Submerged
N/A	PRHR Actuation
N/A	IRWST Injection Initiated
N/A	IRWST Low Level - Switchover to Recirculation
N/A	Creep Rupture of RCS

Table 34-10

3BE-3 EVENT SUMMARY

Time (sec)	Description
0.0	DVI Line Break to PXS Compartment
20.5	Reactor Scram
25.3	Main Coolant Pump Trip
25.3	CMT Actuation
58.1	PCS Actuation
613.0	ADS Stage 1 Actuation - Automatic
733.0	ADS Stage 2 Actuation - Automatic
853.0	ADS Stage 3 Actuation - Automatic
898.2	Accumulator Water Depleted
1588.5	ADS Stage 4 Actuation - Automatic
1700.0	Cavity Water Level @ 83'
3347.0	Cavity Flooding Actuation
3394.4	Onset of Core Melting
5000.0	Cavity Water Level @ 98'
10010.0	Containment Failure
N/A	Hot Leg Submerged
N/A	PRHR Actuation
N/A	IRWST Injection Initiated
N/A	IRWST Low Level - Switchover to Recirculation
N/A	Begin Core Relocation to Lower Plenum
N/A	Lower Plenum Dryout
N/A	Vessel Failure
N/A	Creep Rupture of RCS

Table 34-11

3BL-1 EVENT SUMMARY

Time (sec)	Description
0.0	2-inch Hot Leg Break to Steam Generator Compartment
149.0	Reactor Scram
165.3	Main Coolant Pump Trip
165.3	CMT Actuation
289.5	PCS Actuation
2043.7	ADS Stage 1 Actuation - Automatic
2100.0	Cavity Water Level @ 83'
2163.7	ADS Stage 2 Actuation - Automatic
2283.7	ADS Stage 3 Actuation - Automatic
2511.0	Accumulator Water Depleted
2945.3	ADS Stage 4 Actuation - Automatic
2945.3	IRWST Injection Initiated
5750.0	Cavity Water Level @ 98'
27651.1	Onset of Core Melting
30456.0	Begin Core Relocation to Lower Plenum
40000.0	Lower Plenum Dryout
N/A	Hot Leg Submerged
N/A	PRHR Actuation
N/A	IRWST Low Level - Switchover to Recirculation
N/A	Cavity Flooding Actuation
N/A	Vessel Failure
N/A	Containment Failure
N/A	Creep Rupture of RCS

Table 34-12

3BL-2 EVENT SUMMARY

Time (sec)	Description
0.0	DVI Line Break to PXS Compartment
20.5	Reactor Scram
25.3	Main Coolant Pump Trip
25.3	CMT Actuation
56.0	PCS Actuation
617.2	ADS Stage 1 Actuation - Automatic
737.2	ADS Stage 2 Actuation - Automatic
857.2	ADS Stage 3 Actuation - Automatic
902.0	Accumulator Water Depleted
1500.0	Cavity Water Level @ 83'
1594.4	ADS Stage 4 Actuation - Automatic
1594.4	IRWST Injection Initiated
8800.0	Cavity Water Level @ 98'
45358.2	Onset of Core Melting
53093.0	Begin Core Relocation to Lower Plenum
64000.0	Lower Plenum Dryout
N/A	Hot Leg Submerged
N/A	PRHR Actuation
N/A	IRWST Low Level - Switchover to Recirculation
N/A	Cavity Flooding Actuation
N/A	Vessel Failure
N/A	Containment Failure
N/A	Creep Rupture of RCS

Table 34-13

3BR-1 EVENT SUMMARY

Time (sec)	Description
0.0	Large LOCA in Cold Leg to Steam Generator Compartment
0.6	Reactor Scram
1.3	Main Coolant Pump Trip
1.3	CMT Actuation
1.3	PCS Actuation
383.8	ADS Stage 1 Actuation - Automatic
503.8	ADS Stage 2 Actuation - Automatic
618.8	ADS Stage 3 Actuation - Automatic
700.0	Cavity Water Level @ 83'
1134.6	ADS Stage 4 Actuation - Automatic
3900.0	Cavity Water Level @ 98'
N/A	Hot Leg Submerged
N/A	Onset of Core Melting
N/A	Begin Core Relocation to Lower Plenum
N/A	Accumulator Water Depleted
N/A	PRHR Actuation
N/A	IRWST Injection Initiated
N/A	IRWST Low Level - Switchover to Recirculation
N/A	Cavity Flooding Actuation
N/A	Lower Plenum Dryout
N/A	Vessel Failure
N/A	Containment Failure
N/A	Creep Rupture of RCS

Table 34-14

3BR-1a EVENT SUMMARY

Time (sec)	Description
0.0	Large LOCA in Cold Leg to Steam Generator Compartment
0.2	Reactor Scram
0.7	Main Coolant Pump Trip
0.7	CMT Actuation
0.7	PCS Actuation
372.3	ADS Stage 1 Actuation - Automatic
492.3	ADS Stage 2 Actuation - Automatic
612.3	ADS Stage 3 Actuation - Automatic
1000.0	Cavity Water Level @ 83'
1131.5	ADS Stage 4 Actuation - Automatic
2848.2	Onset of Core Melting
5157.0	Begin Core Relocation to Lower Plenum
7000.0	Lower Plenum Dryout
N/A	Cavity Water Level @ 98'
N/A	Hot Leg Submerged
N/A	Accumulator Water Depleted
N/A	PRHR Actuation
N/A	IRWST Injection Initiated
N/A	IRWST Low Level - Switchover to Recirculation
N/A	Cavity Flooding Actuation
N/A	Vessel Failure
N/A	Containment Failure
N/A	Creep Rupture of RCS

Table 34-15

3C-1 EVENT SUMMARY

Time (sec)	Description
0.0	Large LOCA at Belt of Reactor Vessel
0.05	Reactor Scram
0.6	Main Coolant Pump Trip
0.6	CMT Actuation
0.6	PCS Actuation
50.0	Cavity Water Level @ 83'
302.8	Accumulator Water Depleted
555.5	ADS Stage 1 Actuation – Automatic
675.5	ADS Stage 2 Actuation – Automatic
795.5	ADS Stage 3 Actuation – Automatic
1312.5	ADS Stage 4 Actuation - Automatic
1312.5	IRWST Injection Initiated
1511.0	Begin Core Relocation to Lower Plenum
4300.0	Cavity Water Level @ 98'
7611.8	Onset of Core Melting
N/A	Hot Leg Submerged
N/A	PRHR Actuation
N/A	IRWST Low Level - Switchover to Recirculation
N/A	Cavity Flooding Actuation
N/A	Lower Plenum Dryout
N/A	Vessel Failure
N/A	Containment Failure
N/A	Creep Rupture of RCS

Table 34-16

3C-2 EVENT SUMMARY

Time (sec)	Description
0.0	Large LOCA at Belt of Reactor Vessel
0.0	Containment Failure
0.1	Reactor Scram
0.6	Main Coolant Pump Trip
0.6	CMT Actuation
0.6	PCS Actuation
30.0	Cavity Water Level @ 83'
293.8	Accumulator Water Depleted
352.8	Onset of Core Melting
561.2	ADS Stage 1 Actuation - Automatic
681.2	ADS Stage 2 Actuation - Automatic
801.2	ADS Stage 3 Actuation - Automatic
1318.0	ADS Stage 4 Actuation - Automatic
1318.0	IRWST Injection Initiated
1533.0	Begin Core Relocation to Lower Plenum
4350 0	Cavity Water Level @ 98'
N/A	Hot Leg Submerged
N/A	PRHR Actuation
N/A	IRWST Low Level - Switchover to Recirculation
N/A	Cavity Flooding Actuation
N/A	Lower Plenum Dryout
N/A	Vessel Failure
N/A	Creep Rupture of RCS

Table 34-17

3D-1 EVENT SUMMARY

Time (sec)	Description
0.0	Spurious ADS Stage 4
5.0	Reactor Scram
5.3	Main Coolant Pump Trip
5.3	PCS Actuation
300.0	Cavity Water Level @ 83'
372.3	Accumulator Water Depleted
1490.0	Cavity Flooding Actuation
1532.5	Onset of Core Melting
3400.0	Cavity Water Level @ 98'
3468.0	Begin Core Relocation to Lower Plenum
4900.0	Lower Plenum Dryout
N/A	Hot Leg Submerged
N/A	CMT Actuation
N/A	ADS Stage 1 Actuation - Automatic
N/A	ADS Stage 2 Actuation - Automatic
N/A	ADS Stage 3 Actuation - Automatic
N/A	ADS Stage 4 Actuation - Automatic
N/A	PRHR Actuation
N/A	IRWST Injection Initiated
N/A	IRWST Low Level - Switchover to Recirculation
N/A	Vessel Failure
N/A	Containment Failure
N/A	Creep Rupture of RCS

Table 34-18

3D-2 EVENT SUMMARY

Time (sec)	Description
0.0	Spurious ADS Stage 2
2.9	Reactor Scram
4.0	Main Coolant Pump Trip
22.2	PCS Actuation
1927.5	Accumulator Water Depleted
2000.0	Cavity Water Level @ 83'
3427.4	Cavity Flooding Actuation
3491.3	Onset of Core Melting
5300.0	Cavity Water Level @ 98'
5825.0	Begin Core Relocation to Lower Plenum
7500.0	Lower Plenum Dryout
N/A	Hot Leg Submerged
N/A	CMT Actuation
N/A	ADS Stage 1 Actuation - Automatic
N/A	ADS Stage 2 Actuation - Automatic
N/A	ADS Stage 3 Actuation - Automatic
N/A	ADS Stage 4 Actuation - Automatic
N/A	PRHR Actuation
N/A	IRWST Injection Initiated
N/A	IRWST Low Level - Switchover to Recirculation
N/A	Vessel Failure
N/A	Containment Failure
N/A	Creep Rupture of RCS

Table 34-19

3D-3 EVENT SUMMARY

Time (sec)	Description
0.0	DVI Line Break to PXS Compartment
20.5	Reactor Scram
25.3	Main Coolant Pump Trip
25.3	CMT Actuation
56.1	PCS Actuation
1800.0	Cavity Water Level @ 83'
4227.9	Accumulator Water Depleted
4767.8	Cavity Flooding Actuation
4881.3	Onset of Core Melting
6400.0	Cavity Water Level @ 98'
7714.0	Begin Core Relocation to Lower Plenum
9500.0	Lower Plenum Dryout
N/A	Hot Leg Submerged
N/A	ADS Stage 1 Actuation - Automatic
N/A	ADS Stage 2 Actuation - Automatic
N/A	ADS Stage 3 Actuation - Automatic
N/A	ADS Stage 4 Actuation - Automatic
N/A	PRHR Actuation
N/A	IRWST Injection Initiated
N/A	IRWST Low Level - Switchover to Recirculation
N/A	Vessel Failure
N/A	Containment Failure
N/A	Creep Rupture of RCS

Table 34-20

3D-4 EVENT SUMMARY

Time (sec)	Description
0.0	Spurious ADS Stage 2
2.9	Reactor Scram
4.0	Main Coolant Pump Trip
22.2	PCS Actuation
1927.5	Accumulator Water Depleted
2000.0	Cavity Water Level @ 83'
3491.3	Onset of Core Melting
4491.0	Containment Failure
5350.0	Cavity Water Level @ 98'
5831.0	Begin Core Relocation to Lower Plenum
7500.0	Lower Plenum Dryout
N/A	Hot Leg Submerged
N/A	ADS Stage 1 Actuation – Automatic
N/A	ADS Stage 2 Actuation – Automatic
N/A	ADS Stage 3 Actuation – Automatic
N/A	ADS Stage 4 Actuation - Automatic
N/A	PRHR Actuation
N/A	IRWST Injection Initiated
N/A	IRWST Low Level - Switchover to Recirculation
N/A	CMT Actuation
N/A	Cavity Flooding Actuation
N/A	Vessel Failure
N/A	Creep Rupture of RCS

Table 34-21

6E-1 EVENT SUMMARY

Time (sec)	Description
0.0	Steam Generator Tube Rupture (5 tubes)
147.7	Reactor Scram
164.6	Main Coolant Pump Trip
164.6	CMT Actuation
166.8	PRHR Actuation
3673.3	Accumulator Water Depleted
19184.0	IRWST Injection Initiated
32612.0	Cavity Flooding Actuation
32706.0	Onset of Core Melting
33000.0	Cavity Water Level @ 83'
35050.0	Cavity Water Level @ 98'
36844.0	Begin Core Relocation to Lower Plenum
38500.0	Lower Plenum Dryout
39911.3	IRWST Low Level - Switchover to Recirculation
68637.0	PCS Actuation
N/A	Hot Leg Submerged
N/A	ADS Stage 1 Actuation - Automatic
N/A	ADS Stage 2 Actuation - Automatic
N/A	ADS Stage 3 Actuation - Automatic
N/A	ADS Stage 4 Actuation - Automatic
N/A	Vessel Failure
N/A	Containment Failure
N/A	Creep Rupture of RCS

Table 34-22

6L-1 EVENT SUMMARY

Time (sec)	Description
0.0	Steam Generator Tube Rupture (5 tubes)
148.7	Reactor Scram
165	Main Coolant Pump Trip
165	CMT Actuation
167.0	PRHR Actuation
3672.5	Accumulator Water Depleted
17028.0	ADS Stage 1 Actuation - Automatic
17148.0	ADS Stage 2 Actuation - Automatic
17268.0	ADS Stage 3 Actuation - Automatic
17863.0	ADS Stage 4 Actuation - Automatic
17863.0	IRWST Injection Initiated
18500.0	Cavity Water Level @ 83'
22000.0	Cavity Water Level @ 98'
23793.0	PCS Actuation
44464.0	Onset of Core Melting
48447.0	Begin Core Relocation to Lower Plenum
53000.0	Lower Plenum Dryout
N/A	Hot Leg Submerged
N/A	IRWST Low Level - Switchover to Recirculation
N/A	Cavity Flooding Actuation
N/A	Vessel Failure
N/A	Containment Failure
N/A	Creep Rupture of RCS

Table 34-23

1AP-1 EVENT SUMMARY

Time (sec)	Description
0.0	3/8-inch Hot Leg Break to Steam Generator Compartment
4689.8	Reactor Scram
4697.2	Main Coolant Pump Trip
4698.0	PRHR Actuation
14001.0	PCS Actuation
36000.0	Cavity Water Level @ 83'
86381.8	Accumulator Water Depleted
133253.0	Creep Rupture of RCS (Steam Generator Tube Creep)
137540.1	Cavity Flooding Actuation
137740.7	Onset of Core Melting
139000.0	Cavity Water Level @ 98'
144724.0	Begin Core Relocation to Lower Plenum
146000.0	Lower Plenum Dryout
N/A	Hot Leg Submerged
N/A	ADS Stage 1 Actuation - Automatic
N/A	ADS Stage 2 Actuation - Automatic
N/A	ADS Stage 3 Actuation - Automatic
N/A	ADS Stage 4 Actuation - Automatic
N/A	CMT Actuation
N/A	IRWST Injection Initiated
N/A	IRWST Low Level - Switchover to Recirculation
N/A	Vessel Failure
N/A	Containment Failure

Table 34-24

1AP-2 EVENT SUMMARY

Time (sec)	Description
0.0	3/8-inch Hot Leg Break to Steam Generator Compartment
4689.8	Reactor Scram
4697.2	Main Coolant Pump Trip
4697.2	CMT Actuation
4698.0	PRHR Actuation
15556.1	PCS Actuation
40000.0	Cavity Water Level @ 83'
92439.2	Accumulator Water Depleted
139113.0	Creep Rupture of RCS (Steam Generator Tube Creep)
150556.0	Onset of Core Melting
157909.0	Begin Core Relocation to Lower Plenum
160000.0	Lower Plenum Dryout
N/A	Cavity Water Level @ 98'
N/A	Hot Leg Submerged
N/A	ADS Stage 1 Actuation - Automatic
N/A	ADS Stage 2 Actuation - Automatic
N/A	ADS Stage 3 Actuation - Automatic
N/A	ADS Stage 4 Actuation - Automatic
N/A	IRWST Injection Initiated
N/A	IRWST Low Level - Switchover to Recirculation
N/A	Cavity Flooding Actuation
N/A	Vessel Failure
N/A	Containment Failure

Table 34-25

1A-1 EVENT SUMMARY

Time (sec)	Description
0.0	Feedwater Failure
3.8	Reactor Scram
4015.5	Main Coolant Pump Trip
4015.5	CMT Actuation
4015.5	PCS Actuation
10500.0	Cavity Water Level @ 83'
14000.0	Creep Rupture of RCS (Steam Generator Tube Creep)
15413.0	IRWST Injection Initiated
15721.5	Cavity Flooding Actuation
15864.0	Onset of Core Melting
17700.0	Cavity Water Level @ 98'
19604.0	Begin Core Relocation to Lower Plenum
20500.0	Lower Plenum Dryout
N/A	Hot Leg Submerged
N/A	ADS Stage 1 Actuation - Automatic
N/A	ADS Stage 2 Actuation - Automatic
N/A	ADS Stage 3 Actuation - Automatic
N/A	ADS Stage 4 Actuation - Automatic
N/A	Accumulator Water Depleted
N/A	PRHR Actuation
N/A	IRWST Low Level - Switchover to Recirculation
N/A	Vessel Failure
N/A	Containment Failure

Table 34-26

1A-2 EVENT SUMMARY

Time (sec)	Description
0 0	Feedwater Failure
3 8	Reactor Scram
4015 5	Main Coolant Pump Trip
4015.5	PCS Actuation
7000.0	Creep Rupture of RCS (Steam Generator Tube Creep)
8550.1	Onset of Core Melting
11495 0	Begin Core Relocation to Lower Plenum
12250.0	Lower Plenum Dryout
22175.0	Creep Rupture of RCS (Hot Leg Creep)
22333.8	Accumulator Water Depleted
22500 0	Cavity Water Level @ 83'
N/A	Cavity Water Level @ 98'
N/A	Hot Leg Submerged
N/A	ADS Stage 1 Actuation - Automatic
N/A	ADS Stage 2 Actuation - Automatic
N/A	ADS Stage 3 Actuation - Automatic
N/A	ADS Stage 4 Actuation - Automatic
N/A	CMT Actuation
N/A	PRHR Actuation
N/A	IRWST Injection Initiated
N/A	IRWST Low Level - Switchover to Recirculation
N/A	Cavity Flooding Actuation
N/A	Vessel Failure
N/A	Containment Failure

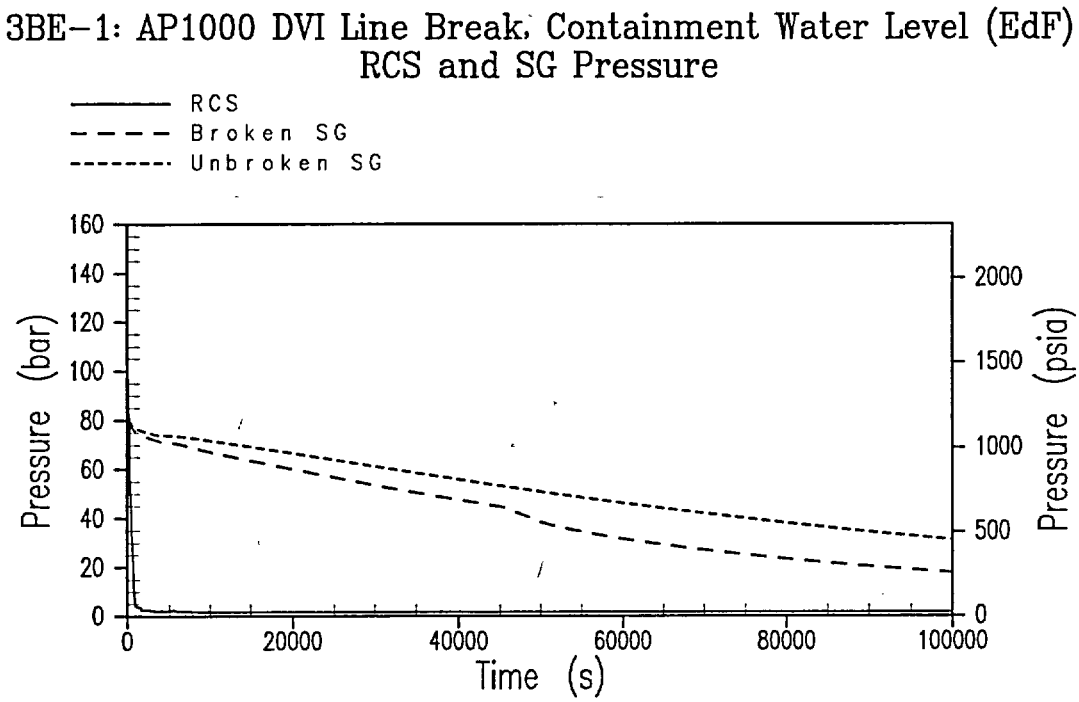

Figure 34-1

Case 3BE-1: RCS and Steam Generator Pressure

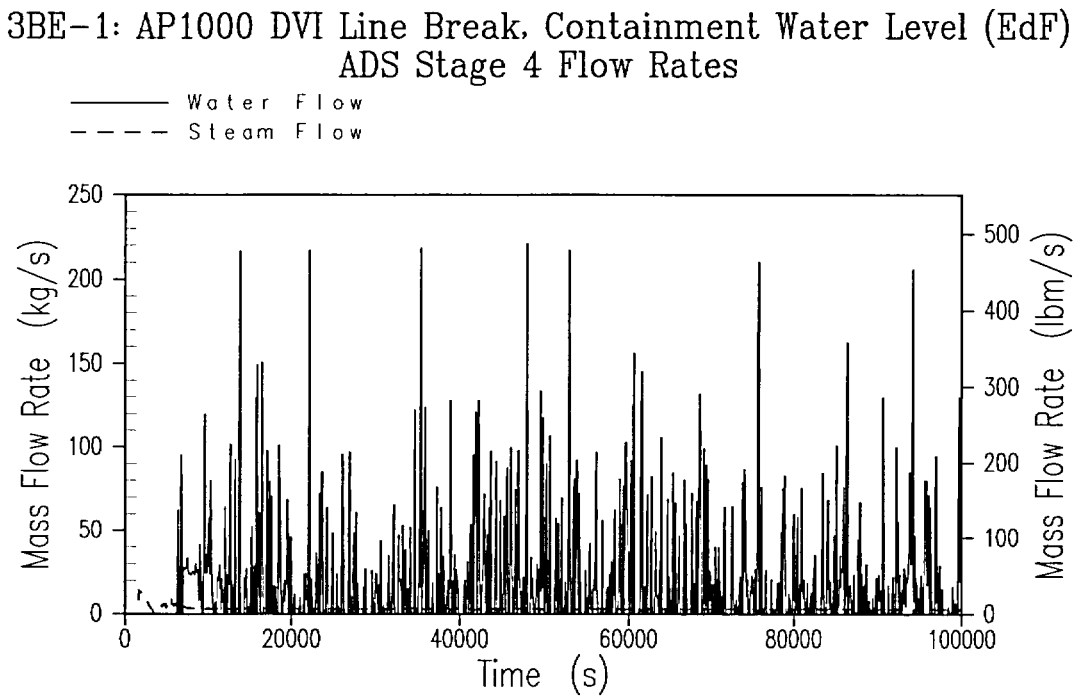

Figure 34-2

Case 3BE-1: ADS Stage 4 Flow Rates

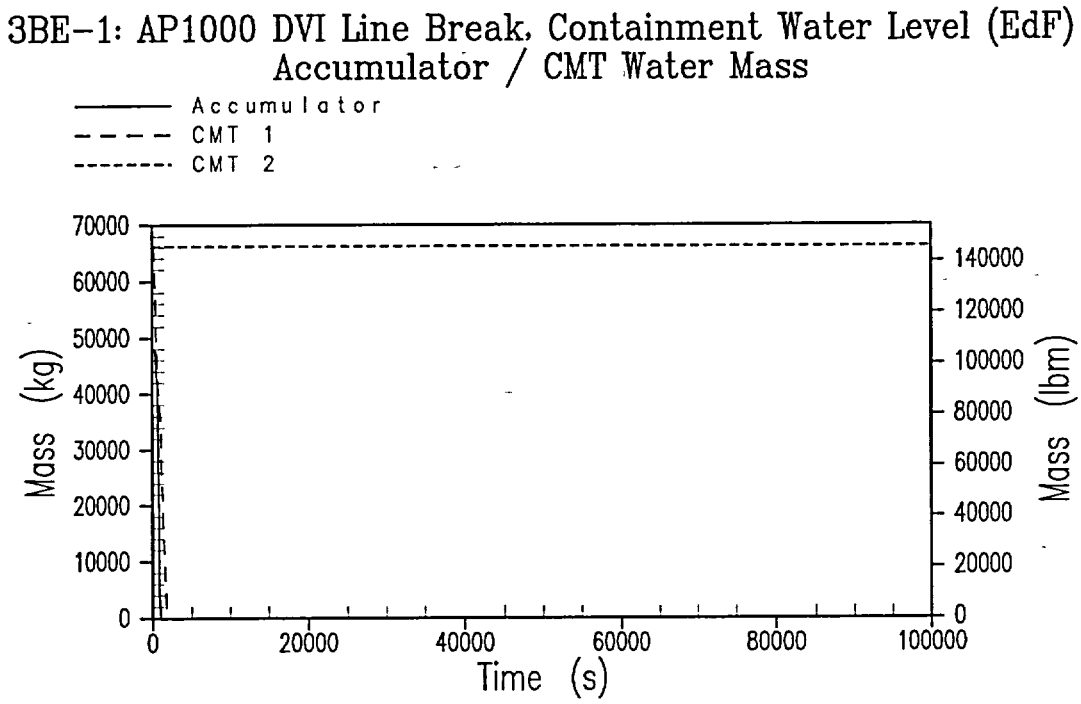

Figure 34-3

Case 3BE-1: Accumulator / CMT Water Mass

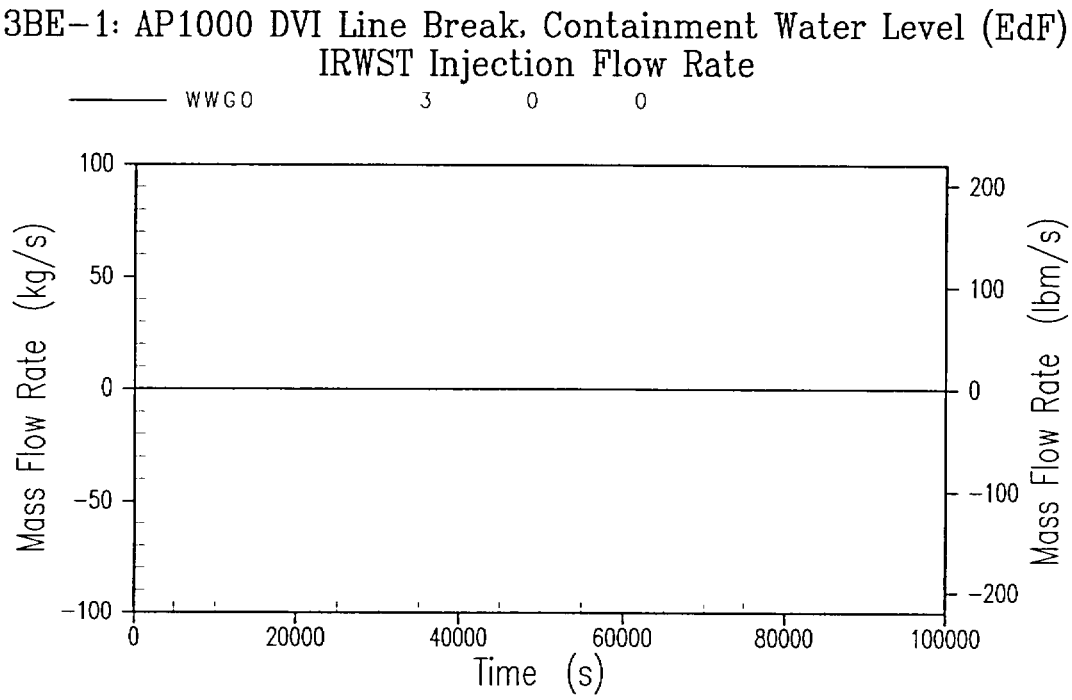

Figure 34-4

Case 3BE-1: IRWST Injection Flow Rate

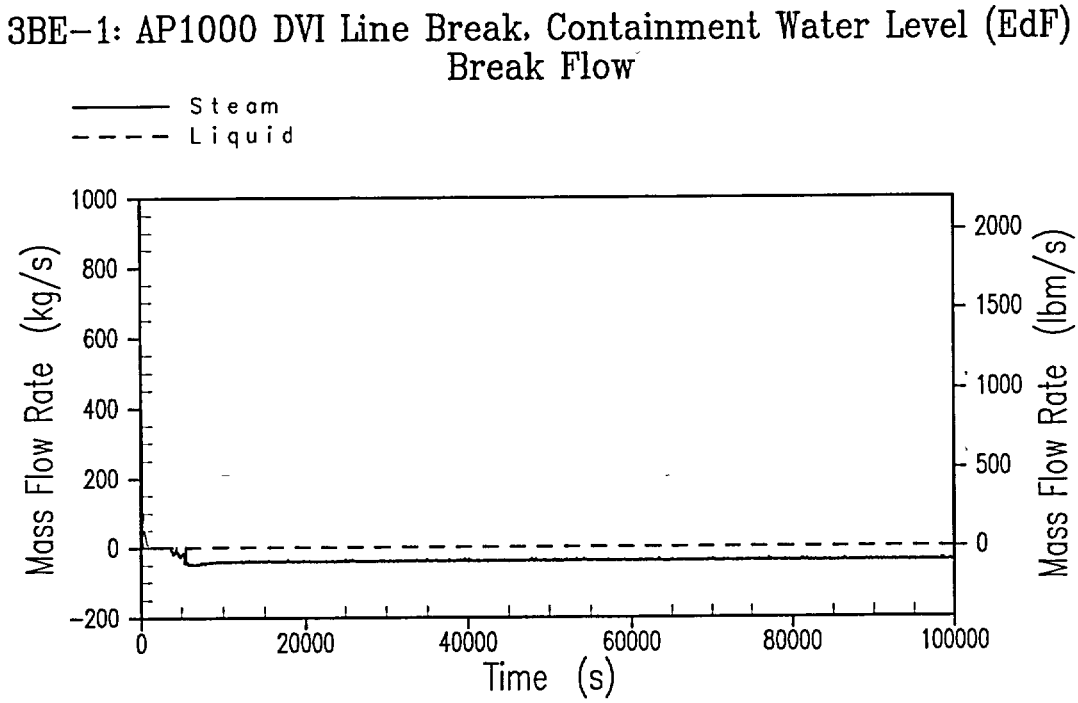

Figure 34-5

Case 3BE-1: Break Flow Rate

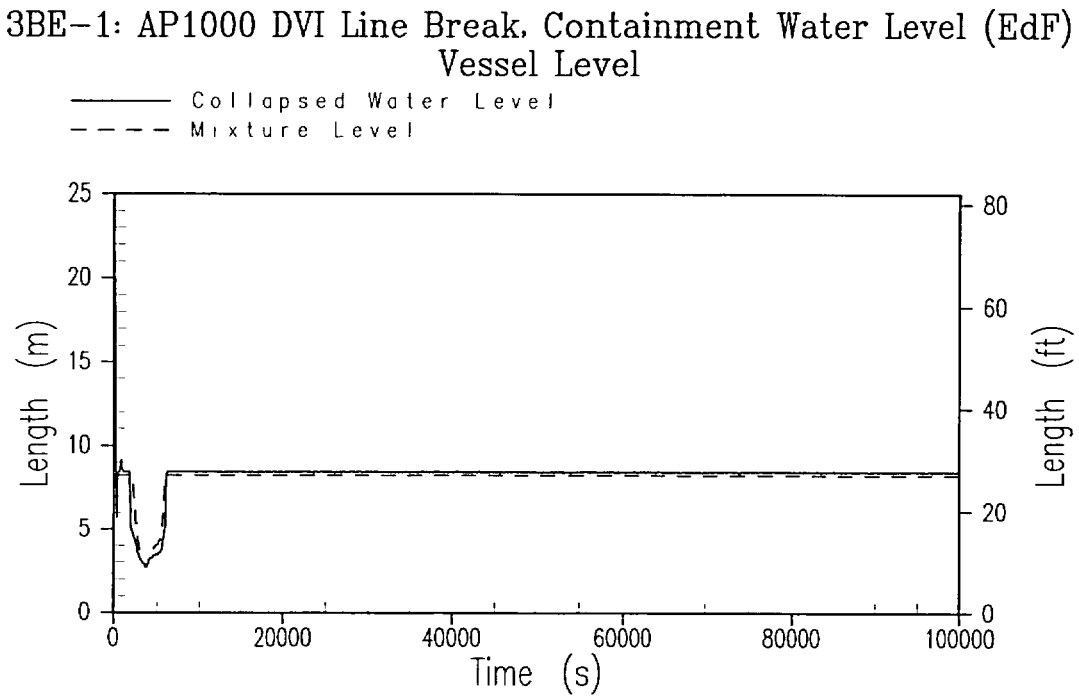

Figure 34-6

Case 3BE-1: Reactor Vessel Water Level

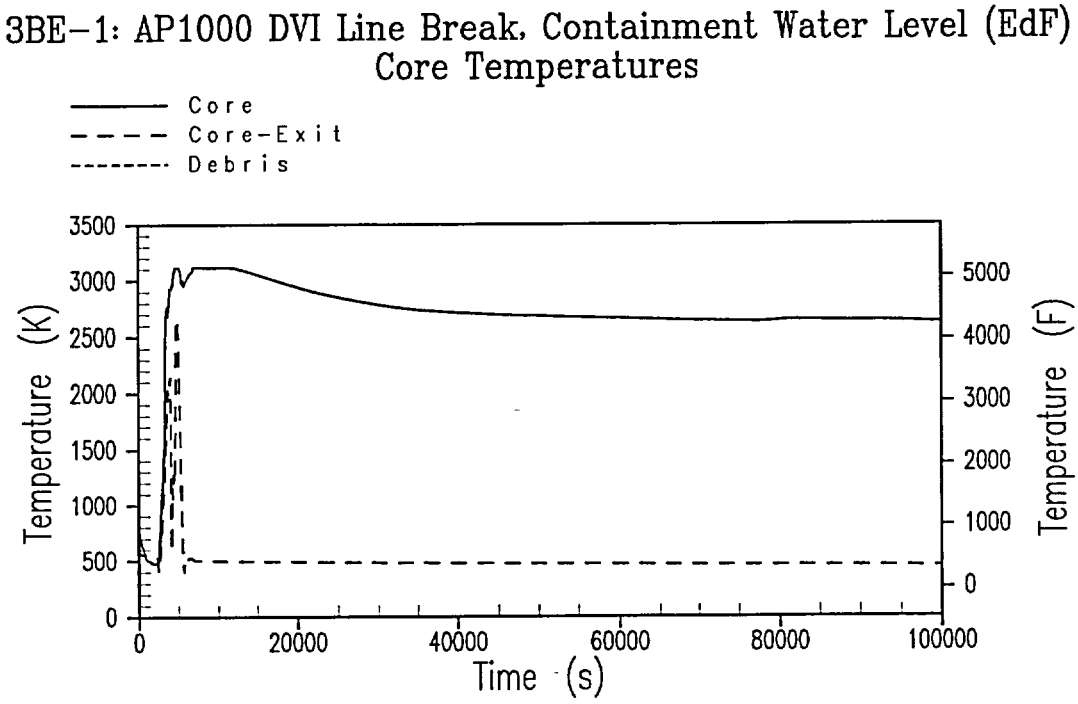

Figure 34-7

Case 3BE-1: Core Temperatures

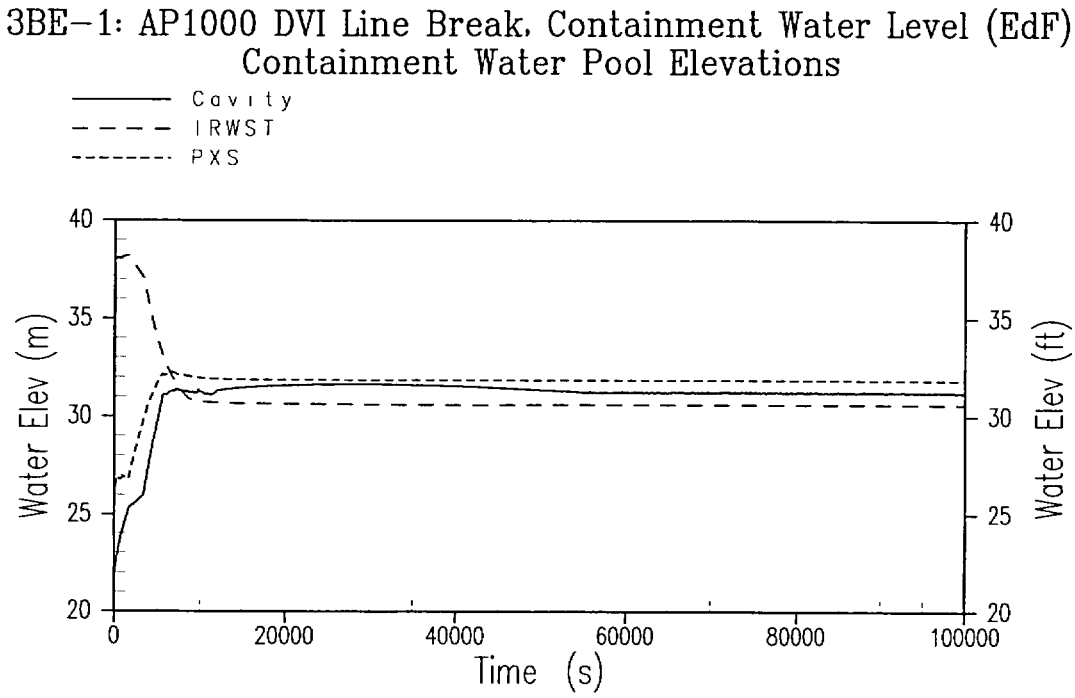

Figure 34-8

Case 3BE-1: Containment Water Pool Elevations

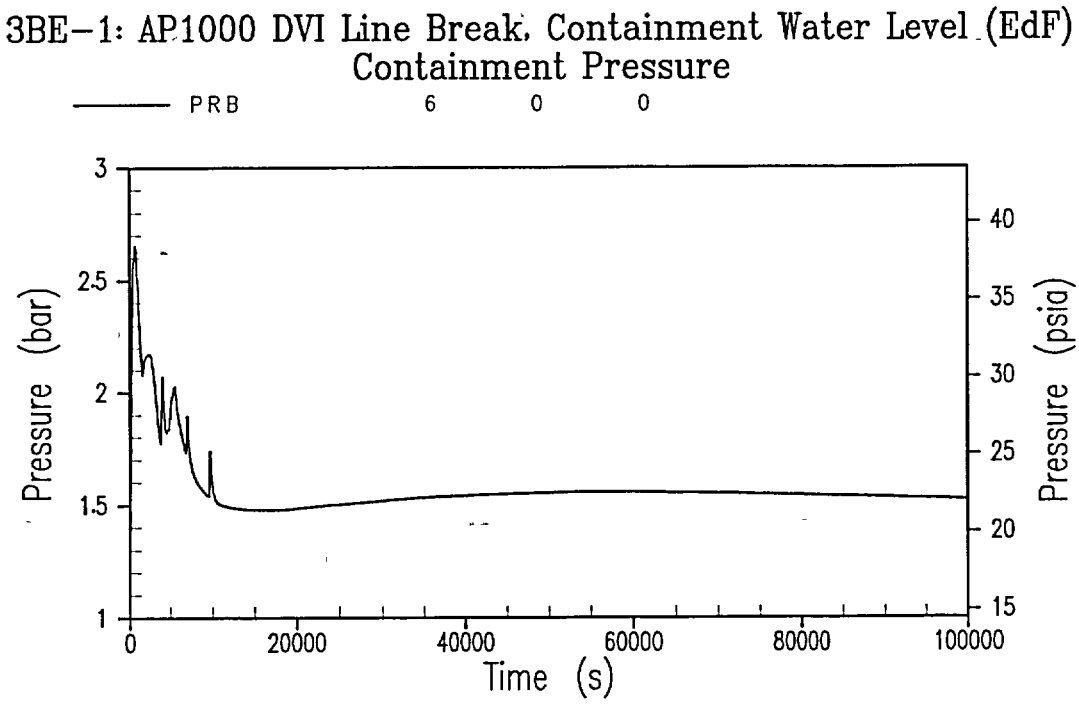

Figure 34-9

Case 3BE-1: Containment Pressure

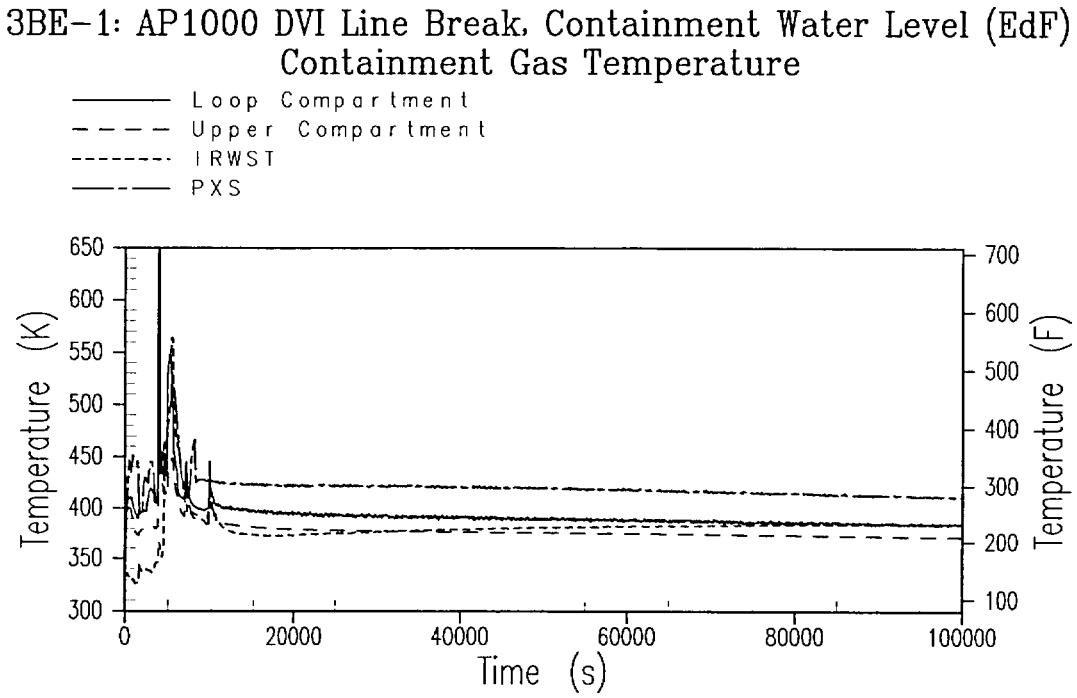

Figure 34-10

Case 3BE-1: Containment Gas Temperatures

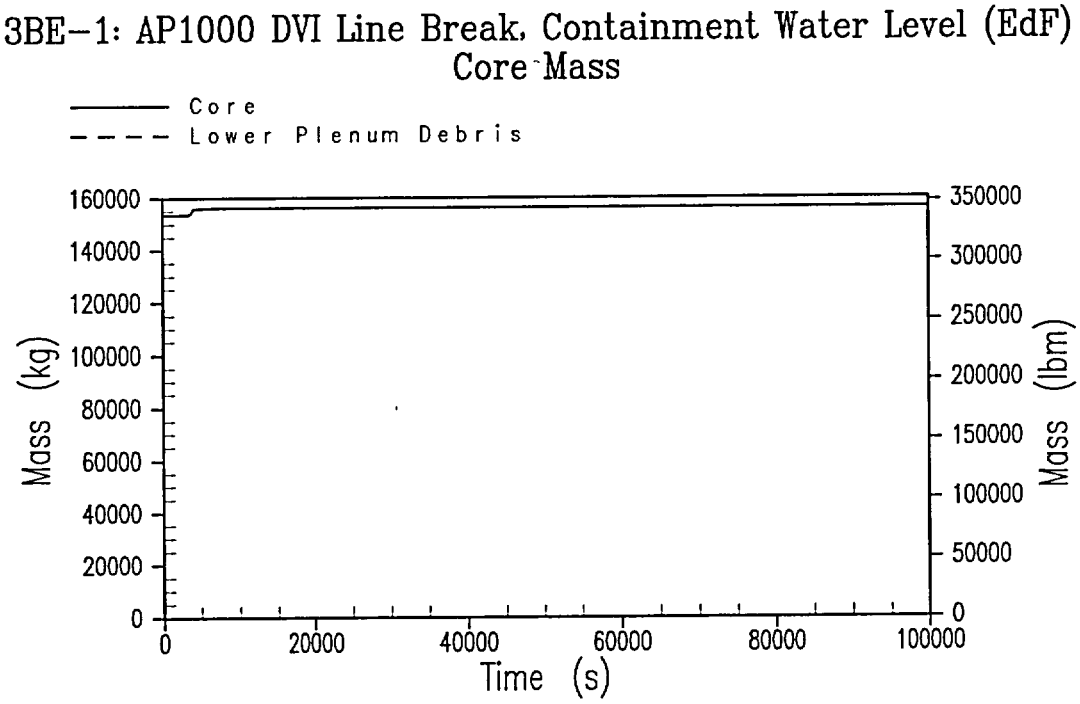

Figure 34-11

Case 3BE-1: Core Mass

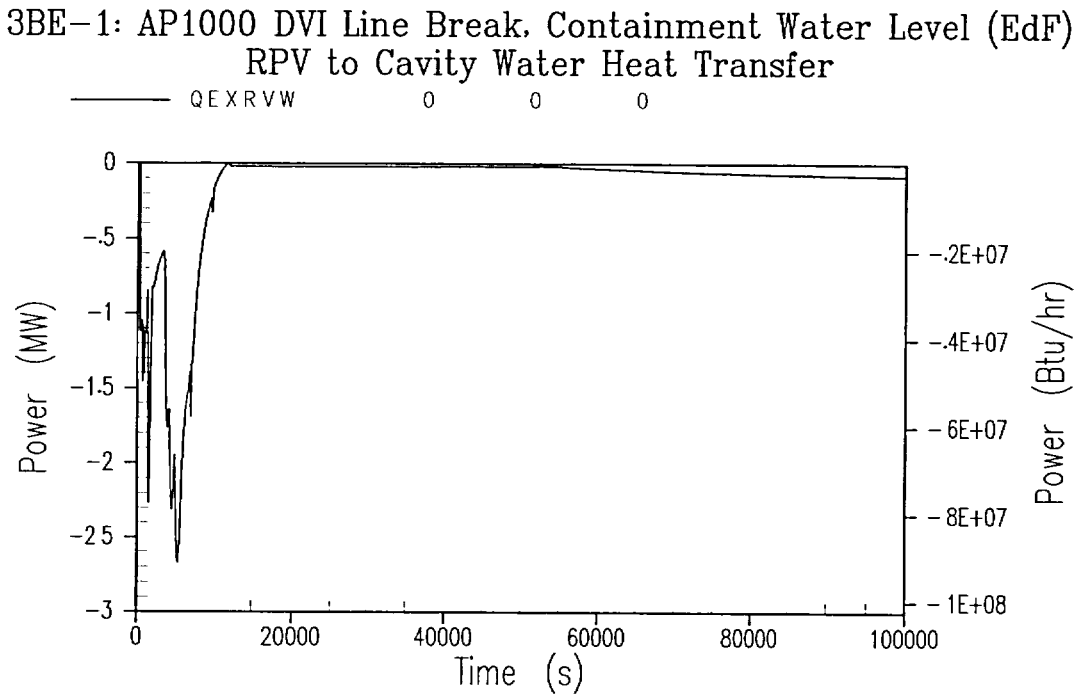

Figure 34-12

Case 3BE-1: Reactor Pressure Vessel to Cavity Water Heat Transfer

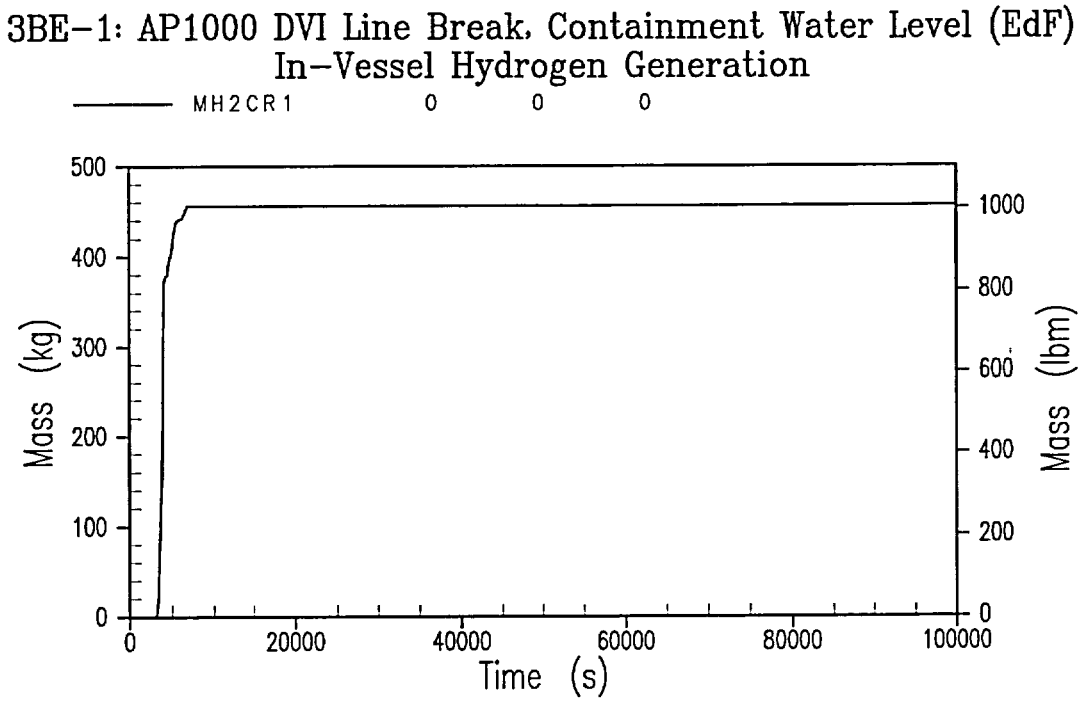

Figure 34-13

Case 3BE-1: In-Vessel Hydrogen Generation

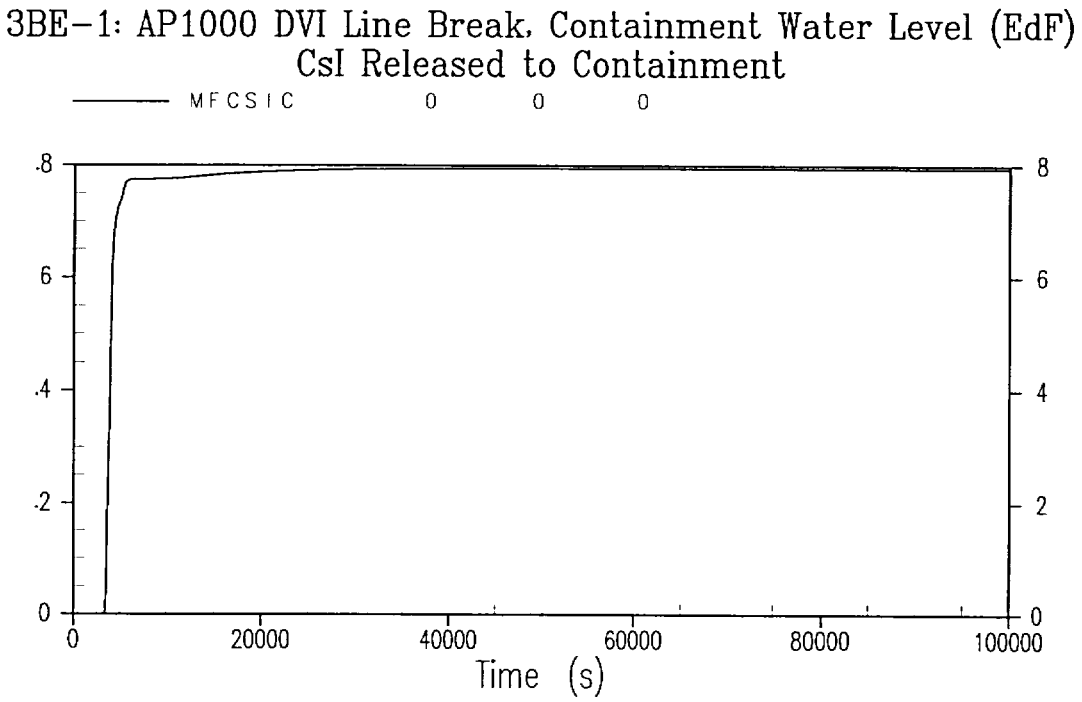

Figure 34-14

Case 3BE-1: Mass Fraction of CsI Released to Containment

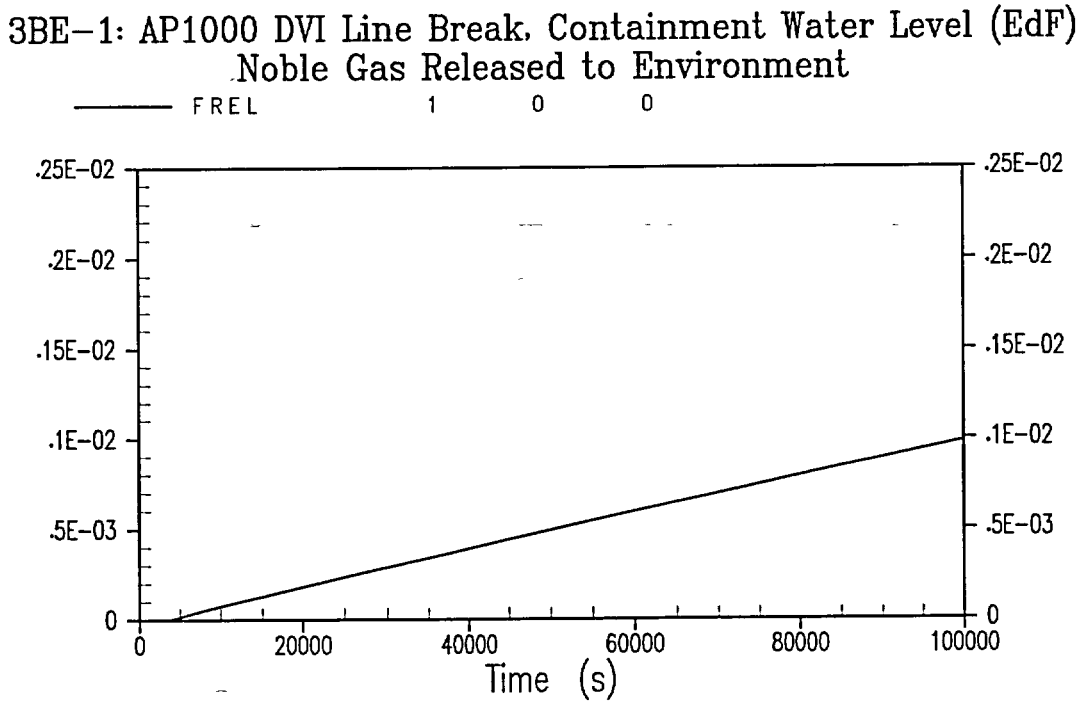

Figure 34-15

Case 3BE-1: Mass Fraction of Noble Gases Released to Environment

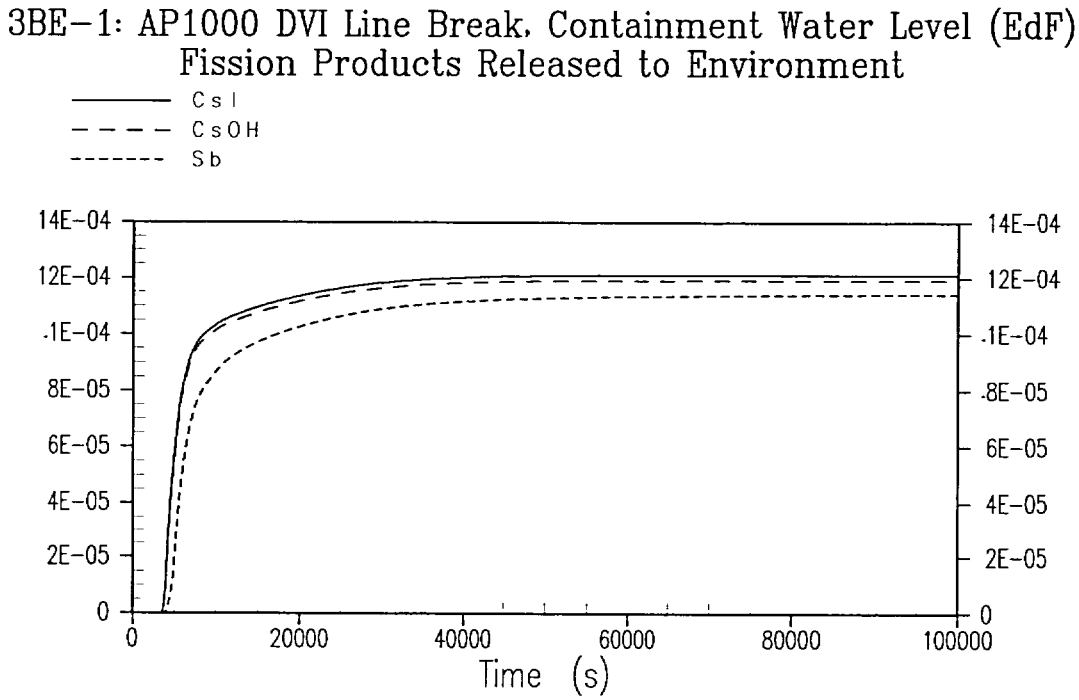

Figure 34-16

Case 3BE-1: Mass Fraction of Fission Products Released to Environment

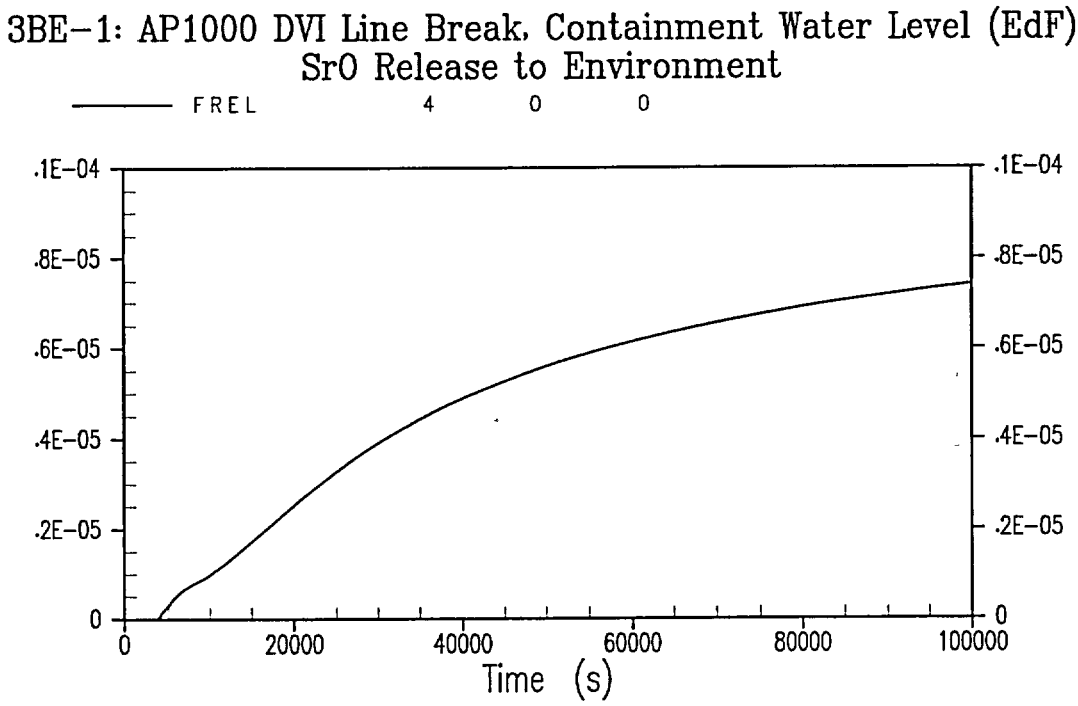

Figure 34-17

Case 3BE-1: Mass Fraction of SrO Released to Environment

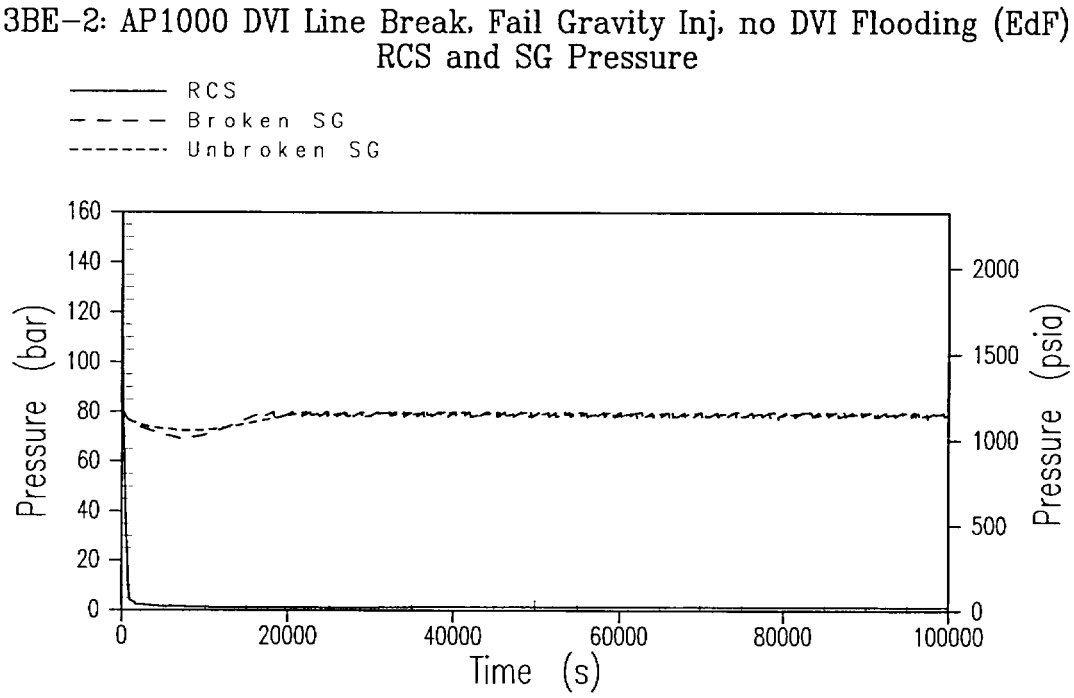

Figure 34-18

Case 3BE-2: RCS and Steam Generator Pressure

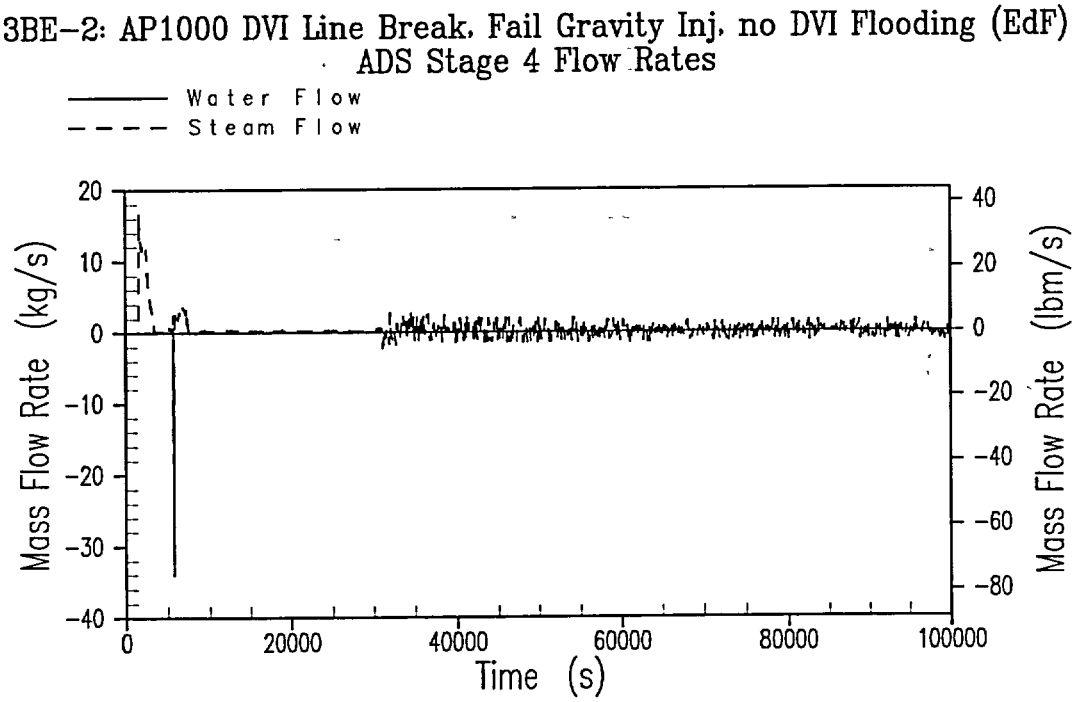

Figure 34-19

Case 3BE-2: ADS Stage 4 Flow Rates

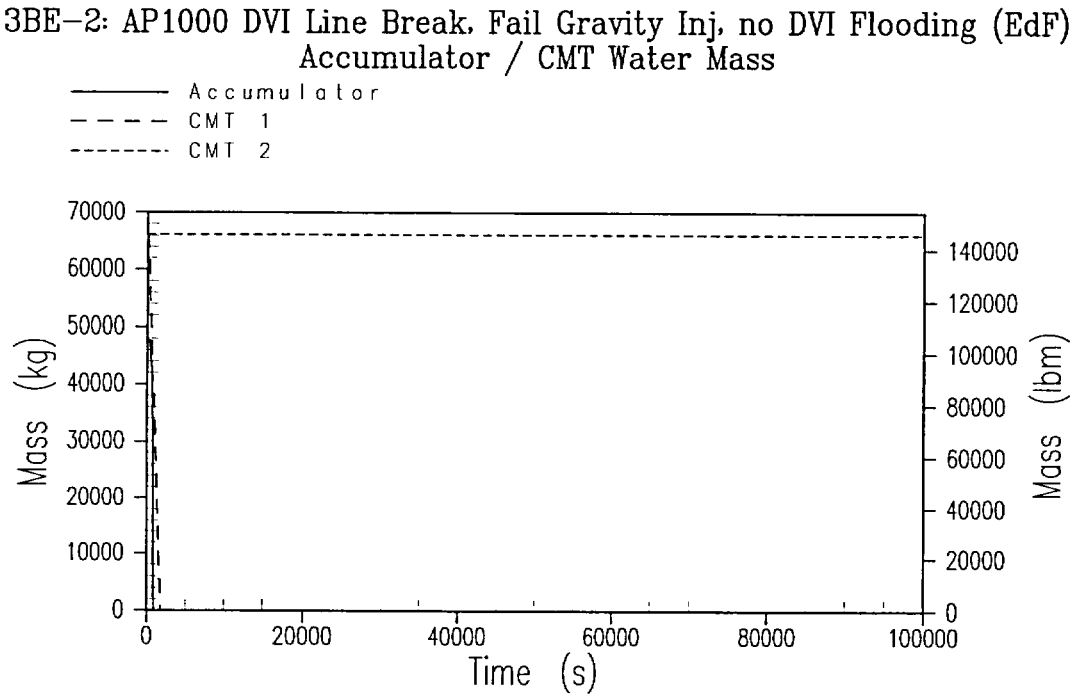

Figure 34-20

Case 3BE-2: Accumulator / CMT Water Mass

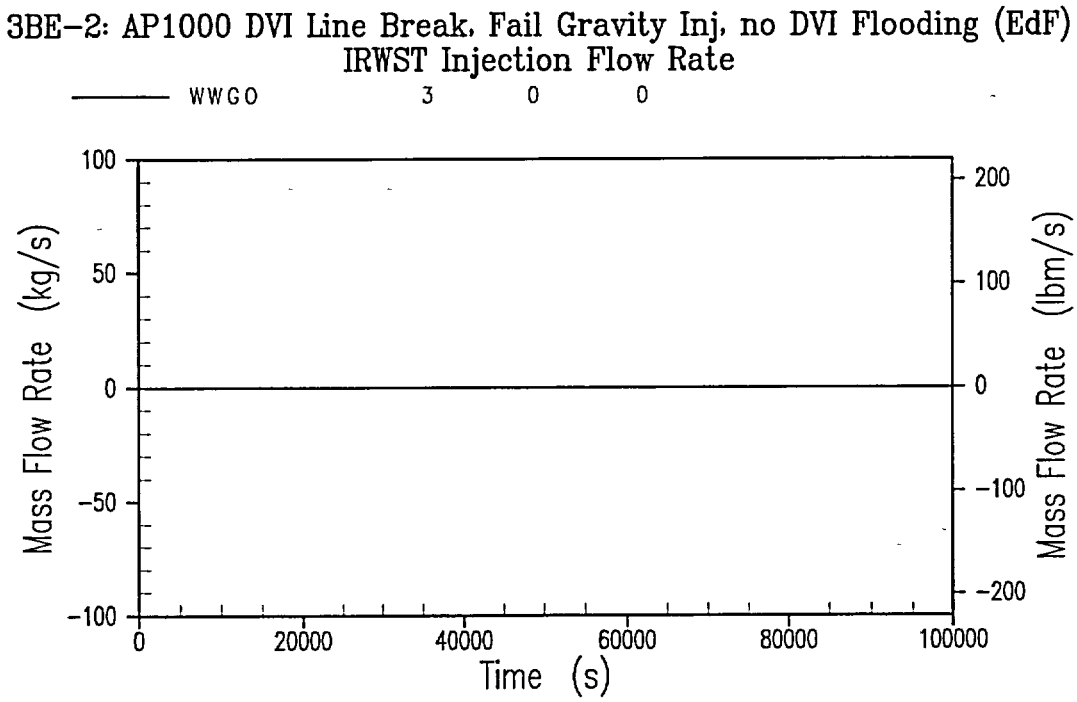

Figure 34-21

Case 3BE-2: IRWST Injection Flow Rate

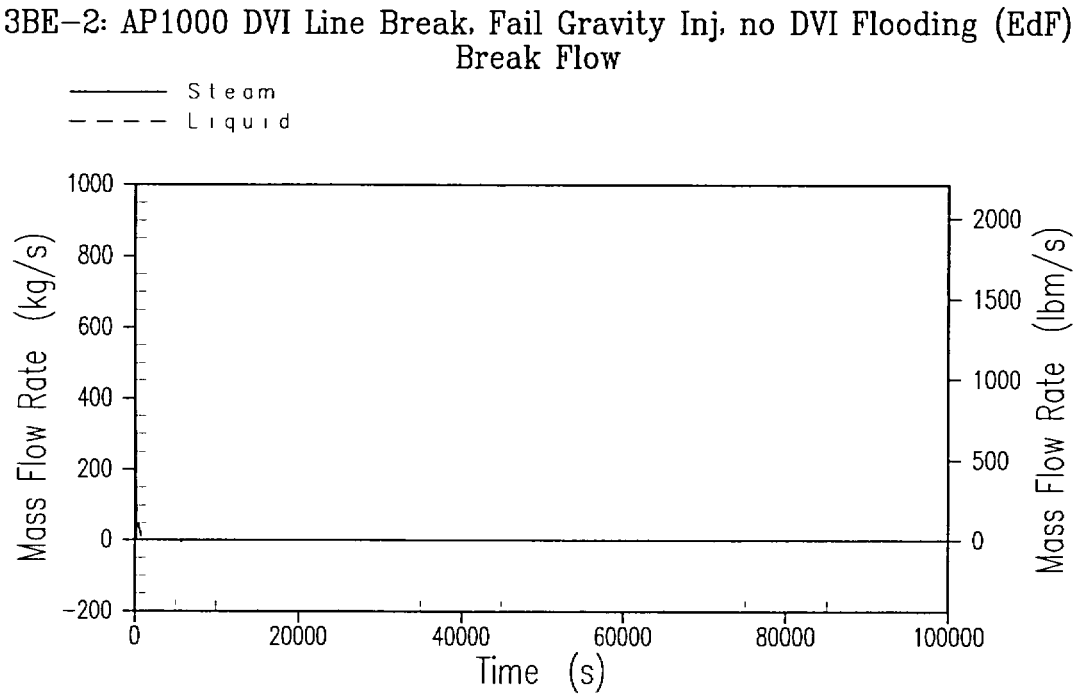

Figure 34-22

Case 3BE-2: Break Flow Rate

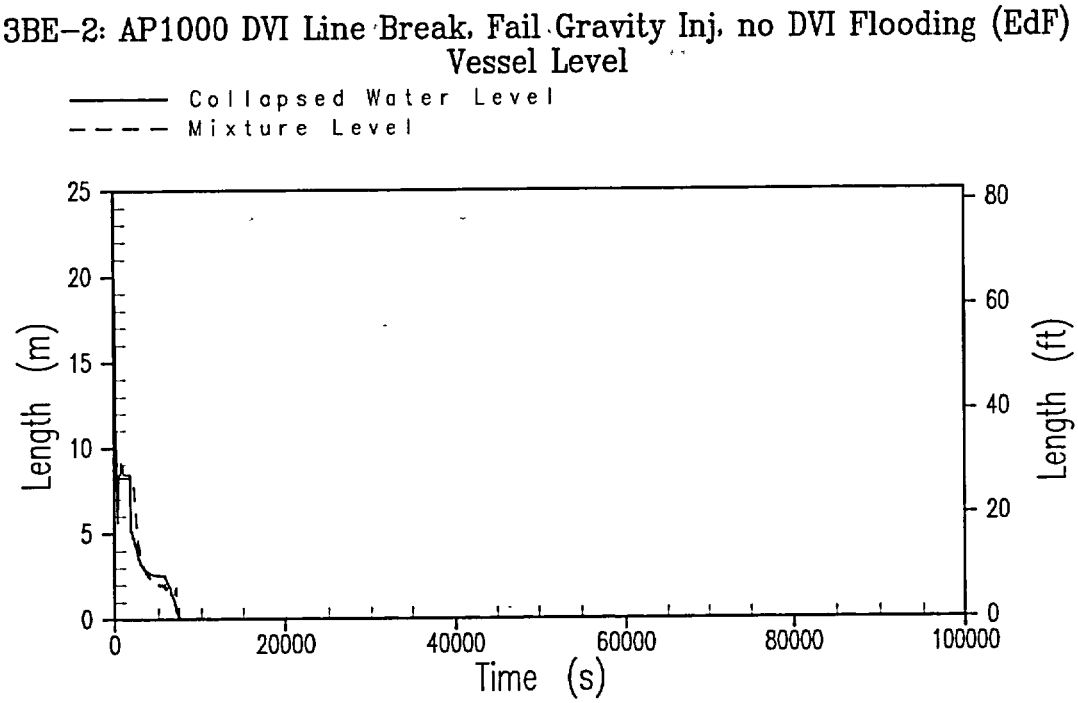

Figure 34-23

Case 3BE-2: Reactor Vessel Water Level

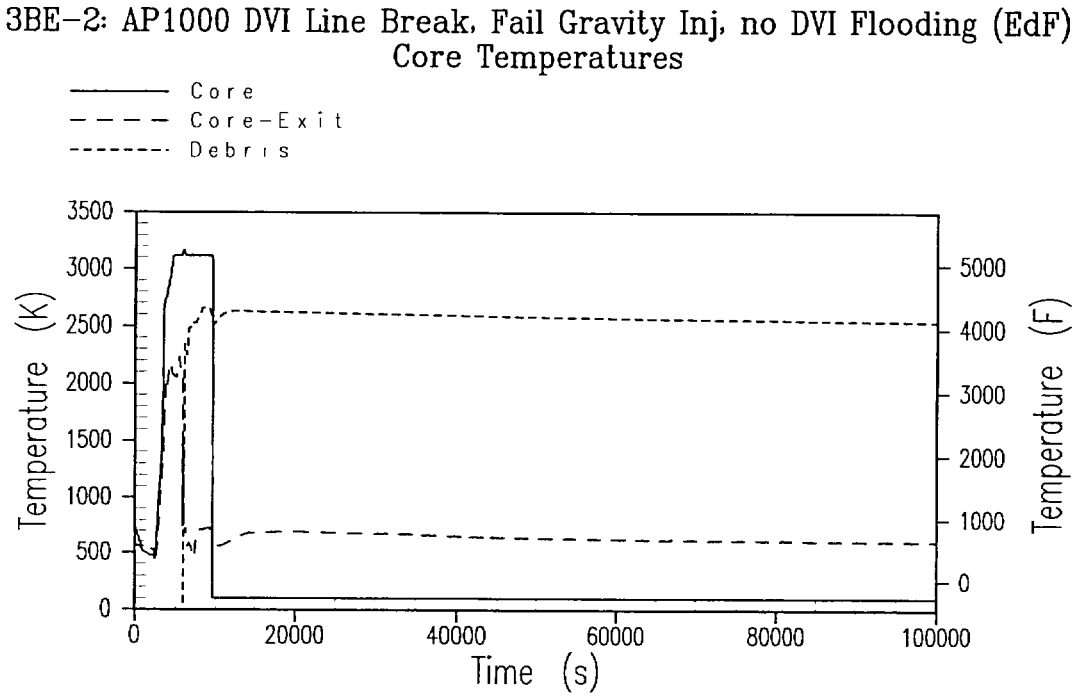

Figure 34-24

Case 3BE-2: Core Temperatures

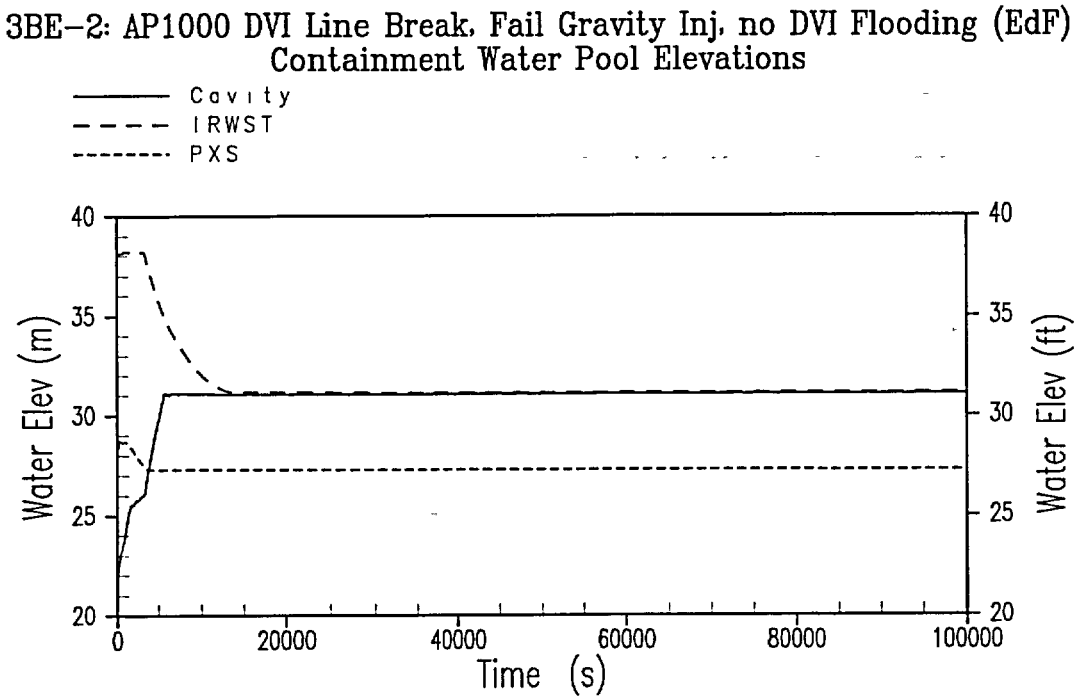

Figure 34-25

Case 3BE-2: Containment Water Pool Elevations

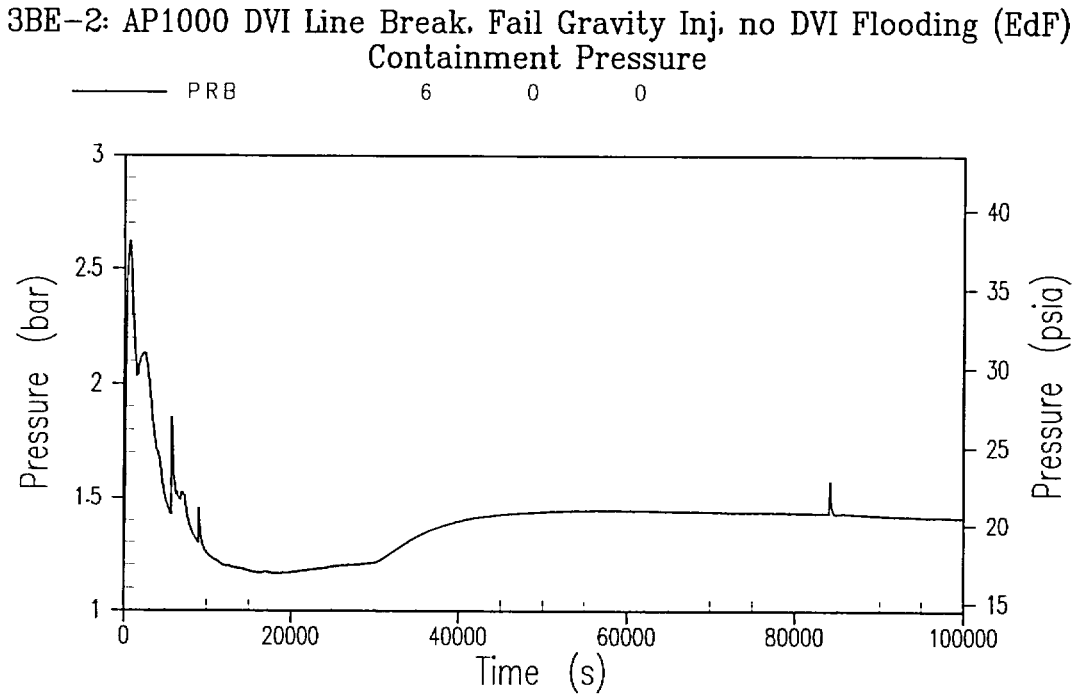

Figure 34-26

Case 3BE-2: Containment Pressure

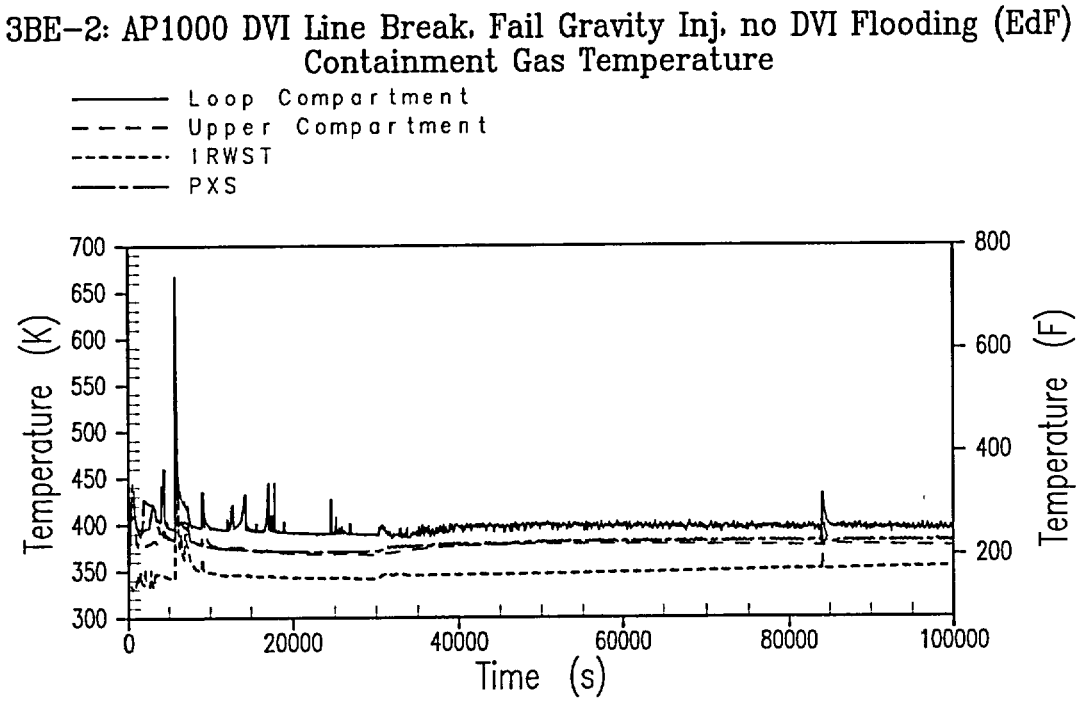

Figure 34-27

Case 3BE-2: Containment Gas Temperatures

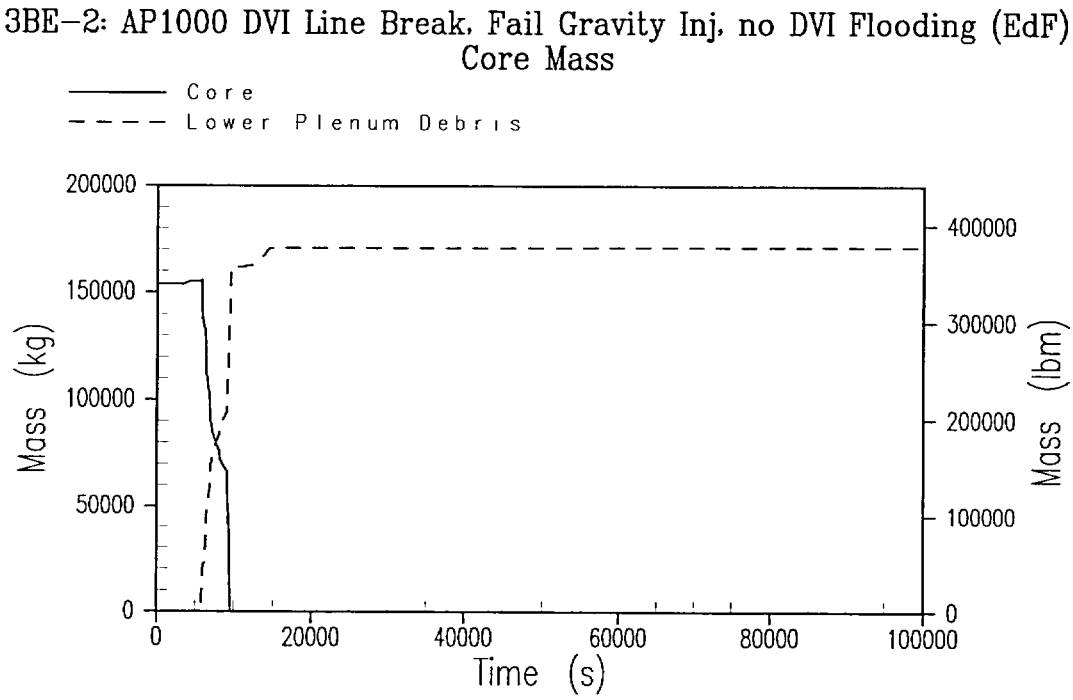

Figure 34-28

Case 3BE-2: Core Mass

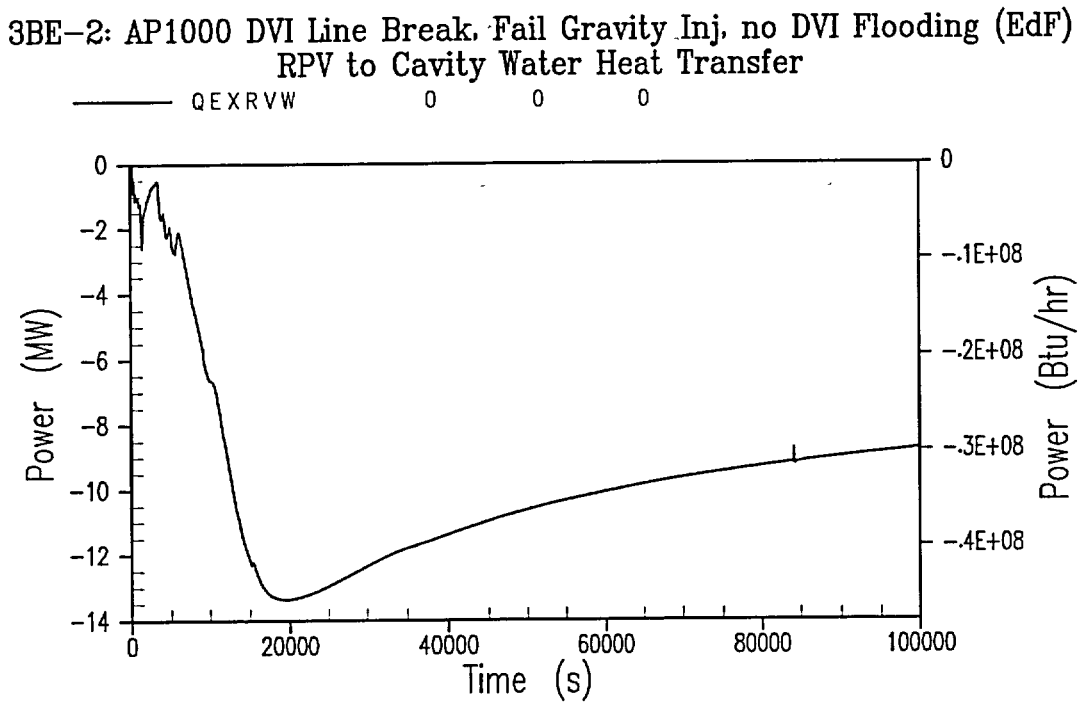

Figure 34-29

Case 3BE-2: Reactor Pressure Vessel to Cavity Water Heat Transfer

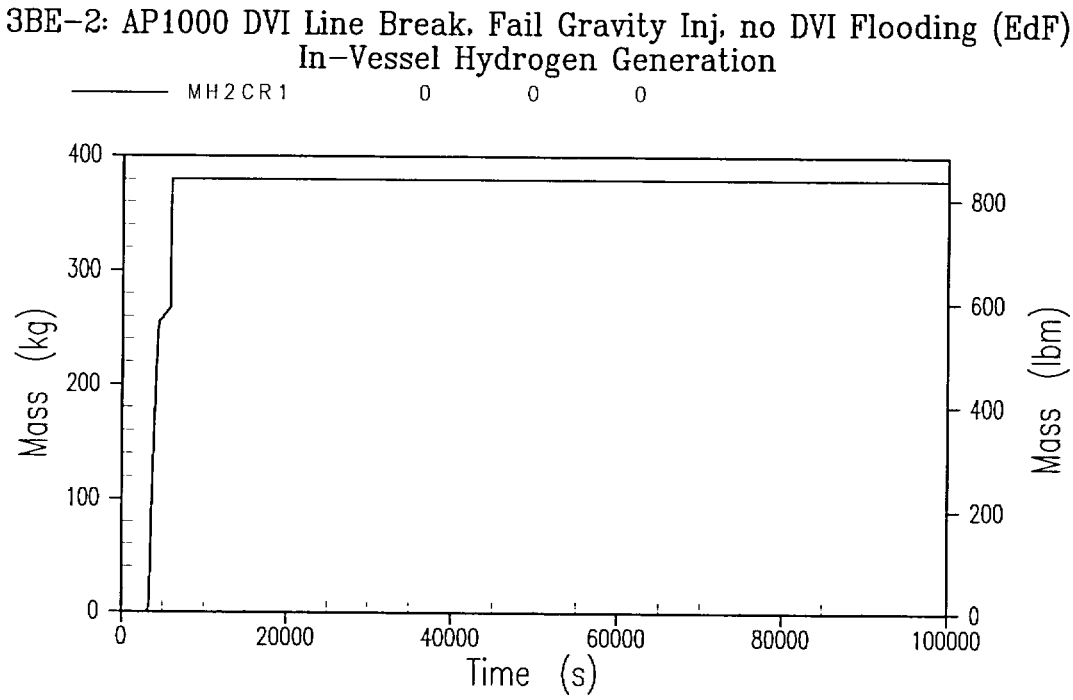

Figure 34-30

Case 3BE-2: In-Vessel Hydrogen Generation

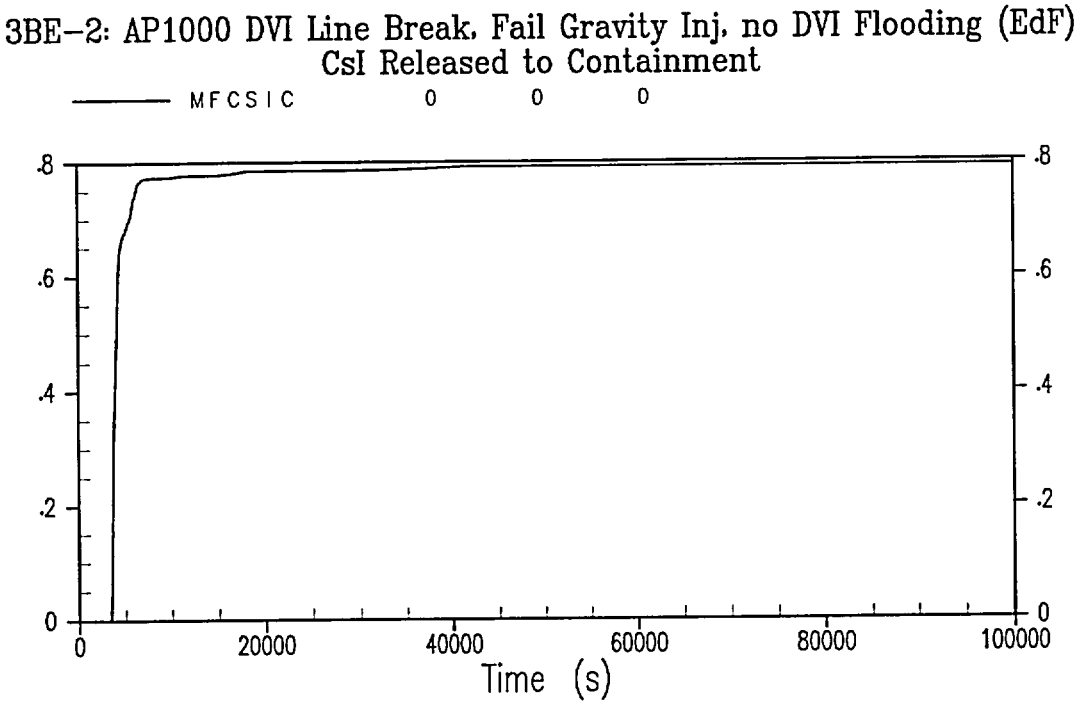

Figure 34-31

Case 3BE-2: Mass Fraction of CsI Released to Containment

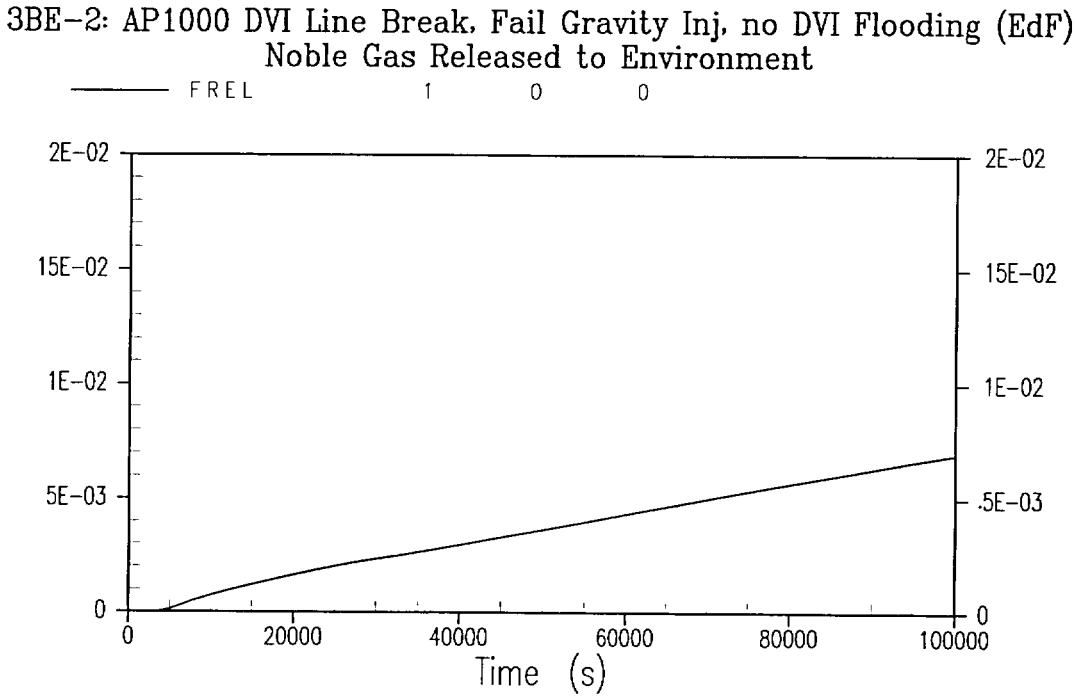

Figure 34-32

Case 3BE-2: Mass Fraction of Noble Gases Released to Environment

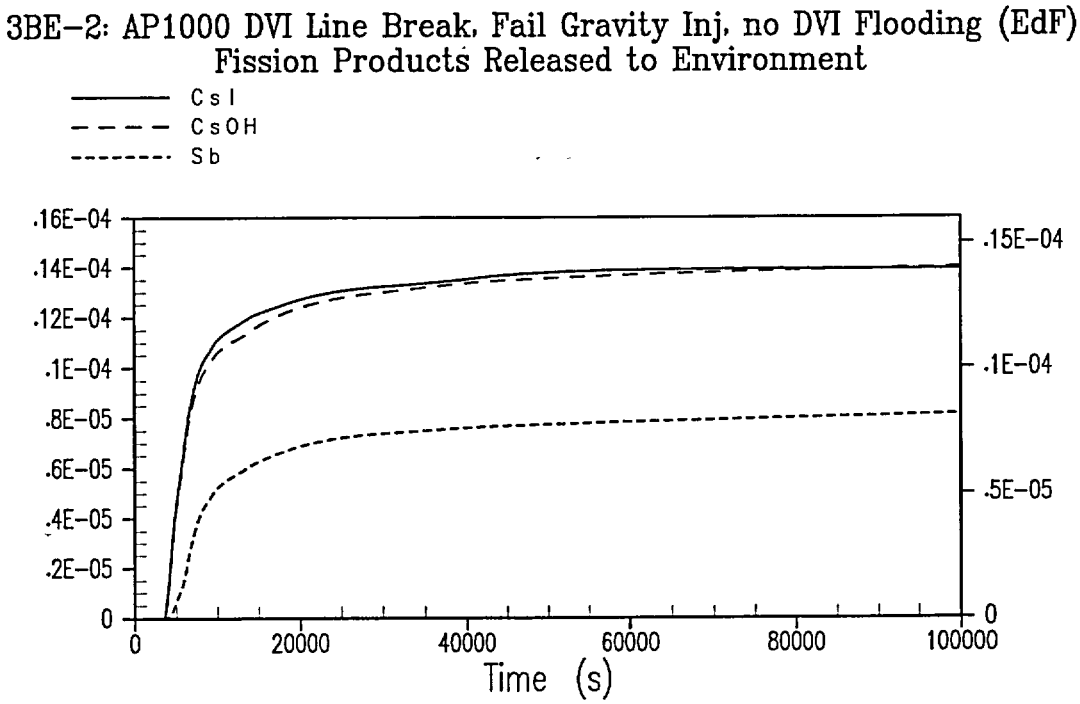

Figure 34-33

Case 3BE-2: Mass Fraction of Fission Products Released to Environment

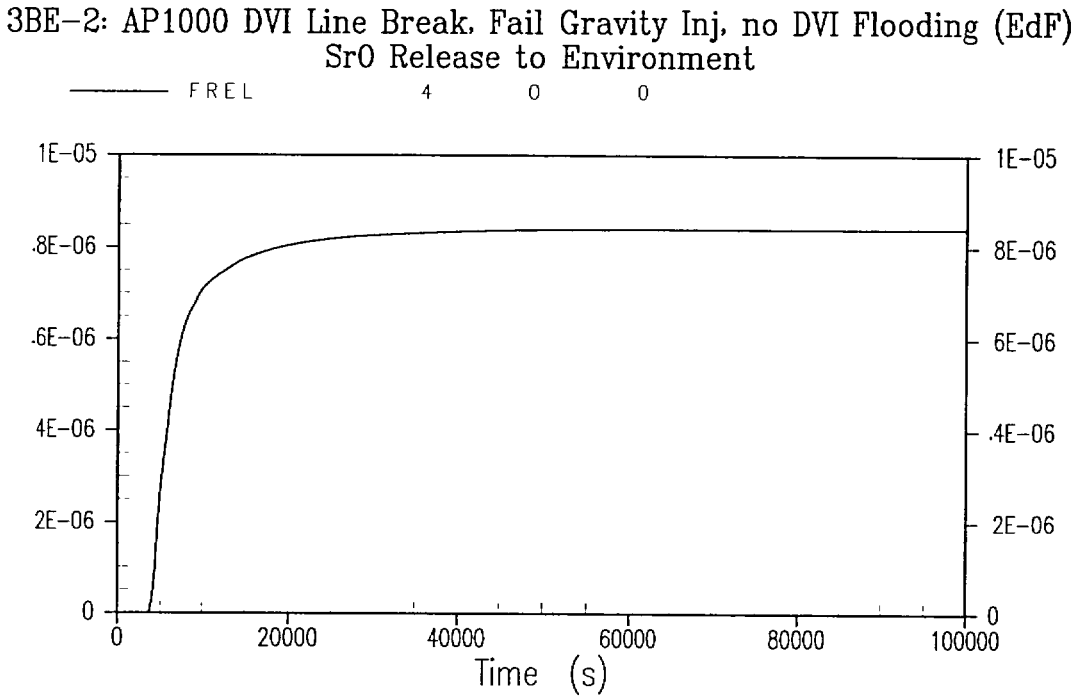

Figure 34-34

Case 3BE-2: Mass Fraction of SrO Released to Environment

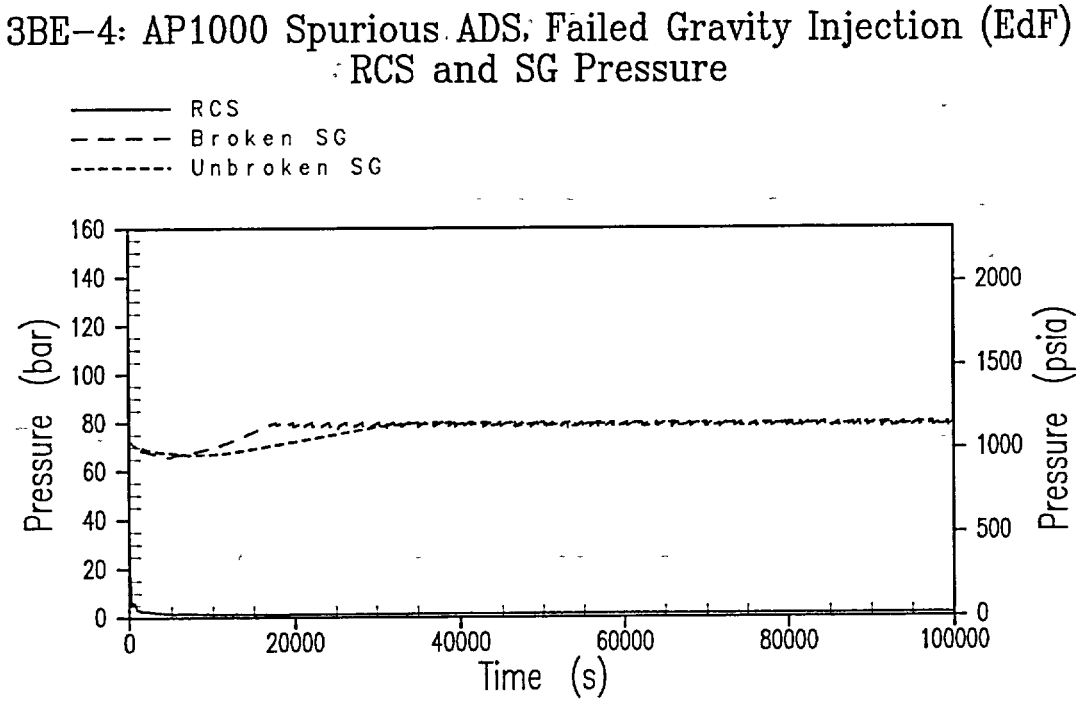

Figure 34-35

Case 3BE-4: RCS and Steam Generator Pressure

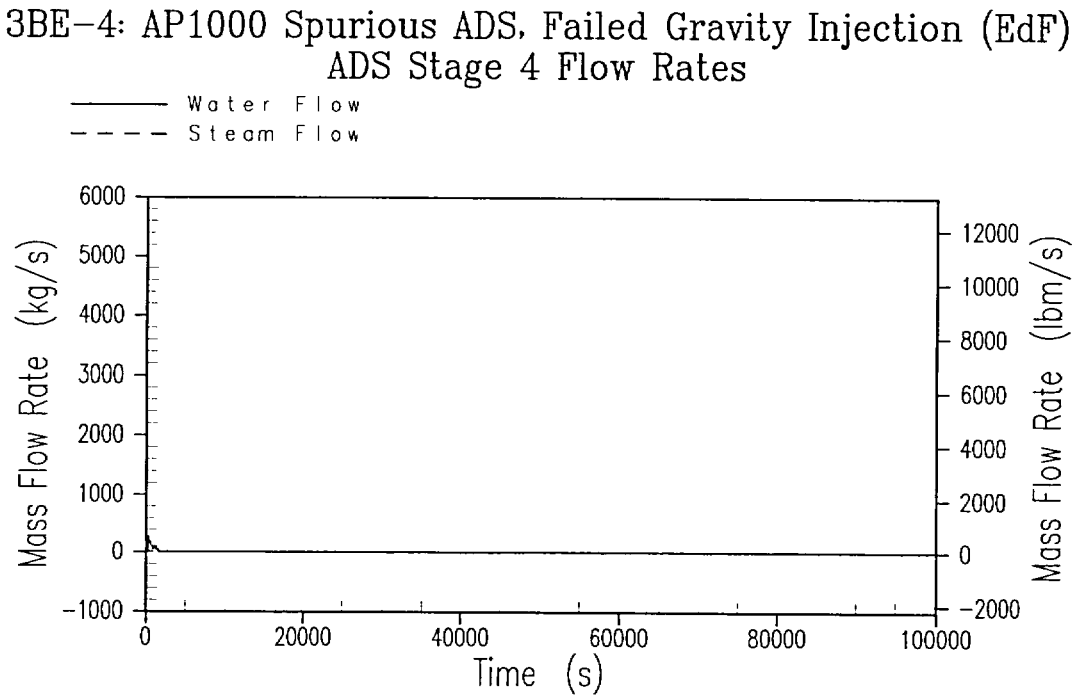

Figure 34-36

Case 3BE-4: ADS Stage 4 Flow Rates